

**SOIL EROSION RISK ASSESSMENT IN KUNTHIPPUZHA  
SUB-WATERSHED USING REMOTE SENSING AND GIS**

by

**SHAHEEMATH SUHARA, K.K**

**(2016 - 18 - 009)**

**THESIS**

Submitted in partial fulfillment of the requirements for the degree of

***MASTER OF TECHNOLOGY***

***IN***

***AGRICULTURAL ENGINEERING***

**(Soil and Water Engineering)**

**Faculty of Agricultural Engineering & Technology**

**Kerala Agricultural University**



***Department of Soil and Water Conservation Engineering***

**KELAPPAJI COLLEGE OF AGRICULTURAL ENGINEERING AND TECHNOLOGY**

**TAVANUR, MALAPPURAM-679573**


**KERALA, INDIA**

**2018**

## DECLARATION

I, hereby declare that this thesis entitled “**SOIL EROSION RISK ASSESSMENT IN KUNTHIPPUZHA SUB-WATERSHED USING REMOTE SENSING AND GIS**” is a bonafide record of research work done by me during the course of research and the thesis has not previously formed the basis for the award to me of any degree, diploma, associateship, fellowship or other similar title, of any other University or Society.

Tavanur,  
Date:

  
**Shaheemath Suhara, K.K**  
(2016-18-009)

## CERTIFICATE

Certified that this thesis entitled “**SOIL EROSION RISK ASSESSMENT IN KUNTHIPPUZHA SUB-WATERSHED USING REMOTE SENSING AND GIS**” is a record of research work done independently by Ms. Shaheemath Suhara, K.K. under my guidance and supervision and that it has not previously formed the basis for the award of any degree, diploma, fellowship or associateship to her.

Tavanur,  
Date:



**Dr. Abdul Hakkim, V.M.**  
(Major Advisor, Advisory Committee)  
Professor (Soil and Water Engineering)  
ARS, Anakkayam



## CERTIFICATE

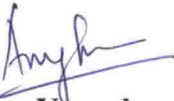
We, the undersigned members of the advisory committee of Ms. Shaheemath Suhara, K.K. (2016-18-009), a candidate for the degree of **Master of Technology in Agricultural Engineering** with major in Soil and Water Engineering, agree that the thesis entitled “**SOIL EROSION RISK ASSESSMENT IN KUNTHIPPUZHA SUB-WATERSHED USING REMOTE SENSING AND GIS**” may be submitted by Ms. Shaheemath Suhara, K.K. (2016-18-009), in partial fulfilment of the requirement for the degree.



**Dr. Abdul Hakkim V.M.**  
(Chairman, Advisory Committee)  
Professor (Soil and Water Engineering)  
ARS, Anakkayam.



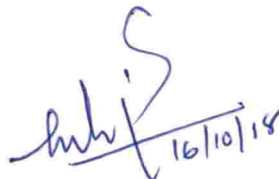
**Dr. Sathian K.K.**  
(Member, Advisory Committee)  
Dean, Professor and Head  
Department of SWCE  
KCAET, Tavanur.



**Dr. Anu Varughese**  
(Member, Advisory Committee)  
Assistant Professor  
Department of IDE  
KCAET, Tavanur.



**Er. Shivaji K.P.**  
(Member, Advisory Committee)  
Assistant Professor  
Department of FPME  
KCAET, Tavanur.



16/10/18

**EXTERNAL EXAMINER**

**Dr. Manoj P Samuel**

## ACKNOWLEDGEMENT

First of all, I praise Allah, the almighty, merciful and passionate, for providing me this opportunity, for lighting up the lamp of hope and granting me the capability to proceed successfully. The thesis appears in its current form due to the assistance and guidance of several people. I would consider this work nothing more than incomplete without attending to the task of acknowledging the overwhelming help I received during this endeavor.

I express my deep and sincere regards, profound sense of gratitude and indebtedness to my guide as well as Chairman of the Advisory Committee, **Dr. Abdul Hakkim, V.M.**, Professor, Soil and Water Engineering, ARS, Anakkayam for untiring supervision, meticulous guidance and benevolent criticisms during the entire course of this investigation. It is my proud privilege to express my heartfelt indebtedness and deepest sense of gratitude for laying out the guidelines of research work.

It is my pleasure to pay tribute to **Dr. Sathian, K.K.**, Dean, Professor & Head, Department of Soil and Water Conservation Engineering, K.C.A.E.T, Tavanur, and member of advisory committee for his advice and guidance rendered during this study. I have real admiration, gratitude and regards for his full hearted support and untiring help.

True kindness lies within the act of giving without the expectation of anything in return. My sincere and heartfelt thanks go to **Dr. Anu Varughese**, Assistant Professor, Department of Irrigation and Drainage Engineering, K.C.A.E.T, Tavanur and member of advisory committee for her sustained guidance, constant encouragement, untiring help and insightful consults throughout the period of the study. Thank you for always supporting me and encouraging me.

I express my deep gratitude to **Er. Shivaji K.P.**, Assistant Professor, Department of Farm Power Machinery and Energy, K.C.A.E.T, Tavanur as a member of advisory committee. I am indebted to you for your encouragement and support in my research.

It is my pleasure to offer whole hearted and special thanks to **Er. Priya G Nair**, Assistant Professor, Soil and Water Conservation Engineering for her guidance, constant encouragement, untiring help and support throughout the period of the study. I place my special thanks to **Dr. Rema, K.P.**, Professor, Department of Irrigation and Drainage Engineering, K.C.A.E.T, Tavanur, and **Dr. Asha Joseph**, Professor, Department of Irrigation and Drainage Engineering, K.C.A.E.T, Tavanur and **Dr. Sasikala, D.**, Professor, Department of Irrigation and Drainage Engineering, K.C.A.E.T, Tavanur, **Er. Jinu, A.**, Assistant Professor, Soil and Water Conservation Engineering, **Dr. Sajeena, S.**, Assistant Professor, KVK, Malappuram for their unreserved help. I was surprised for their passion and solicitude towards students. I place my special thanks to all teachers in department of Soil and water Conservation Engineering as well as Department of Irrigation and Drainage Engineering.

I express my deep sense and sincere gratitude and indebtedness to whole **CGIT** team. It is my responsibility and proud privilege to express my heartfelt thanks to **Jithesh Kumar T.J.**, for the help he had rendered. Also it is my pleasure to pay tribute to **Nogy Augustine** for his encouragement and sustained guidelines during this endeavor. I place my special thanks to **Mrs. Geethu C.G., Mr. Anup P.C., and Mr. Denish** for the generous support needed by me. My completion of this project could not have been accomplished without the help of you people.

I express my sincere thanks to the officers and employees of the **Department of Soil Survey and Soil Conservation, Palakkad** for providing the data required for this study. In addition, I am extremely grateful to the **RARS, Pattambi**, also to **Ilangovan, R** for providing the weather data required in this study without any delay.

I am extremely grateful to **Dr. Prince, M.V.**, Professor and Academic Officer, Department of PFE, KCAET, Tavanur for the support he has rendered.

I am extremely grateful to the all teachers, officers, library staffs of the KCAET, Tavanur for their sincere support.

I take this opportunity to express my greatest regards to my classmates, friends and seniors especially, **Er. Ardra Wilson, Er. Chethan B.J., Er. Gilsha Bhai, Er. Jyothy Narayanan, Er. Anjana S.R., Er. Hari Sairam, Er. Sharon L George, Er. Pooja M.R., Er. Shahama K., Er. Mamatha Prabhakar** and my favorite junior **Shili** for their constant and invaluable help and support rendered during the conduct of project work.

My sincere thanks to my M.Tech batchmates **Er. Uday Bhanu Prakash, Er. Venkata Sai, Er. Athira Prasad, Er. Rasmi J., Er. Akhila J.C., Er. Remya, Er. Aswathi, Er. Pooja V., Er. Venkata Reddy, Er. Sreedhara** and to my seniors **Er. Ashitha G.N., Er. Salsan, Er. Yunus A. and Er. Anjaly C.** for their supports. I place my thanks to my juniors **Er. Arya. K.T., Er. Amrutha, Er. Nandu Lal, Er. Aksa and Er. Riyola** for their sincere support rendered during the conduct of project work. Also, I am extremely grateful to my friends **Er. Arjun, Er. Yadhu Krishnan, Rajeevan, Rashida K.P., Sruthi K.V., Krishnalekha and Aju Thomas** for their supports.

My heartfelt thanks to **Kerala Agricultural University** for providing me a chance to study in this institution.

I am in dearth of words to express my unboundful gratitude and love to the living gods, my parents **Kunhamu, C.N. and Thahira, C.L.** for their unbounding love and dedicated efforts to educate me to this level which were the sustaining factors in carrying out this work successfully. I extend my gratitude to **Shakkira, Adv. Shafi, Tajudheen, Thaslim, Abdu Rahiman, Shameela, Safvana, Shaheena,**

**Surayya, Lubaina, Rubeena, Munavvira, Abbas Ibrahim, Ashraf and Rizwan** and each members of the **CN family** and **CL family** for the support, caring and love rendered throughout my study.

Above all, I humbly acknowledge the grace and blessings of the supreme power for enlighten my life and fulfilling this well nurtured dream.

**Shaheemath Suhara, K.K.**



Dedicated to

Agricultural  
Engineers

## CONTENTS

<b>Chapter No:</b>	<b>Title</b>	<b>Page No:</b>
	LIST OF TABLES	i
	LIST OF FIGURES	ii
	LIST OF PLATES	vi
	SYMBOLS AND ABBREVIATIONS	vii
1	INTRODUCTION	1
2	REVIEW OF LITERATURE	6
3	MATERIALS AND METHODS	47
4	RESULTS AND DISCUSSION	77
5	SUMMARY AND CONCLUSIONS	118
	REFERENCES	122
	APPENDICES	144
	ABSTRACT	

## LIST OF TABLES

<b>Table No.</b>	<b>Title</b>	<b>Page No.</b>
2.1	Estimation of R factor from rainfall amount by different authors	27
2.2	Variation of K factor with respect to texture and organic matter content	30
2.3	Slope classification	32
2.4	C factors and Land use	33
2.5	P factor values	35
3.1	The variation of P factor with respect to landuse and land slope	64
3.2	Soil parameters for MMF model	70
3.3	Plant parameters for MMF model	71
4.1	Sediment delivery ratio calculation	103
4.2	Soil erosion severity classes with area covered	110
4.3	Spatial and temporal variations in NDVI and mean soil erosion with the changes in land use in the year 2000 and 2013	115

## LIST OF FIGURES

Figure No.	Title	Page No.
3.1	Location of the study area	48
3.2	USGS Earth Explorer user interface	50
3.3	User interface of OpenTopography	51
3.4	User interface of OpenstreetMap	52
3.5	User interface of Bhuvan	52
3.6	The delineated boundary of the study area ( <i>'Bound.shp'</i> )	55
3.7	GIS interface for IDW interpolation	57
3.8	Soil map of the Bharathapuzha river basin	59
3.9	Digitization of the soil map of the study area	59
3.10	ArcGIS interface for raster calculator	61
3.11	Flow chart for LS factor determination	62
3.12	Image analysis tool with LISS III image clipped for the study area	63
3.13	The clipped Landsat image of the year 2000	65
3.14	The clipped Landsat image of the year 2013	66
3.15	Methodological framework adopted in RUSLE model	67

3.16	Texture triangle	69
3.17	USDA soil texture calculator	69
3.18	ArcGIS polygon to raster tool with selected value field 'BD'	70
3.19	Attribute data management of the plant parameters for the MMF model	71
3.20	Methodological framework adopted in MMF model	73
3.21	Cell statistics tool in ArcGIS	74
4.1	Spatial distribution of R factor in the year 2000 ( <i>R2000</i> )	78
4.2	Spatial distribution of R factor in the year 2013 ( <i>R2013</i> )	79
4.3	Spatial distribution of K factor ( <i>K_soil</i> )	80
4.4	Spatial distribution of LS factor in the year 2000 ( <i>LS2000</i> )	81
4.5	Spatial distribution of LS factor in the year 2013 ( <i>LS2013</i> )	82
4.6	Spatial distribution of C factor in the year 2000 ( <i>C2000</i> )	83
4.7	Spatial distribution of C factor in the year 2013 ( <i>C2013</i> )	83
4.8	Spatial variation of C factor in the years 2000 and 2013	84
4.9	Spatial distribution of P factor in the year 2000 ( <i>P2000</i> )	85
4.10	Spatial distribution of P factor in the year 2013 ( <i>P2013</i> )	85
4.11	Spatial distribution of MS values ( <i>MS_soil</i> )	87
4.12	Spatial distribution of BD values ( <i>BD_soil</i> )	87

4.13	Spatial distribution of EHD values ( <i>EHD_soil</i> )	88
4.14	Spatial distribution of 'A' values of the year 2000 ( <i>A2000</i> )	88
4.15	Spatial distribution of 'A' values of the year 2013 ( <i>A2013</i> )	89
4.16	Spatial distribution of $E_t/E_0$ values of the year 2000 ( <i>E<sub>t</sub>/E<sub>0</sub>2000</i> )	89
4.17	Spatial distribution of $E_t/E_0$ values of the year 2013 ( <i>E<sub>t</sub>/E<sub>0</sub>2013</i> )	90
4.18	Slope steepness map of the year 2000 ( <i>S2000</i> )	90
4.19	Slope steepness map of the year 2013 ( <i>S2013</i> )	91
4.20	Spatial distribution of E factor in the year 2000 ( <i>E2000</i> )	92
4.21	Spatial distribution of E factor in the year 2013 ( <i>E2013</i> )	93
4.22	Spatial distribution of $R_c$ factor in the year 2000 ( <i>R<sub>c</sub> 2000</i> )	94
4.23	Spatial distribution of $R_c$ factor in the year 2013 ( <i>R<sub>c</sub> 2013</i> )	95
4.24	Spatial distribution of Q factor in the year 2000 ( <i>Q2000</i> )	95
4.25	Spatial distribution of Q factor in the year 2013 ( <i>Q2013</i> )	96
4.26	Variation F values with A factor for the year 2000 and 2013	97
4.27	Spatial distribution of 'G' factor in the year 2000 ( <i>G2000</i> )	98
4.28	Spatial distribution of 'G' factor in the year 2013 ( <i>G2013</i> )	98
4.29	Spatial distribution of 'F' factor in the year 2000 ( <i>F2000</i> )	99
4.30	Spatial distribution of 'F' factor in the year 2013 ( <i>F2013</i> )	99
4.31	Spatial distribution of soil erosion by RUSLE (2000)	100

4.32	Spatial distribution of soil erosion by RUSLE (2013)	101
4.33	Spatial distribution of soil erosion by MMF (2000)	101
4.34	Spatial distribution of soil erosion by MMF (2013)	102
4.35	Kunthippuzha sub-basin with 16 micro-watersheds	102
4.36	Zonal elements of rainfall and slope with their corresponding mean soil erosion by RUSLE and MMF	105
4.37	Zonal elements of soil with mean soil erosion by RUSLE and MMF	105
4.38	Zonal elements of vegetation with mean soil erosion by RUSLE and MMF	106
4.39	Soil loss scores for major soil loss factor layers: (a) land use score (b) slope score (c) soil score (d) rainfall score (RUSLE)	107
4.40	Soil loss scores for major soil loss factor layers: (a) soil score (b) slope score (c) rainfall score (d) and land use score (MMF)	108
4.41	Soil erosion map with severity ranges A) RUSLE B) MMF	109
4.42	NDVI maps for the year 2000 and 2013	111
4.43	Landuse maps generated for Kunthippuzha sub-basin for the year a) 2000 b) 2013	112
4.44	Variation of pixel count with NDVI values	114

## LIST OF PLATES

Plate No.	TITLE	Page No.
4.1	Field photographs of the study area	113



## SYMBOLS AND ABBREVIATIONS

%	:	Percentage
<	:	Less than
>	:	Greater than
$\Sigma$	:	Sum
$\leq$	:	Less than or equal to
$\geq$	:	Greater than or equal to
$^{\circ}$	:	Degree
$^{\circ}\text{C}$	:	Degree Celsius
a	:	acre
ACED	:	Assessment of Current Erosion Damage
AGNPS	:	Agricultural-Non-Point-Source Pollution
ANN	:	Artificial Neural Network
ANOVA	:	Analysis of Variance
ANSWERS	:	Areal Nonpoint Source Watershed Environment Simulation model
ASTER	:	Advanced Space Borne Thermal Emission and Reflection Radiometer
cm	:	Centimeter
CMIP	:	Coupled Model Intercomparison Project
CREAMS	:	Chemicals, Runoff and Erosion from Agricultural Management Systems
DEM	:	Digital Elevation Model
DGPS	:	Differential Global Positioning System
DTM	:	Digital Terrain Model
E	:	East
ERDAS	:	Earth Resources Data Analysis System
i.e.,	:	Which is to say, in other words
ESRI	:	Environmental Systems Research Institute

ET	:	Evapotranspiration
et al.,	:	and others
etc	:	et cetra
ft	:	feet
GIS	:	Geographical Information System
GPS	:	Global Positioning System
GRSII	:	Guelph Rainfall Simulator II
h	:	Hour
ha	:	hectare
I <sub>30</sub>	:	30 minute intensity
IDW	:	Inverse Distance Weighted
ILWIS	:	Integrated Land and Water Information System
IMD	:	Indian Meteorological Department
IRS	:	Indian Remote-Sensing Satellite
ISRO	:	Indian Space Research Organization
J	:	Joule
km	:	Kilometer
k-NN	:	K-nearest neighbors
LISS	:	Linear Imaging And Self Scanning
LULC	:	Landuse Land Cover
m	:	meter
MFI	:	Modified Fournier Index
MJ	:	Mega Joule
mm	:	millimeter
Mg	:	Mega gram
MMF	:	Morgan, Morgan and Finney model
m-tonnes	:	Million tonnes

MUSLE	:	Modified Universal Soil Loss Equation
N	:	North
NDVI	:	Normalized Difference Vegetation Indices
NIMET	:	Nigerian Metrological Agency
NIR	:	Near infrared
R <sup>2</sup>	:	Coefficient of Determination
RARS	:	Regional Agricultural Research Station
RMSE	:	Root Mean Square Error
RUSLE	:	Revised Universal Soil Loss Equation
s	:	Second
SOI	:	Survey of India
SPI	:	Stream Power Index
SRTM	:	Shuttle Radar Topography Mission
SWAT	:	Soil and Water Assessment Tool
t	:	ton
TLSD	:	Transport Limited Sediment Delivery
TRMM	:	Tropical Rainfall Measuring Mission
TWI	:	Topographic Wetness Index
UMR	:	Upper Min River
USDA	:	United States Department of Agriculture
USGS	:	United States Geological Survey
USLE	:	Universal Soil Loss Equation
UTM	:	Universal Transverse Mercator Co-ordinate System
vfS	:	Very fine sand
viz.,	:	Namely
w/w	:	Weight/Weight
WEPP	:	Water Erosion Prediction Project

WGS : World Geodetic System  
WIO : Weighted Index Overlay  
y : year

# **INTRODUCTION**

# CHAPTER 1

## INTRODUCTION

Land and water are two fundamental natural resources essential for the existence of life. These two components of the biosphere are connected with each other in different phases of the hydrologic cycle. The socio-economic development of all countries is based on efficient utilization of these two resources, its conservation and management through an integrated approach. Rise in population, urbanization and agricultural intensification have led to the over exploitation of these resources ultimately resulting in resource depletion and degradation (Amore *et al.*, 2004). Among all troubles associated with land and water, soil erosion is the most perplexing, common, well-distributed and complex problem mostly in humid and sub-humid mountain regions. It has been estimated that in India about 5334 million tonnes of soil is displaced annually either due to natural reasons or by unscientific human interventions (Bhattacharya *et al.*, 2007; Pandey *et al.*, 2007; Karthik *et al.*, 2017).

Basically, the process of soil erosion is defined as a combination of three actions, detachment or entrainment of the soil particles, transportation of detached soil particles and deposition of transported soil particles to new depositional area by the action of erosive agents like wind, water or gravity forces (SCSA, 1982).

Contemplating on the reasons of soil erosion, it is accounted that consequences of deforestation, removal of natural vegetation and overgrazing in the mountainous regions are the major contributors, which speed up the erosion process. The inherent tendency of a soil to get eroded is also one of the reasons of soil erosion, wherein this tendency of the soil is significantly influenced by the various soil characteristics such as rate of infiltration, permeability, structure, texture, organic matter content, total water holding capacity, etc (Belasri and Lakhouili, 2016).

Soil erosion is one of the most serious environmental troubles encountered nowadays as this phenomenon degrades soil fertility, water quality, soil productivity as well as it affects the biodiversity. Apart from this, it increases the natural level of sedimentation in the rivers and reservoirs, which in turn reduces their storage capacity as well as life span thereby increases the possibility of flood (Amore *et al.*, 2004; Pandey *et al.*, 2007; Bouaziz *et al.*, 2011, Anache *et al.*, 2017).

In several regions, unrestrained soil erosion and related land degradation have left vast areas economically unproductive. The risk assessment of soil erosion is very much essential, which helps to evaluate the magnitude, spatial extent and severity of the soil erosion, so that application of management and mitigation actions becomes feasible to protect the soil from further degradation. Soil erosion risk assessment in sub-watershed scale significantly supports the planning for soil conservation and management of the entire watershed.

Focusing on the agricultural development to ensure food and economic security in future, assessment of soil erosion particularly in agriculture field is very much essential. The transportation of topsoil from the cropland, the disruption of soil structure and the reduction in organic matter content and level of nutrients present in the soil causes the notable reduction of productive depth of soil and fertility (Prasannakumar *et al.*, 2011a).

Soil erosion is highly dependent on the rainfall, soil characteristics, topographical features, land use-land cover, human interventions and agricultural practices adopted in the field. In addition to these parameters financial, social and political components also influence the soil erosion. Analysis of the erosion rate under each factor will help to identify extent of effects contributed by each of these factors on erosion. Furthermore, its quantification helps to prioritize the watershed and identify the erosion prone areas which will in turn aid in implementing soil conservation measures for sustainable development (Biswas, 2012).

Conventional methods mainly carried out for prediction and assessment of soil erosion are field surveys, using runoff plots, multi slot devicer, Coshocton wheel sampler (Miller, 1926) and erosion pin method. These methods are time-consuming and expensive and need extensive data collection. Generation of results and thorough understanding of the erosion processes by incorporating all the complex interaction occurring among the various factors in a watershed through field studies is very difficult (AbdelRahman *et al.*, 2016). The accuracy of data is also not assured owing to the lack of exact information about the location from which soil gets eroded and chances of deposition of eroded soil particles in other locations before reaching the runoff plots or gauging station (Hudson, 1993). Hence, it is difficult to accept the soil loss output obtained through such methods while considering larger expenditures.

To overcome the limitations of the conventional methods, soil erosion models have been popularized. Major advantage of the erosion models is its capability to handle most of the complex interactions which greatly influences the rate of erosion. Many kinds of models like empirical model, semi empirical model, physical model, distributed model and process based models are used for the assessment of rate of erosion by simulating erosion processes occurring in the watershed (King and Delpont, 1993; Siakeu and Oguchi, 2000).

The input data or information required for a model is the main challenge in selecting the model since these models require variety of input data relating to soil, vegetation, climate and topography, drainage networks, morphology etc. The models are basically developed for specific set of conditions of particular area. The empirical models like Universal Soil Loss Equation (USLE) (Wischmeier and Smith, 1965; Balasubramani *et al.*, 2015), Modified Universal Soil Loss Equation (MUSLE) (Williams, 1975) and Revised Universal Soil Loss Equation (RUSLE: Knneth *et al.*, 1991; Kouli *et al.*, 2008) have been commonly applied to various scales and regions. Semi empirical models include Morgan, Morgan and Finney model (Morgan *et al.*, 1984), having strong physical base for the assessment of soil erosion. Furthermore,



several process-based or event-based models such as Water Erosion Prediction Project model (WEPP : Nearing, 1989; Renard *et al.*, 1996; Amore *et al.*, 2004; Atakora *et al.*, 2013), Agricultural-Non-Point-Source Pollution (AGNPS : Young *et al.*, 1989), European Soil Erosion Model (EUROSUM : Morgan *et al.*, 1998), Areal Nonpoint Source Watershed Environment Simulation model (ANWERS : Beasley and Huggins, 1981) and CREAMS model (Silburn and Loch, 1989) are also available for the prediction of soil erosion. Mostly empirical and semi empirical models carries an important role in estimation of the rate of soil loss and planning of soil conservation measures since most of the event/process based models are not well proved and need many input data (Suresh, 1993).

Soil characteristics, topographical features, land use patterns and rainfall distribution within a watershed vary spatially. Most of the erosion models estimate the spatial average of soil erosion which gives single average value representing the soil erosion rate occurring in the entire watershed. The idea on the extent and magnitude of the soil erosion and contribution of each parameter on the erosion rate at different points of the watershed will give thorough idea about what conservation measures have to be adopted and where and how to adopt it (Balasubramani *et al.*, 2015).

The combined use of remote sensing, GIS and erosion models have been proved to be efficient and appropriate for assessing the severity, temporal and spatial distribution of erosion (AbdelRahman *et al.*, 2016). With the introduction of remote sensing technology, collection and generation of spatial input data becomes easier and cost effective. Remote sensing technology provides accurate data related to land use, climate, topography and soil of various time periods and locations, which will be impossible to obtain through field survey as it requires great amount of time and incur high costs (Biswas, 2012).

GIS technology helps to derive slope factor from Digital Elevation Models (DEM) and cover management factor from satellite imageries (Barman *et al.*, 2013). Apart from this, GIS has the capability to interpolate the data such as rainfall for applying to the ungauged watershed using nearby gauged watershed data. The handling capability of geo-referenced data comprising spatial and non spatial information makes GIS more attractive. Remote sensing and GIS techniques used along with erosion models could help to generate visually pleasing and more informative input and output map layers, which makes the assessment more easier (Boggs *et al.*, 2001; Gelagay and Minale, 2016).

In the present study, RUSLE and Morgan, Morgan and Finney (MMF) models are employed within Geographic Information System (GIS) environment to analyse erosion risk of Kunthippuzha sub-watershed and to assess land capability in the watershed for soil conservation planning.

The specific objectives of the study are:

1. To identify the erosion prone areas in the watershed based on soil erosion models using remote sensing and GIS.
2. To analyse the effect of spatial and temporal variations in land use-land cover on soil erosion based on vegetation index.

# **REVIEW OF LITERATURE**

## CHAPTER II

### REVIEW OF LITERATURE

A review of the important studies related to soil erosion, various factors affecting erosion and assessment of soil erosion risk by adopting different methodologies are described in this chapter.

#### 2.1 SOIL EROSION

The term erosion is derived from the Latin word “erodere”, which is often used to designate all exogenic processes occurred at the earth surface which affects the earth relief (Zorn and Komac, 2011). According to the Soil Conservation Society of America, soil erosion is wearing away of the soil from the earth surface by the action of the erosive agents including water, wind, glaciers etc (SCSA, 1982). There are mainly two types of erosion, geologic erosion and accelerated erosion. Geologic erosion which occurs due to the action of natural agents, leads to wearing away of the soil mass and deposits it in new locations. The accelerated erosion which mainly happens due to agriculture and unscientific human interventions disturbs both soil and environment (Lal, 1990). Soil erosion can be described as the combination of the three major processes, which includes detachment, transportation and deposition (Huang *et al.*, 1999). The main significance of soil erosion processes is either on-site or off-site impact produced on the ecosystem (Bilotta *et al.*, 2012).

The newly deposited soil mass is more threatened and vulnerable to erosion because the bonds formed after the deposition of the soil mass on the new location may not be stronger than the original bond (Woo *et al.*, 1997). Hence it is very essential to identify the factors which cause erosion, which helps to adopt suitable soil erosion control measures in those areas.

## **2.2 FACTORS AFFECTING SOIL EROSION**

There are a number of factors which affect soil erosion considerably such as climatic factors, vegetation, soil type and topography. This section describes the effect of these factors on erosion.

### **2.2.1 Climate**

The climatic factors that influence soil erosion are rainfall, wind speed and atmospheric temperature.

#### **2.2.1.1 Rainfall**

Soil erosion rate varies considerably with intensity of rainfall, amount of rainfall, its duration and the size of rain droplets. Among these, intensity plays major role such that the high intense rainfall makes the erosion processes faster (Fraser *et al.*, 1999). Nearing *et al.* (2004) assessed the impacts of climate change on the rate of soil erosion by analysing previous studies associated with climate change and soil erosion. The study observed the changes in soil loss with the changes in rainfall amount and intensity, number of rainy days/year especially because increasing global temperature results in frequent and intense storms. The study showed that both amount and intensity of rainfall have direct influence on soil erosion, which is approximated as around 1.7% increase in erosion rate with each 1% increase in rainfall amount occurred in a year.

To identify the relationship between soil erosion and rainfall characteristics, so many field studies and laboratory studies (using rainfall simulators) have been conducted by different researchers. Ahmed *et al.* (2012) evaluated the effect of rainfall distribution on the soil erosion rate with the help of Guelph Rainfall Simulator II (GRSII), which was used to simulate the rainfall with different patterns and intensities. The study observed that the average soil loss rates for sandy soil and

loamy soil under different intensity of rainfall were notably higher than the soil loss rates for the same type of soil under constant rainfall intensity for the same duration.

Fang *et al.* (2012) analysed the variation of soil loss in accordance to the rainfall regimes. The study performed in a small hilly watershed of China. Three regimes were identified based on the amount and duration of rainfall viz. regime I (medium amount of rainfall with medium duration), regime II (high amount of rainfall with long duration) and regime III (less amount of rainfall with short duration). Higher soil loss was experienced during regime I (medium amount of rainfall with medium duration) and regime II (high amount of rainfall with long duration).

Mohamadi and Kavian (2015) conducted a study to evaluate the effects of pattern of the rainfall on soil erosion using 18 field plots and ANOVA (Analysis of Variance). Study was conducted during the rainy season for the year 2010-2011. Four types of storm patterns were considered for the study such as rainfall with increasing intensity, rainfall intensity increasing and then falling, rainfall with falling intensity and finally rainfall with falling and then increasing intensity. Analysis of the results showed that highest soil erosion occurred by rainfall events with increasing intensity.

#### **2.2.1.2 Wind**

In arid and semi-arid region, wind is the major erosive agent which declines the agricultural production. The extent of erosion caused by the wind depends on both wind characteristics (wind speed and direction) and soil characteristics (soil surface roughness and soil susceptibility). Zamani and Mahmoodabadi (2013) found the direct relationship between wind velocity and erosion rate through wind tunnel experiment.

Wind also produces some effects on the raindrop impact on the soil and incident angle of rain. Due to this, the energy of the particular rain event enhances and thereby ability of the rain to make the soil erosion increases. The sealing and compaction properties of the soil get affected by the wind velocity and its direction. In this case, surface roughness acts as a dominant factor in the incident angle (Helming, 2001).

### **2.2.1.3 Temperature**

Temperature is another climatic factor which influences soil erosion. Sudden thawing of the soil due to the warm rain can cause serious erosion whereas frozen soils are unsusceptible to erosion. Temperature also influences the organic matter concentration on the top soil layer. The thickness of the organic cover reduces with temperature. Organic layer protects the soil by covering it from the impact of falling rain and thereby protects the soil from erosion (Drift, 1995).

## **2.2.2 Topography**

The topographical factor which affects the soil erosion includes length, steepness and shape of the slope.

### **2.2.2.1 Length and Steepness**

Topographical factors contribute a major role in soil erosion especially in slopes. Two major characteristics of the slope, viz. length and steepness of the slope are to be taken into account while describing the effect of topography on soil erosion. Mainly in hilly areas, it is very much essential to identify how slope will affect the soil erosion. Steepness of the slope exerts high impacts on the soil erosion compared to other slope features. Sun *et al.* (2014) reported that cultivation in hilly terrain with steep slopes leads to serious erosion which results in the formation of rills and gullies on the Loess Plateau, north China.

Zhang *et al.* (2015) divided the Zuoma watershed into five slope gradient classes, 0-3, 3-7, 7-15, 15-25 and  $> 25^\circ$  for analysing the effect of slope on soil loss under different land uses. The soil erosion increased with increasing slope gradient irrespective of the land uses. Zhang *et al.* (2018) concluded based on the study conducted on the effect of topographic factors on soil loss in southwest China that, with increase in the gradient of slope soil loss on slopes showed an increasing-declining-increasing trend. Soil loss increased upto  $15^\circ$  and erosion rate increased nearly linearly with slope length. When both gradient and length of the slope increases, soil loss was directly related to rainfall amounts. Furthermore, soil loss showed a power function correlation with topographic factors.

#### **2.2.2.2 Slope Shape**

Apart from the slope length and steepness, shape of the slope also has considerable influence on the erosion potential. Convex, concave, planar and uniform slope are some peculiar shapes of the slope. Sensoy and Kara (2014) conducted a field experiment during 2007-2009 on a hillside field plot with different slope shapes and identified that the shape of slope also has a significant role on soil erosion. Uniform slope generates more soil erosion compared to other shapes, whereas concave shaped slope generates the least.

Gray (2016) also made an attempt through field observation as well as laboratory tests to find out the effect of the shape of slope on the erosion. The study ensured that concave slope is much better as it generates lesser sediments compared to planar or uniform slopes. The result was validated using conceptual model and computer modeling of soil erosion with Digital Terrain Model (DTM).

#### **2.2.3 Vegetation**

Vegetation plays an important role in retarding soil erosion, as it contributes to two important hydrologic processes such as evapotranspiration and interception, the



amount of water available for runoff reduces. Also, it increases the infiltration of water into the soil which eventually retards the erosion. Furthermore, the vegetal cover lowers the impact of rain drops hitting on the land surface, thereby reduces the erosion (Suresh, 1993).

Restoration of vegetation seems to be a better measure to reduce the wind as well as water erosion. Kosmas *et al.* (2000) proved that the restoration of the natural vegetation is very less in soils having smaller depth and erosion processes will be very active resulting in further desertification and deterioration of the land. When the erosion process continued up to the depth of about 10 cm or less, perennial vegetation is very difficult to support and which leads to further erosion.

Vegetation also acts as a hindrance to the flowing water thereby to the flow velocity, which in turn reduces the erosive ability of the runoff. Additional to the biomass cover on the surface, root system also provides vital contribution to prevent the soil loss. The rooting system of the plants, shrubs, herbs and grasses makes the soil more porous which enhances the infiltration of water in to the soil. In addition, water absorption by roots reduces the amount of water which causes soil erosion and runoff (Gyssels *et al.*, 2005). Soils with roots are more erosion resistant compared to soil without roots. Root diameter has the direct correlation with rate of soil erosion as it makes the soil more permeable (Khanal and Fox, 2016).

Fen-Li (2006) proved the effect of vegetation through the study conducted in the Loess Plateau. The dramatic decrement of soil erosion was observed in the area after the restoration of vegetation, where it was very severe problem before. Furthermore, accelerated erosion occurred through the destruction of vegetation played a fantastic role in land degradation and eco-environmental deterioration in deforested regions.

Plant cover maintains vital interrelationship with properties of the soil, which enhances the biodiversity even in the steep sloped areas those are highly susceptible

to erosion. Plant cover carries a pivotal role in soil erosion management and restoration of ecosystems. The improper removal of vegetal cover and the extreme cultivation practices in mountain areas severely affect the land conservation (Zuazo and Pleguezuelo, 2008).

Ouyang *et al.* (2018) proved the role of land use on mitigating soil erosion by identifying the impacts of land cover together with soil characteristics. Even though the variation happened on soil physical characteristics indicated that the rate of erosion should increase, due to the increment of forest and paddy fields, soil erosion get reduced  $187.7 \text{ t km}^{-2} \text{ a}^{-1}$  in 1979 to  $158.4 \text{ t km}^{-2} \text{ a}^{-1}$  in 2014.

#### 2.2.4 Soil

Soil also exerts greater influence on the soil erosion, which have erosion promoting and retarding ability. Major concerning soil factors include permeability of the soil, structure, texture etc. Soil with greater permeability will reduce the amount of water contributing soil erosion. Biological activities performing in the soil will make the soil more porous one, which will promote the downward movement of water. In erosion point of view, erodibility of the soil is very important, which is the property of the soil to get eroded. The erosion process detachment and transportation of soil particle is greatly depends on the soil characteristics mainly soil texture, where sandy soil is easier to detach, whereas it is difficult to transport to other location (Suresh, 1993). The surface roughness also influences soil erosion as smoother surface shows less soil loss compared to rough surface with the storms of same intensity (Romkens *et al.*, 2001).

Soil erosion rate is highly influenced by the texture of soil in correlation with rainfall characteristics, mainly intensity of the rainfall and its duration. Soil with high organic matter content will exert enough resistance to erosion, especially soil organic carbon as it increases the infiltrating capacity of the soil through reducing its bulk density (Franzluebbers, 2002). Considering kaolinitic, montmorillonitic and

nonphyllosilicate soils, kaolinitic soil exhibits lowest soil loss as it shows the lowest detachment and lowest runoff due to its high aggregate stability. Montmorillonitic soil experienced highest soil erosion (Wakindiki and Ben-Hur, 2002).

Vannoppen *et al.* (2017) showed how soil characteristics contribute in mitigating soil erosion along with root systems. The study revealed the negative correlation of rate of soil loss with soil cohesion and positive correlation with sand content. Fibrous roots in sandy soil showed remarkable effect in reducing soil erosion as the soil is less cohesive. Dry bulk density of the soil also exerts stronger effect on erosion decreasing ability of the plant roots as fibrous roots were more effective in soil with less dry bulk density.

Rate of erosion will vary with the variation of soil type. But the extent of variation is very much dependent on the intensity of the rainfall. Wu *et al.* (2018) examined effect of soil type along with rainfall intensity on sheet erosion process through the experiment conducted in different provinces of central south China. The selected soils were classified into Calcic Luvisol, Ferric Luvisol, Plinthic Alisol, Plinthic Acrisol and Acric Ferralsol and for each soil type, separate field plots were prepared. Lowest erosion was observed in Ferralsol soil and highest in Luvisol type.

### **2.2.5 Tillage Practices**

In agricultural lands, major factor promoting soil erosion is tillage practices. Commonly the term tillage erosion is used to describe the effect of tillage practices on erosion. The extent of tillage erosion depends on the degree of mechanical manipulation performing on the soil, more specifically on the extent to which soil is lifted or turned. Mostly conservation tillage practices perform as alternatives of tillage operation as it leads to excessive fertile soil losses (Gould *et al.*, 1989). For a hilly terrain, eroded soil due to tillage from upslope areas get deposited on the down slope. Tillage erosion greatly affects by the tilling depth, direction of tillage and the

speed of operation. Soil loss can be reduced by reducing the tilling depth and speed and the size of the tilling implements (Li *et al.*, 2008).

Wildemeersch *et al.* (2014) analysed soil erosion rate by considering tillage direction as parallel to the contour bund and up and down the slope. Soil erosion was less while tilling by alternating the direction i.e., tilling up and down the slope as soil movement get neutralized in this method. Downward and upward movement of soil is very important factor where to reduce the erosion; downward movement of soil should not be more than upward movement of soil. Contour tillage using *Arado Americano* does not make soil erosion as it moves less soil in downward direction in moderate slopes.

Mhazo *et al.* (2016) examined the impact of tillage practices on soil erosion based on 282 runoff plots through meta-analysis. Study compared the results during no tillage and conventional tillage practices. Results proved that the soil loss were higher with conventional tillage compared to no tillage. Rate of soil erosion were observed 60% lower under no tillage than conventional tillage. In soils with low clay content under temperate climates showed higher differences in soil losses between no tillage and conventional tillage. Wang *et al.* (2016) suggested performing any method among artificial digging, artificial hoeing or contour plow which will control runoff and sediment transport compared to conventional practices by improving the infiltration characteristics of the soil.

In steep sloped areas, relocation of soil through runoff is much easier if soil is redistributed by the tillage practices. Wang *et al.* (2016) conducted a study in Zhongxian, southwest China in 2014, to identify the impacts of tillage erosion on runoff in a hilly area. Tillage erosion leads to change characteristics of soil which adversely affect the soil-water-plant relationships, water quality and productivity of the soil. Water erosion increased with increasing tillage intensity. It deteriorates soil

structure by declining its rate of infiltration, water holding capacity and effective depth of soil.

Tillage intensifies the soil loss from farm land along with it reduces the soil organic carbon content in the soil (Zhao *et al.*, 2018). Conservation tillage practices like mulch tillage reduces soil erosion rate. According to the study conducted by the Auerswald *et al.* (2018), mulch tillage decreases the soil loss 1.5 times from those experienced by the conventional tillage practices. Ryken *et al.* (2018) conducted similar study in central Belgium. In addition to no tillage and conventional tillage practices, the study considered strip tillage also. Soil loss was less in case of strip till and no tillage compared to conventional tillage. Soil loss rate increased in all the three types of practices with wheel track compaction because of the increment in bulk density of the soil. Strip till practice is far better to reduce the sediment transport than no tillage which can be proved by the presence of land cover due to the more crop residues. Reduced tillage like strip till will increase the macro pores in the soil and thereby increases the hydraulic conductivity.

Wang *et al.* (2018) considered five tillage practices and studied the rate of soil erosion associated with each practices. The practices like straw mulch, manure, intercropping with peanut and orange, crop rotation with peanut and radish and conventional down slope furrows were selected. The soil detachment rate was as follows: conventional down slope furrows > crop rotation with peanut and radish > intercropping with peanut and orange > manure > straw mulch. The probability of effective reduction of soil erosion rate is more in case of no tillage compared to the conventional tillage and deep tillage. Prolonged conventional tillage may leads to the formation of hardpan in subsoil region (Bogunovic *et al.*, 2018).

### **2.3 METHODS FOR ESTIMATING SOIL EROSION**

Various methods can be adopted for assessing soil erosion ranging from conventional techniques comprising runoff plots, erosion pin methods, sampling etc.

to the estimation using soil erosion models assisted with emerging technologies like remote sensing, GIS and Artificial Neural Network (ANN) etc.

### **2.3.1 Conventional Methods for Estimating Soil Erosion**

This section includes critical reviews which give the description of various conventional methods, their advantages and disadvantages.

#### **2.3.1.1 Reconnaissance Method**

This is the most simple and less expensive method for estimation of soil erosion as it requires less skilled person and less maintenance. Erosion pin method is one among them. The wooden or metallic pin was driven into the soil, where upper portion of the pin will act as reference point and based on that erosion is possible to measure. Hardley and Lusby (1967) applied this method in western Colorado with plot size of 5 ha and pin spacing of 1.5 m. The obtained soil loss was compared with the sediment load estimated during the reservoir survey, which were 2.7 mm and 2.3 mm respectively. This method was also adopted in Tanakami mountain region, Japan, where pins were installed in the 3 plots having area of 100 m<sup>2</sup>. Experiment was prolonged for 10 years and pin height was noted at each month. The annual soil erosion rate was found to be 13 mm/y (Takei *et al.*, 1981).

#### **2.3.1.2 Runoff Plots**

Runoff plot method is the most commonly accepted soil loss measuring method in which it is laid on the predominant slope of the sample field plot where the rate of soil loss is going to measure. Land grading is necessary operation in the runoff plot method to obtain the required gradient uniformly all over the field. Runoff plots have all the problems and difficulties of agronomic trials in addition to the problems of collecting, catching and recording the soil and water. There are possibilities for faults and errors and runoff plots are costly, in terms of initial construction, maintenance and operation (Michael and Ojha, 1996). Furthermore, the chances of occurrence of

errors are more as it needs to catch and record the sediment and water come into the plot. Leakage around the boundaries of the plot also raises the error. Skilled operators and frequent investigations are necessary to reduce these errors (FAO, 1991). The soil erosion study was conducted in China using various sizes of plot varying from 60 m<sup>2</sup> to 1000 m<sup>2</sup> within the watershed having 2 ha area (Jinze, 1981) and concluded that plots which extended over the entire slope length of gully slopes were essential to evaluate erosion on a watershed scale.

#### **2.3.1.3 Soil Loss and Sediment Load**

Soil loss can be estimated from the sediment load comprising suspended load and bed load using various types of samplers and devices. But this method is not efficient as all the eroded materials from the watershed area need not be contributed to sediment. The estimation incorporates concentrated sediment in the streams and the rate of flow (Wade and Heady, 1978). Grab samplers like dip sampling techniques adopted in the South Africa to estimate the suspended load. Bottles were used for dip sampling. The result obtained was 25% lesser compared to other well proved methods (Rooseboom and Annandale, 1981).

#### **2.3.1.4 Multi Slot Divisor and Coshocton Wheel Sampler**

When the situations come in to encounter the large volume of soil loss and runoff, it is necessary to install large sized plot. In some situations, series of connected plots can be adopted. Coarser particles are allowed to settle in the first tank. The outflow from the tank is guided to the multi slot divisor containing numerous slots, out of which one slot is active at a time which allows passing known quantity of water to lower tank. The sediment samples are collected, dried and weighed to estimate the soil loss. Multi-slot divisors along with storage tanks were installed to estimate the sediment deposition from small plots in New South Wales, Australia. The designed system has better storage capacity. The capacity of sludge tank and storage tank was 0.3 cm and 10 cm respectively. The permissible flow rate

was  $0.009 \text{ m}^3 \text{ s}^{-1}$  (Ryan, 1981). Due to the limited capacity of such samplers, multi slot devisors are limited to small watersheds.

Coshocton wheel sampler is the arrangement used to estimate soil loss directly from field especially adopts for small watershed. The known quantity of discharge from the measuring flume falls over a water wheel having slight inclination from vertical. At each rotation of the wheel, the slot divides across the jet from the flume and considers a small fraction of the flow (Kinnell *et al.*, 1994).

Devaranavadagi and Bosu (2014) installed a multi-slot devisor on the cotton field of Perumbalur district, Tamil Nadu for the daily monitoring of soil erosion rate. Soil erosion under cotton crops grown on runoff plot was observed as  $10.86 \text{ t ha}^{-1} \text{ y}^{-1}$ .

### **2.3.2 Soil Erosion Estimation Models**

In general, soil erosion models are used to simulate the erosion process occurring in an area by considering number of complex interaction which is affecting the rate of soil loss. Number of soil erosion models has been developed by various scientists during the past 50 years, those include empirical models, semi empirical models and process based soil erosion models (Suresh, 1993). Description and previous studies related to empirical and semi empirical models are included in this chapter.

#### **2.3.2.1 Empirical Models**

These are the empirically derived models and are mainly statistical based. Such models are basically developed for particular region. This particular section includes critical reviews related to various empirical models such as USLE, RUSLE and MUSLE along with its applications.



### 2.3.2.1.1 *Universal Soil Loss Equation (USLE)*

USLE is the widely accepted empirical soil loss equation mainly developed for agricultural lands. This equation considered rainfall, soil, topographical and vegetation parameters in its design. According to this model,

$$A = R K L S C P \quad (2.1)$$

Where, A is the annual average soil loss in t/ha/y; R is the factor indicating erosivity of rainfall expressed in MJ mm ha<sup>-1</sup> h<sup>-1</sup> y<sup>-1</sup>. K is the factor related to soil erodibility, L is the slope length factor and S is the slope steepness factor. C is the cover management factor and P indicates the soil conservation practices factor (Wischmeier and Smith, 1978).

There are number of shortcomings in USLE model which limited its application in soil loss estimation. Major drawback associated with this is its empirical nature, so that it may not consider erosion process actually happens in the watershed. Furthermore, it is not considering the snowmelt and irrigation in R factor estimation. It measures annual average soil loss rather than the event based soil loss. This method does not compute the gully erosion and sediment transport (Williams *et al.*, 1972).

### 2.3.2.1.2 *Revised Universal Soil Loss Equation (RUSLE)*

The fundamental equation in the case of RUSLE model is same as that of the USLE model. Preparation of isoerodent map of the location and consideration of 1000s of gauge location to collect data for the computation of R factor differentiates this method from USLE. Seasonal K factor is considered in this method. The value of K factor ranges from 0.10 to 0.45 based on the textural composition of the soil. In RUSLE model, complex slopes can be easily represented by using a series of segments, which helps to estimate the topographic effect at its better way (Renard and Ferreira, 1993). The C factor in RUSLE model has significant importance as it

directly has the influences on the conservation of soil. In this method, C factor will vary from zero to 1.5 where the value zero can be adopted for well protected lands where as 1.5 is for the lands which produce more runoff. For the computation of RUSLE C factor, various sub factor values are accounted as follows:

$$C = PLU * CC * SC * SR \quad (2.2)$$

In which, PLU: sub factor related to prior crop canopy; CC: sub factor related to canopy of crops; SC: sub factor related to surface cover; and SR: sub factor related to surface roughness (Morgan, 2005).

### 2.3.2.1.3 Modified Universal Soil Loss Equation (MUSLE)

This model helps to estimate the sediment yield mainly based on the rainfall event and runoff characteristics. Williams and Berndt (1972) developed this storm based soil loss estimation model by analysing 778 rainfall events in a 15 watershed. According to the model, sediment yield for an individual rainfall event (Y, tones) can be expressed as  $Y = 11.8(Q * q_p)^{0.56} K L S C P$ , where Q is runoff volume in  $m^3$ ,  $q_p$  indicates rate of peak flow ( $m^3/s$ ) and K, L, S, C and P are the same factors those used in USLE.

Sadeghi and Mizuyama (2010) conducted a soil erosion assessment study using MUSLE model in Khanmirza watershed, Iran with an arial extent of  $395 \text{ km}^2$ . A total of six rainfall events were taken and hydrographs and sediment graphs were prepared to get flow discharge data and sediment flux data. The hydrographs and sediment graphs were prepared using limnigraph and one litre plastic bottle samplers respectively. The values of K, L, S, C, and P were allotted as 0.0462, 2.599, 2.875, 0.222 and  $0.706 \text{ Mg MJ}^{-1} \text{ mm}^{-1}$  respectively. The observed and estimated sediment yields was 7495.753 and 7791.957 tonnes and were calculated and analysed using statistical t test and regression analysis. The errors in estimation were found to be 18.56% which is considered in acceptable range as it is the modeling of natural

phenomena. The prior hydrological condition exists in the watershed, variation in rainfall distribution and unequal distribution of eroded sediment through entire watershed made difference in hydrological reactions of the area.

### **2.3.2.2 Semi Empirical Models**

There are semi empirical models also to estimate soil erosion rate, which are partly empirical and partly physical based. Morgan, Morgan and Finney (MMF), Revised Morgan, Morgan and Finney (RMMF) and Modified Morgan, Morgan and Finney (MMMMF) are some examples of the semi empirical models.

#### **2.3.2.2.1 Morgan, Morgan and Finney (MMF) Model**

It is the semi empirical model for estimating rate of soil loss. The MMF model separates the soil erosion process into a water phase and sediment phase. The water phase includes two predictive equations, one for the kinetic energy of the rainfall and another for the depth of overland flow. The sediment phase comprises two equations, one for the rate of splash detachment and one for the transport capacity of overland flow. In this method, the computed rate of detachment by raindrop and the transport capacity of overland flow are compared and lower of these two values is assigned as the annual rate of soil loss (Morgan, 2001).

## **2.4 RUSLE PARAMETERS**

The RUSLE model comprises five parameters as described in the section 2.3.2.1.2. The different attempts made by different researchers are given in this section.

### **2.4.1 R Factor**

It is the index of rainfall erosivity which quantifies the ability of rainfall to cause erosion in a field. It highlights the role of rainfall in the erosion processes.

Numerically, it can be calculated by multiplying the kinetic energy of rainfall (E) event with maximum 30 minute intensity ( $I_{30}$ ).

$$R = \sum (EI_{30}) \quad (2.3)$$

This factor clubs the rainfall characteristics like intensity, duration and rainfall amount (Wischmeier and Smith, 1978).

Arnoldus (1980) is brought a new index in erosivity factor computation called Fournier index (F) as it linearly related to R factor. From the experiments conducted using 40 Sicilian rain gauge data, F was identified as a best estimator of R.

$$F = \sum_{i=1}^{12} P_i^2 / P \quad (2.4)$$

Where,  $P_i$  is the monthly rainfall and P is the annual rainfall in mm. Erosivity factor can be calculated as  $R = mF + n$ , where m and n varies according to region (Ferro *et al.*, 1991).

Loureiro and Coutinho (2001) proposed a new model to compute the monthly R factor from the amount of precipitation in Algarve region of Portugal. The model was as follows:

$$R = (7.05 \times \text{rain}_{10} - 88.92 \times \text{days}_{10}) \quad (2.5)$$

Where,  $\text{rain}_{10}$  is the monthly rainfall amount for days  $\geq 10$  mm;  $\text{days}_{10}$  is the number of rainy days with rainfall  $\geq 10$  mm per month. In Cameron highlands region of Malaysia adopted this model to find out the R factor using 23 years (1991-2013) of monthly precipitation data (Sholagberu *et al.*, 2016).

Xie *et al.* (2002) conducted a study to develop a method for determining practical thresholds for erosive rainfall event. For the study, rainfall and runoff data were measured for a small watershed and three plots at the Yellow River basin in China for the years of 1961 to 1969. The thresholds corresponding to rainfall

amount, rainfall intensity and peak intensity were calculated using amount, average and peak intensity of rainfall respectively. The method chosen for the determination of threshold was  $EI_{30}$  method, in which the first step was calculating the  $EI_{30}$  values for only the storms where soil loss occurred. Then the second was used to find the cumulative  $EI_{30}$  values from the higher precipitation amount until it approached to the target  $EI_{30}$  of all erosive events. To find out the peak intensity thresholds, all rainfalls and corresponding soil losses were arranged in decreasing order of rainfall amount and finally cumulative percentage of soil erosion were obtained. To evaluate the efficiency of thresholds on estimation of rainfall erosivity, REI (Relative Error Indices) and MI (Mixing Indices) were proposed. The study concluded that more accurate way to fix the threshold is based on the peak intensity than average intensity as well as rainfall amount. Three thresholds such as 1.2 cm of precipitation amount, average intensity of rainfall 0.24 cm/h and 13.3 mm/h for the maximum 30-minutes rainfall intensity were fixed as erosive rainfall.

Petkovsek and Mikos (2004) estimated RUSLE R factor from daily rainfall data of the south-west Slovenia coming under the sub-Mediterranean climate. The addition of rainfall amount obtained within 24 h interval provided the daily precipitation amount ( $P_d$ ). The parameters such as maximum  $P_d$  ( $P_{max}$ ), sum of precipitation of days with more than 0.1 cm of rainfall ( $P_{10}$ ) and the number of days with more than 0.1 cm of rainfall ( $d_{10}$ ) were calculated for each month. Two statistical models were used to predict monthly R factor based on the multiple linear regression value. The goodness of fit was assessed with efficiency coefficient 'e'. For different average periods, the modelled and observed value was compared and assessed by means of the Root Mean Square Error (RMSE). The spatial as well as temporal analysis of rainfall erosivity is possible to calculate with the obtained daily precipitation data using statistical models.

Janecek *et al.* (2006) made an attempt to calculate R factor by collecting 40 years of rainfall data (1961 to 2000) from 13 rain gauge stations. Rainfall with 12.5

mm or more or else the intensity of 6 mm in 15 min were considered as the erosive storm events. Isoerodent maps from the selective rainfall events were prepared and statistical principles were applied to calculate the R factor. The average rainfall erosivity of 20 MJ/ha.cm/h was obtained. The calculated value were analysed using ombrographic records from other stations by considering two variants such as: variant I: for all storms rainfall >12.5 mm or intensity > 6 mm/15 min and variant II: for all storms rainfall less than 12.5 mm or intensity > 6.25 mm/15 min. Average R factor obtained according to variant I was 57.2 and those according to II was 45.6. The R factor obtained according to variant I is considered as more appropriate.

Elangovan and Seetharaman (2011) used above mentioned formula (equation 2.3) to generate erosivity factor from the precipitation depth data of Krishnagiri watershed region. Collected rainfall data for the period 2005-2009 from the four self recording type rain gauge station located within a watershed were adopted for the study. Erosivity factor were calculated as:

$$R \text{ (MJ mm ha}^{-1} \text{ h}^{-1} \text{ y}^{-1}) = \sum (0.29[1 - 0.72 \exp(-0.082 I)])_k * \Delta V_k * I_{30} \quad (2.6)$$

Where, I is the intensity of rainfall in mm/h and  $\Delta V_k$  is the amount of rainfall in  $k^{\text{th}}$  period. Using ArcGIS interpolation tool, spatial distribution of erosivity factor was done. The factor  $\sum (0.29[1 - 0.72 \exp(-0.082i)])_k * \Delta V_k$  in the above mentioned equation denotes the value of kinetic energy (E).

Rawat *et al.* (2013) applied same model incorporating rainfall intensity to find out the USLE R factor of small portion of the Nirjuli catchment. The study area basically comes under jhum cultivation with tropical climatic conditions. The kinetic energy of the rainfall calculated using the equation:

$$KE \text{ (MJ/ha/cm)} = 210 + 89 \log_{10} I \quad (2.7)$$

Where, I denote the intensity of rainfall in cm/h. The rainfall with 12.7 cm or more were considered for the study. The estimated R factor was 974.8 MJ cm ha<sup>-1</sup> h<sup>-1</sup>.

Tirkey *et al.* (2013) applied another model for Daltonganj catchment which was actually developed for the Damodar valley by Babu *et al.* (2004). Fifteen years of rainfall data were used to calculate the R factor. According to this model

$$R = 81.5 + 0.375 r \quad (340 \leq r \leq 3500 \text{ mm}) \quad (2.8)$$

Where,  $r$  is the annual rainfall in mm. The estimated value of erosivity factor was  $114.3 \text{ MJ mm ha}^{-1} \text{ h}^{-1}$ .

Nigussie *et al.* (2014) conducted a study to obtain daily, monthly, seasonal and annual rainfall erosivity factor (R) for the upper Blue Nile River basin in Ethiopia. Ten years of rainfall data were collected from eight automatic rain gauge stations in the basin from national meteorology agency of Ethiopia. For the computations of erosivity (R) factor, rainfall events with less than 12.5 mm amount were not included. The erosivity factor was then determined by the equation  $R=E \cdot I_{30}$ . A relationship between rainfall and erosivity is formulated by plotting erosivity indices (annual, seasonal, monthly and daily) against rainfall amounts using Microsoft Excel. The best curve of fit was obtained based on the highest coefficient of determination  $R^2$ . The model was validated using remaining two years rainfall data of each rain gauge station. The higher peaks of rainfall erosivity were obtained throughout the basin in the months of July and August. For the entire basin, the model efficiency of the monthly rainfall erosivity was 0.85. The rainfall erosivity models at the basin level carry a major role in planning and selecting effective soil conservation measures for the watershed management.

Antal *et al.* (2015) tried to compute of rainfall erosivity factor for the areas of Slovak Republic. The one minute rainfall data were available for the area in digital format so that analysis of data became much easier in Microsoft Excel environment. Rainfall data from five gauging stations were collected for various time periods. In this particular study, rainfall amount greater than 12.5 mm or rainfall having intensity  $24 \text{ mm/h}$  were considered as erosive events.

Panagos *et al.* (2015) calculated this E value to calculate the R factor for Europe using the equation 2.4. In this experiment, the rainfall data is collected from 28 countries of Europe, which include various data resolutions like 60 min, 30 min, 15 min, 10 min and 5 min. Finally all these data are aggregated to 30 min resolution data to ensure homogeneity in calculation. The erosivity factor was successfully represented in map form with resolution of 1 km x 1 km. The same formula suggested by the Panagos *et al.* (2015) is followed by the Ballabio *et al.* (2017) to assess the monthly R factor in Europe. Moreover, the assessment of monthly erosivity factor will help to identify the month along with area where experiencing high risk of soil erosion.

Rahaman *et al.* (2015) estimated annual average soil loss using RUSLE model in Kallar watershed, Tamil Nadu. The particular watershed has the area of about 1281.2 km<sup>2</sup>. For the calculation of R factor, 30 years of monthly rainfall data (1980 to 2010) were collected from Indian meteorological department. The rainfall erosivity value was calculated using the formula modified by Arnoldus (1980):

$$R = \sum_{i=1}^{12} 17.35 \times (1.5 \log_{10} (P_i^2 / P) - 0.08188) \quad (2.9)$$

Where rainfall erosivity factor, R is expressed in the unit MJ mm ha<sup>-1</sup> h<sup>-1</sup> y<sup>-1</sup>, annual rainfall, P as well as monthly rainfall, P<sub>i</sub> is in mm. The annual average erosivity value for the particular watershed was found in the range of 251.5 to 798.5 MJ mm ha<sup>-1</sup> h<sup>-1</sup> y<sup>-1</sup>.

Calibration of the methods for estimating erosivity for time scales ranging from daily to average annual can be performed based on symmetric mean absolute percentage errors and Nash-Sutcliffe model efficiency coefficients (Yin *et al.*, 2015).



**Table 2.1 Estimation of R factor from rainfall amount by different authors**

Authors	R factor equation	Applied by	Description
Roose (1975)	Developed for west Africa. $R = 0.5 P, 0.6 P, 0.2-0.3 P$ and $0.1 P$ for general cases, coastal areas, tropical hilly region, Mediterranean region respectively.	Adediji <i>et al.</i> (2010)	Katsina region, Nigeria. Tropical climate Rainfall 1100 mm
Moore (1979)	$R = 47.5 + 0.38 P$	Lufafa <i>et al.</i> (2003)	Catchment of lake Victoria
Arnoldus (1980)	$R = \sum_{i=1}^{12} 17.35 \times (1.5^* \log_{10} (P_i^2 / P) - 0.08188)$	Jain <i>et al.</i> (2001)	Doon valley, uttar Pradesh 52 km <sup>2</sup> area
	”	Prasannakumar <i>et al.</i> (2011a)	Siruvani river basin, Kerala Rainfall-1061 mm Tropical climate
	”	Prasannakumar <i>et al.</i> (2012)	Pamba river basin, Kerala Highlands rainfall- 3046mm
	”	Kumar <i>et al.</i> (2014)	Kothagiri taluk Temperate climate Rainfall - 3046 mm
Hurni (1985)	$R = -8.12 + 0.562 P$ Developed for Ethiopia	Gelagay and Minale (2016)	Koga watershed, Ethiopia
Renard and Freimund (1994)	$R = 0.264 F^{1.5}$ Developed for Morocco	Kouli <i>et al.</i> (2008)	Crete, Greece Rainfall - 900 mm Semi arid region
Ferro <i>et al.</i> (1999)	$R = 0.6120 F^{1.56}$ Developed for Sicily Italy	Alexakis <i>et al.</i> (2013)	Yialias of Cyprus region

Okorafor *et al.* (2017) conducted a study to obtain the R factor for Imo state of Nigeria. Around 31 years of monthly rainfall data (1980-2010) were collected from the Nigerian Metrological Agency (NIMET) and data having the mean of 199.2 and standard deviation 144.8 MJ.mm/ha/h. The erosivity factor was calculated using the equation 2.3. where kinetic energy of rainfall events was calculated using the equation  $E=210.3+87\log_{10} I$ , in which I is rainfall intensity (cm/hr). Intensity of rainfall is normally calculated from the amount of rainfall and its duration. Rainfall erosivity map was prepared using ArcGIS 10.2. The study obtained highest erosivity of 6033.4 MJ.mm/ha/h.

Vijith *et al.* (2017) applied same model in Sarawak region of Malaysia. The area was found to receive about 350-460 cm of annual rainfall. R factor was computed for the year 2014 by collecting monthly rainfall data from the department of irrigation and drainage. Inter month change in precipitation led to select this model. R factor found to be in the range of 2353 to 5380 MJ.mm/ha/h/y.

There are so many well calibrated models existing to calculate the rainfall erosivity factor from the rainfall amount rather than rainfall intensity. Such models are very much suitable and recommended for the watersheds where the intensity of the rainfall data is not available. Most of the studies adopted monthly and annual precipitation data to find out RUSLE R factor due to the lack of rainfall intensity data. Roose (1975) proposed a new erosivity model to compute R factor from mean annual precipitation. This model can be adopted in the regions where hourly, daily and monthly precipitation data are not available. Half of the rainfall amount numerically considered as erosivity in this approach. Vemu and Pinnamaneni (2011) applied this model in Indravati Catchment, Orissa. The observed erosivity factor was 602 MJ.mm.ha<sup>-1</sup> h<sup>-1</sup> with standard deviation of 25 MJ.mm.ha<sup>-1</sup> h<sup>-1</sup>.

### 2.4.2 K Factor

This factor measures the susceptibility of soil to get erode. It clubs various soil properties like soil structure, texture, organic matter content, permeability of the soil etc. The value of K factor numerically ranges from 0 to 1. The soil with zero k value denotes the toughness to get erode whereas it is very easy to erode in the case of soils with K=1. Wischmeier *et al.* (1971) developed a relationship connecting soil texture, soil structure, percentage organic matter content and permeability which is given below:

$$K = [[2.1 \cdot 10^{-4} (12-M) [(Si+vfS) (100-C)]^{1.14} + 3.25 (A-2) + 2.5 (P-3)]/759] \dots (2.10)$$

In which, M is the percentage organic matter content of the soil, Si indicates the percentage composition of the silt, vfS denotes the percentage composition of very fine sand, C denotes the percentage composition of clay, A indicates value corresponding to structural classes and P indicates the value corresponding to the permeability classes. The A value varies as follows: 1 for very fine granular; 2 for fine granular; 3 for medium or coarse granular and 4 for blocky, platy or massive structure. Variation of P value is as follows: 1 for rapid; 2 for moderate to rapid; 3 for moderate; 4 for slow to moderate; 5 for slow and 6 for very slow permeability rate. The nomograph for USLE K factor determination is available, which is basically derived from this formula, considered as one of the most rapid method to calculate the soil erodibility (Wischmeier and smith, 1978). Karydas *et al.* (2013) prepared K factor map using the field data (textural composition, organic matter content, permeability and structure of the soil) and USDA nomograph. The result was spatially compared with geologic map of the study area. Imani *et al.* (2014) determined and mapped the K factor in Yamchi watershed of Iran having an areal extent of 562.7 km<sup>2</sup> using the equation 2.9. The 38 soil samples were collected from the plot from a depth of 0 to 15 cm. The observed K factor was varied from 0.3 to 0.8 t ha h ha<sup>-1</sup>MJ<sup>-1</sup> mm<sup>-1</sup>.

Renard *et al.* (1997) developed formulae to estimate the K which was found out from global data of measured K values. The equation was as follows:

$$K = 0.0034 + 0.0405 * \exp (-0.5 (\log D_g + 1.659)^2 / 0.7101) \quad (2.11)$$

$$\text{Where, } D_g = \exp \sum f_i \ln [ (d_i - d_{i-1}) / 2 ] \quad (2.12)$$

Where  $D_g$  is the geometric mean particle size for each particle size class (clay, silt, sand),  $d_i$  is the maximum diameter (mm),  $d_{i-1}$  is the minimum diameter and  $f_i$  is the corresponding mass fraction (Kouli, 2008).

Schwab *et al.* (1981) summarised K factor values according to textural classes and percentage organic matter content as given in Table 2.2. The Parveen and Kumar (2012) followed Table 2.2 for the study conducted in the south Koel basin, India.

**Table 2.2 Variation of K factor with respect to texture and organic matter content**

Textural class \ OM (%)	OM (%)		
	0.5	2.0	4.0
Fine sand	0.16	0.14	0.10
Very fine sand	0.42	0.36	0.28
Loamy sand	0.12	0.10	0.08
Loamy very fine sand	0.44	0.38	0.30
Sandy loam	0.27	0.24	0.19
Very fine sandy loam	0.47	0.41	0.33
Silt loam	0.48	0.42	0.33
Clay loam	0.28	0.25	0.21
Silt clay loam	0.37	0.32	0.26
Silty clay	0.25	0.23	0.19

\* OM: Organic matter content

Alexakis *et al.* (2013) estimated K values for the textural groups as 0.07, 0.13, and 0.26 t ha h ha<sup>-1</sup> MJ<sup>-1</sup> mm<sup>-1</sup> respectively for coarse sandy loam, sandy loam and silty clay.

### 2.4.3 LS Factor (Topographical Factor)

LS factor is the collective representation of the slope length and slope steepness factor. Soil erosion rate varies exponentially with slope length, where exponent is varying from 0.1 to 0.9 (Zingg, 1940). Steepness of the slope also directly influences the soil erosion rate. Conventionally, slope gradient measures in field using inclinometers, abney level etc. The implication of LS factor in RUSLE is such that the ratio of soil loss experiences under given slope length and steepness to that from the slope length of 72.6 feet and steepness of 9%. Smith and Wischmeier (1957) proposed a formula to calculate the topographical factor by connecting slope length (L, ft) and land slope (S, %) as follows:

$$LS = L^{0.5} / 100 (0.76 + 0.53 S + 0.076 S^2) \quad (2.13)$$

The slope length and steepness data can be getting from the Digital Elevation Model (DEM) of the study location. Shiono *et al.* (2002) prepared a DEM with 2 m resolution in ERDAS IMAGINE software. CalcLS tool was used to get slope length and steepness values. The topographical factor was found to be in the range between 0.03 and 13.50 in Kanto area of Japan.

Wischmeier and Smith (1978) were proposed an equation to estimate the slope steepness factor as given in the equation 2.13.

$$S = (65.41 \times \sin 2\theta) + (4.56 \times \sin\theta) + 0.065 \quad (2.14)$$

Where,  $\theta$  represents slope angle in degrees. The RUSLE model usually applies on the field having slope greater than 9% as the erosion occurs faster on steeper slopes. McCool (1987) proposed another equation for calculating L and S factor as follows:

$$S = 10.8 \times \sin \theta + 0.03 \text{ for slope } < 9\% \quad (2.15)$$

$$S = 16.8 \times \sin \theta - 0.50 \text{ for slope } \geq 9\% \quad (2.16)$$

Where,  $\theta$  represents slope angle in degrees.

$$L = (l / 22.13)^m \quad (2.17)$$

Where, 'l' is the slope length; exponent  $m = 0.5$  where  $\theta \geq 9\%$

$$m = 0.4; 9 > \theta \geq 3\%; m = 0.3; 3 > \theta \geq 1\%; m = 0.2; 1 > \theta$$

The SRTM and ASTER digital elevation model can be use to derive slope value (AbdelRahman *et al.*, 2016). The LS factor can be calculated with the help of ArcGIS spatial analyst and ArcHydro tools.

$$LS = ((\text{Flow Accumulation} * \text{Cell size})/22.13)^m \times (\sin \text{slope}/0.0896)^{1.3} \quad (2.18)$$

Where, slopes in degree were considered. The exponent  $m$  for the equation 2.18 was derived by the Wischmeier and Smith (1978) based on the slope steepness as follows; 0.5 for slopes  $> 4.5\%$ , 0.4 for 3-4.5% slopes, 0.3 for 1-3%, and 0.2 for slopes  $< 1\%$ . Alexakis *et al.* (2013) classified range of slopes into 4 major classes as given in Table 2.3.

**Table 2.3 Slope classification (Alexakis *et al.*, 2013)**

Sl. No	Slope range (%)	Slope type
1	<5	Very gentle
2	5-15	Gentle
3	15-30	Steep
4	>30	Very steep

#### 2.4.4 C Factor

It is numerically same as the ratio of soil loss from a field of cultivating with specified crop to that from the continuous fallow land, considering that type of soil, topography and rainfall features are identical throughout the field. From planting to the harvesting, the value of C factor will vary considerably. The variation of the C factor is ranging from 0.003 (excellent vegetative cover condition) to 1 (continuous fallow land), which is mainly based on the density of the crop especially the extent of canopy. USDA (1972) suggested some values as C factor corresponding to each land use types as given in Table 2.4.

**Table 2.4. C factor and land use**

<b>Land Use Class</b>	<b>C values</b>
Settlement	1.000
Vacant land	1.000
Brick kilns	1.000
Crop land	0.280
Fallow land	1.000
Plantations	0.280
Dense forest	0.004
Open forest	0.008
Degraded forest	0.008
Land with scrub	0.700
Land without scrub	0.180
Marshy	0.000
Water bodies	0.000

The C factor can be easily obtained from the Normalized Difference Vegetation Indices (NDVI) values. NDVI basically denotes the density of plant cover and at some extent its growth condition too. NDVI values can be easily obtained from the multispectral remote sensing images using the equation 2.19:

$$\text{NDVI} = (\text{NIR band} - \text{RED band}) / (\text{NIR band} + \text{RED band}) \quad (2.19)$$

The value of this index will confine in between -1 and 1. Where highest values of NDVI were possessed by the vegetation where as bare soil, water and urban area carries lowest based on the spectral reflectance (Jensen, 2005). The calculation of C factor from NDVI is as given in equation 2.20 (Kouli *et al.*, 2008):

$$C = \text{EXP} (-2\text{NDVI} / (1 - \text{NDVI})) \quad (2.20)$$

According to this equation 2.20, C factor can possess the values from zero to more than 1. C factor of the Pamba river basin for the year 2008 was calculated by Prasannakumar *et al.* (2012) was found to be in the range of 0.3 to 1.5 which were derived from remote sensing dataset and NDVI method.

Parveen and Kumar (2012) derived C factor for a basin in Jharkhand from NDVI map obtained after the image analysis of the landsat image. The obtained C factor was in the range of 0.06 to 1 as it varies depending on the different land use pattern. The C values were ranged between 0.05 and 0.2 for forest areas, 1 for waterbodies and 0.3-0.6 for agricultural areas. The maximum value of C factor in the watershed area of Yialias of Cyprus was 2.7 (Alexakis *et al.*, 2013).

#### **2.4.5 P Factor**

It is also called support practice factor. P factor is calculated by finding the ratio of loss of soil under a given conservation practices to that from up and down the slope. Number of conservation practices is adopted depending on the slope of the field. Contour cropping, terracing, bunding, mulching and strip cropping are some examples of the commonly used conservation practices in the agricultural lands. The value of P factor varies from zero to one (Wischmeier and Smith, 1978) as given in table 2.5, varies according to the land slope. Rao (1981) assigned 0.28 and 1 for paddy fields and field other than paddy respectively. The lands with no conservation practices carry higher P values as 1 (Shiono *et al.*, 2002).



Singh (1994) suggested P factor for different percentage ranges of land slope as 0.6, 0.5, 0.5, 0.6, 0.7, 0.8 and 0.9 respectively for the slopes 1-3, 3-6, 6-9, 9-13, 13-17, 17-21 and 21-25. Biswas (2012) applied this method in Upper Kangsabati catchment. To ignore this factor in soil erosion estimation, Kouli *et al.* (2008) assigned P factor as one throughout the watershed of Crete.

**Table 2.5. P factor values (Wischmeier and Smith, 1978)**

Land use	Land slope, %	P factor
Agriculture	0-5	0.10
	5-10	0.12
	10-20	0.14
	20-30	0.19
	30-50	0.25
	50-100	0.33
	>100	0.35
All other land use		1.00

Alexakis *et al.* (2013) prepared land use map from the two GeoEye-1 satellite images for the preparation of P factor map. The value of one was assigned for the areas with no support practices. On the other hand the terrace areas which are considered to be less prone to erosion were assigned a value as 0.55.

## 2.5 RUSLE MODEL STUDIES IN GIS ENVIRONMENT

Shiono *et al.* (2002) estimated soil loss and its spatial distribution under the current cropping conditions in a pilot study area of about 3,009 ha comprising 11, 544 crop fields in Japan using RUSLE model combined with GIS. The average soil loss rate of the year 1994-1999 was estimated as 10.5 t/ha/y. The K factor of the USLE was estimated from the sedimentation survey conducted in the small catchment area. The LS factor was derived from the field information and digital elevation model (DEM) constructed using ERDAS. The study suggested that estimation of soil

erosion rate using RUSLE incorporating with GIS was very much useful for soil conservation planning.

Srinivas *et al.* (2002) conducted a soil erosion study in Nagpur district, Maharashtra by employing RUSLE in GIS environment to prioritise the study area for soil conservation and for delineation of suitable conservation units. Isoerodent map, topographic factor map, land cover-land use map were prepared separately and delineation of nine conservation units was done by adopting multi-criteria overlay analysis. The average soil loss was estimated as 23.1 and 15.5 t/ha/y under potential and actual conditions respectively. The C factor values for natural vegetation were calculated from USLE lookup table for different cover types. The P factor for main conservation practices were computed from the slope and crop cover.

Pandey *et al.* (2007) identified critical erosion prone areas in the Karso watershed Hazaribagh, Jharkhand state for an areal extent of 27.93 km<sup>2</sup> using USLE and GIS tools. ERDAS IMAGINE 8.4 image processing software was used to generate and manipulate spatially organized disparate data for sediment yield modeling. The study area were divided into 200×200 grid cells and average annual sediment yields were estimated for each grid cell of the watershed to identify the critical erosion prone areas for prioritization purpose. Sediment yields was estimated by the model as well as from the data collected from the stream gauging station located at the outlet of the watershed and the results obtained were thus compared. Finally, the RUSLE model was validated. The average annual soil erosion for Karso watershed was estimated about 3.66 t ha<sup>-1</sup>. The study concluded that the remote sensing and GIS could play significant role in generation of parameters from remote areas of watersheds/river basins for sediment yield modeling and watershed management.

Zhou *et al.* (2008) conducted a study to find out the effect of vegetation cover on soil erosion in an area located in the Upper Min River (UMR) watershed. The soil

erosion rate was evaluated by RUSLE method on a pixel-by-pixel basis. Raster map of R factor was produced by using a multivariate geostatistic cokriging model. Vegetation cover was estimated using k-NN technique by integrating Landsat ETM+ scenes and field data with optimal parameters. Optimal parameters were determined by evaluating the root mean square errors and significance of biases at the pixel. The accuracy of vegetation cover was predicted by a regression function using Landsat ETM+ bands, field measurements as well as those predicted by the Normalized Difference Vegetation Index (NDVI).

Sharma (2010) integrated terrain and vegetation indices and identified potential soil erosion risk area of Maithon reservoir catchment during 1988 to 2004. By using three terrain indices namely Topographic Wetness Index (TWI), Stream Power Index (SPI) and vegetation index like Normalized Difference Vegetation Index (NDVI) categorize the study area into four soil erosion potential classes. Finally the derived erosion potential map was validated by using RUSLE model which showed a good agreement with the results. Results found that there was a considerable change in the erosion potential of the watershed and a gradual changing of lower erosion potential class to next higher erosion potential class over the study period.

Vemu and Pinnamaneni (2011) made a quantitative assessment of soil loss using USLE for Indravati catchment. All the thematic layers of R, K, LS, C and P are prepared, analysed and finally generated an erosion risk map on 200m x 200m pixel size to find out spatial distribution of soil loss within the GIS environment. Twenty year average rainfall data was used to estimate the annual average soil erosion rate. Yearly soil loss (t/ha/y) was calculated by means of yearly R factor and keeping the remaining factors as constant. Prioritization of all 424 sub-watersheds in the Indravathi basin was done according to the intensity of soil loss for soil conservation purpose. Predicted average erosion rate by the study was 18 t/ha/y and sediment yield at the outlet of the catchment was 22.3 Million tons per annum. The predicted values were verified with the observed data.

Prasannakumar *et al.* (2012) estimated the soil erosion risk within a small mountainous sub-watershed in Pamba river basin using geographic information system and RUSLE model. The climatic and terrain factors which are used in the soil loss equation were calculated from rainfall data collected from Indian Meteorological Department (IMD), soil texture map of soil survey organization, Kerala, satellite image and Survey of India (SOI) toposheets. Vegetation parameters in the area were assessed from IRS-P6 LISS-III digital data of the year 2008 with resolution of 23.5 m. Rainfall erosivity factor were calculated by using the equation 2.8. The average soil erosion rate estimated for the study area ranges from 0 to  $17.73 \text{ t h}^{-1} \text{ y}^{-1}$ . The estimated average annual soil loss of Pamba sub-watershed was grouped into different classes and spatial distribution of each class was presented. From the spatial patterns, it was found that the severe and high levels of soil erosion risk zones are distributed on the grassland, deciduous forest areas and degraded plantation. From the study it was concluded that the areas with high LS-factor and degraded/deciduous forest/grasslands need immediate attention to conserve the soil.

AbdelRahman *et al.* (2016) estimated the soil fertility status in physically degraded land using GIS and remote sensing techniques in Chamarajanagar district, Karnataka, India. He made use of satellite data for qualitative assessment of soil eroded areas and found that the data enabled better delineation of eroded areas. By the visual interpretation of IRS data along with field survey method, soil erosion was found in the tone of none or slight to very severe where by the RUSLE method it was moderate to high. He also found that the compaction reduces water infiltration capacity of the soil and thereby increases the erosion. According to this study, Soil loss increases as slope increases up to 50% and after that soil erosion tends to decrease due to the presence of dense vegetation. Average soil loss dramatically decreases with the increase in vegetation cover. Current soil erosion status was mapped based on soil, slope and land use-land cover of the area. Incorporating

different types of the factors affecting land erosion, it was found that the majority of the study area falls under the moderate erosion classes.

Ganasri and Ramesh (2016) made an assessment of soil erosion by RUSLE model using remote sensing and GIS in Nethravathi River Basin. The estimated rainfall erosivity, soil erodibility, topographic and crop management factors were ranged from 2948.16 to 4711.4 MJ/mm ha<sup>-1</sup> h<sup>-1</sup>/y, 0.10 to 0.44 t ha<sup>-1</sup>MJ<sup>-1</sup>mm<sup>-1</sup>, 0 to 92, and 0 to 0.63 respectively. The study concluded that the empirical soil erosion models are relatively simple and easy to interpret physically, require minimal resources and can be worked out with readily available inputs. They found that the annual average soil loss estimated using RUSLE model is about 473,339 t/y in the Nethravathi Basin. By analysing the impact of increase in agricultural area on soil erosion, they concluded that as the agricultural area increases, erosion risk also increases due the agricultural practices. By implementing Weighted Index Overlay (WIO) method, they classified the area into different zones based on probability of soil erosion which ultimately helpful to derive suitable protection measures.

Hao *et al.* (2017) applied the empirical and contemporary model of RUSLE for simulating the soil erosion rate in a Karst catchment using remote sensing and GIS. Each RUSLE factor was calculated under the GIS environment. The potential soil erosion map was prepared to identify areas under severe soil erosion problem. The erosion rate was reclassified into 6 classes such as minimal, low, medium, high, very high and extremely high. The estimated erosion rate was 30.24 Mg ha<sup>-1</sup> y<sup>-1</sup> from the 1980s to 2000s, which was in good agreement with the result obtained through the in situ measurement from 1980 to 2009.

Ostovari *et al.* (2017) made an attempt to estimate the soil erosion in Semikan watershed, Iran. The study was mainly focused to investigate the effect of K factor on soil erosion. The model was run using ArcGIS 9.3. The K factor was calculated in two ways, one was using erosion plot and other by USLE method. The results

showed that the average measured K factor were two times lower than the estimated K by USLE K-factor. The annual average of soil loss estimated by the RUSLE model was  $5.70 \text{ t h}^{-1} \text{ y}^{-1}$  and comparable with measured soil loss, but it was two times greater than the measured K values. Spatial distribution of soil erosion was done of which most of the areas came under very low category (73.6%).

Singh and Panda (2017) investigated spatial distribution of soil erosion in Kapgari watershed, India. The watershed boundary was delineated using survey of India toposheets and DEM. The RUSLE model was run in GIS environment. The estimated R, K and LS factor was  $6117.8 \text{ MJ mm h}^{-1} \text{ ha}^{-1} \text{ y}^{-1}$ ,  $0.0256 \text{ Mg h MJ}^{-1} \text{ mm}^{-1}$  and 0.643 respectively. Land use classification was done and P and C values were assigned based on the land use category. The accuracy of the classification was analysed on the basis of kappa coefficient. The areal distribution of each erosion classes such as slight, moderate, high, very high and severe were 82.63%, 6.87%, 5.96%, 3.3% and 1.24% respectively.

Thomas *et al.* (2017a) predicted soil erosion rate in Muthirappuzha river basin, one of the tropical mountainous river basins, using RUSLE model along with a function called Transport Limited Sediment Delivery (TLSD). ArcGIS was used to formulate input map layers. R factor were estimated considering the Fournier index value and interpolated throughout the watershed. Sixteen soil samples with two replications for each sample were collected and used for the computation of K factor. ArcHydro tool in ArcGIS was used for the computation of LS factor. NDVI value was derived from the LISS III images and C factor map was generated for the watershed. The value 1 was assigned as P value for forest and open scrub. TLSD value was calculated from DEM using terrain analysis function in ArcGIS. Mean gross soil loss in the study location was  $14.36 \text{ t ha}^{-1} \text{ y}^{-1}$  of which 25% was found as the net soil erosion rate. Based on the net soil erosion values, erosion was reclassified into 6 classes ranging from slight to very severe. Among all the factors

influencing soil erosion, the LS and C factor were found as the most influencing factors.

Thomas *et al.* (2017b) estimated soil erosion rate on Pambar river basin having the areal extend of 289 km<sup>2</sup> by integrating RUSLE and TLSD function with GIS software. The RUSLE R factor was computed from the Fournier index considering the monthly rainfall data collected from the meteorological stations located in the river basin. K factor was calculated from the field sample using the method formulated by the Wischmeier and Smith (1978). DEM for the study area was generated from the topographic map obtained from the SOI. Land use-Land cover (LULC) map was prepared for the computation of P and C factor from the LISS III image with ground truth verification. The estimated mean gross and net erosion rate was 11.7 t/ha/y and 2.9 t/ha/y respectively.

Zare *et al.* (2017) predicted the impacts of land use changes on soil erosion in Kasilian watershed of Iran by the year 2030 by examining the patterns in the years 1981 to 2011. The RUSLE model integrated with GIS was adopted to estimate the soil erosion. Land use map was prepared from the satellite imageries through maximum likelihood classification and calibrated by running the Markov chain model using IDRISI Kilimanjaro software. The results showed that the mean erosion potential will increase 45% from the estimated 104.52 t ha<sup>-1</sup> y<sup>-1</sup> by the year 2030. Moreover, the results indicate that land use change from forest area. The land use change from the forest to the urban area as well as to the settlement found as the key factor influencing the erosion.

Kayet *et al.* (2018) estimated soil erosion rate in Kiruburu and Meghahatuburu mining areas, Jharkhand by adopting RUSLE model. The model was run in GIS environment and remote sensing data were used for the study. Landsat image of the year 2015 and CARTOSAT DEM of the year 2014 were used for the generation of LULC map and LS factor respectively. Rainfall data were collected from the Indian meteorological department. Data verification was done by using field images and

DGPS survey data. Support vector machine algorithm was used for the classification of the C factor. Karl Pearson coefficient of correlation was used to determine the correlation of soil erosion with slope as well as altitude, found to be 0.998 in both the cases. The estimated soil erosion in the area was 40 t/ha.

Teng *et al.* (2018) made an assessment and prediction of soil loss rate in the Tibetan Plateau using RUSLE and CMIP model. Soil erosion for the years 2002 to 2016 were estimated by RUSLE model integrated with ArcGIS. R factor was calculated from the daily rainfall data obtained from the rain gauge stations and TRMM data. To couple these to rainfall data collocated cokriging option was used. K factor was calculated by adopting epic model which mainly considers soil organic carbon content and texture of the soil. The prediction of soil erosion in 2050 was done using multi linear regression model and CMIP model. The estimated rate of erosion was 2.76 t/ha.

Zerihun *et al.* (2018) made soil erosion assessment in the Dembecha district, Ethiopia. The study was done in GIS environment by integrating RUSLE model. Rainfall data were collected from the 8 rain gauge stations located in the study area and interpolated throughout the watershed in ArcGIS. K factor values were assigned for different types of soil types such as 0.25 for Alisols, 0.15 for vertisols and 0.3 for fluvisols. LS factor was derived from the digital elevation model with 30 m resolution. Based on the quantitative assessment of soil erosion, erosion severity classes were prepared. The mean annual rate of soil erosion was  $49 \text{ t ha}^{-1} \text{ yr}^{-1}$ . The consistency of the model was proved by the double mass curve plotted using rainfall data.

## **2.6 MMF MODEL STUDIES IN GIS ENVIRONMENT**

Shrestha (1997) assessed soil erosion in the middle mountain region of Nepal by adopting MMF erosion model and made an attempt to evaluate the applicability of an erosion model in mountainous terrain. The study analysed the effect of land use,



slope exposition and terrace farming on soil erosion. The model was run in the ILWIS and a raster based GIS software package. Rainfall data were processed by using the spreadsheet software package called Quatro-Pro. Soil data were calculated from the soil sample collected from the study area by conducting laboratory test. The study found that annual soil loss rates are the highest (up to 56 t/ha/y) in the areas with rainfed cultivation, which is directly related to the sloping nature of the terraces. The lowest soil losses (< 1 t/ha/y) were recorded under dense forest. In the degraded forest, the soil loss was in the range of 1 to 9 t/ha/y and in the grazing lands it was estimated at 8 t/ha/y.

Jain *et al.* (2001) compared USLE model and MMF model through a study conducted in Sitlarao, a Himalayan watershed. The estimated soil erosion by MMF model was found in the reported range for that region, was around 2200 t/km<sup>2</sup>/y. ILWIS and ERDAS softwares were used for the study. The result was showed the better performance of MMF model in hilly terrain.

Behera *et al.* (2005) conducted a soil erosion study using MMF model in the small portion of Song sub-watershed of Ganga river basin, which covers the areal extent of 167 km<sup>2</sup>. Study was done using ILWIS 2.2 and ERDAS 8.4 softwares. DEM was generated from the elevation details of the study area. Land use and vegetation related parameters were obtained from the LISS III images. Thematic map layers including RD map,  $E_r/E_0$  map, A factor map, C factor map, MS layer, K layer and BD layer were prepared. The erosion was estimated based on the MMF model and areas were reclassified into different classes based on the quantity of erosion. The study showed that scrubs in the area are more susceptible to erosion.

Vigiak *et al.* (2005) successfully attempted to identify the erosion pattern in Kwalei (Tanzania) catchment using ACED survey and MMF model. In Kwalei catchment, erosion features were highly dependent on annual crops. The predicted rate of erosion was ranging from 0.01 to 13.50 kg/m<sup>2</sup>/y. The erosion map obtained by MMF model was compared with those from ACED survey was highly comparable.

Ustun (2008) made an attempt to estimate soil loss in Ganos mountain region, Turkey incorporating with ERDAS and ILWIS software. The MMF model was used to estimate the soil erosion rate of the study area. Slope values were derived from DEM, which were prepared by digitizing the contours. Landsat 5 imageries were used to calculate the vegetation related parameters. The estimated soil erosion rate was 10 t/ha.

Pandey *et al.* (2009) estimated the rate of soil loss in Dikrong basin, Himalaya having the areal extend of 1556 km<sup>2</sup> with the help of remote sensing and GIS incorporated with MMF model. Soil losses were observed for the years from 1988 to 2004. The estimated annual average soil loss was 75.7 t/ha.

Ramasankaran *et al.* (2012) computed the spatial distribution of soil erosion in Pathiri Rao watershed. The particular watershed is basically ungauged and semi mountainous one. Remote sensing data like DEM of 50 m resolution and satellite images (LISS III) were used for the preparation of thematic map layers. ArcGIS software was used for the spatial distribution of data.

Barman *et al.* (2013) attempted to find out the effects exerted on the soil erosion by various factors like land cover, soil, climate etc jointly or separately using MMF model. The study was performed in Majuli Island, Assam. LISS II and LISS III images were used. The LULC map was generated in ArcGIS by digitizing the satellite imageries. Texture of soil over entire area was assumed as sandy loam. Slope related parameters were derived from the ASTER DEM of 30 m resolution. All these parameters were combined in ILWIS software to study and determine the changes in soil erosion obtained in the year 1975, 1998 and 2008. The study found that in the year 1975, total area covered by vegetation was 33.67% and in the year 1998 and 2008, the vegetated area was 26.13% and 17.8% respectively. Accordingly, rate of soil loss for the year 1975, 1998 and 2008 were 7.53 kg/m<sup>2</sup>, 7.65 kg/m<sup>2</sup> and 8.39 kg/m<sup>2</sup> respectively, which shows the influence of land cover on soil erosion.

Tesfahunegn *et al.* (2014) successfully attempted to assess the soil erosion in Mai-Negus catchment, Ethiopia by incorporating MMF model and GIS software. DEM for the study was generated from the topographical map of the study area. Vegetation and land related parameters are directly collected randomly from 117 plots. Zone sampling technique was adopted for the collection of the soil samples. Rainfall intensity of about 25 mm/h was assumed for the entire study area and detachability index values were chosen from the literature corresponding to soil texture. Point data were interpolated using Kriging interpolation techniques in ArcGIS 9.3. The model evaluation was done considering the percent difference between simulated and the data obtained after the survey in reservoir. Average soil loss estimated was 26 t/ha/y. The simulated average soil erosion was 11.64 t/ha.

Shreshta and Jetten (2018) assessed soil erosion on a daily basis in Nam Chum watershed of Thailand and Sehoul commune, Morocco using MMF model. Digital elevation model was derived from the 10 m contour lines and SRTM DEM for the selected study area of Thailand and Morocco respectively. Soil parameters required to run the model were found from the soil samples taken from both the fields. Land cover parameters were derived from the remote sensing data such as landsat multispectral image and ASTER satellite image downloaded for the watersheds in Thailand and Morocco respectively. Daily canopy cover for both the locations was obtained from the NDVI images. Model validation was performed with observed soil loss data. The average soil erosion assessed from the watersheds of Thailand and Morocco was 15 t/ha and 19 t/ha respectively.

## **2.7 Watershed prioritization**

Khan *et al.* (2001) prioritized the Guhiya watershed having areal extent of 1641 km<sup>2</sup> for effective implementation of soil and water conservation measures. Attempt was done in GIS environment using remote sensing data. Watershed was delineated and assessment of erosivity and sediment yield were done using GIS software. Sixty

eight watersheds were considered for the study. Slope map, satellite images and land use map were used and digitized to obtain thematic map layers and prioritization was carried out based on the obtained sediment yield value. The study suggested to apply immediate action in the areas with high sediment yield value.

Adeogun *et al.* (2018) identified the erosion prone areas considering the sediment yield values of the watershed of Kainji hydropower dam, Nigeria. Classification was mainly based on the erosion severity, aimed to apply management practices in the watershed. The results showed that 11 sub-basins are under low erosion prone areas, 23 are in moderate, 12 are in severe erosion area whereas 8 sub-basins came under extreme category. Filter strips and stone bunds were introduced in the severe erosion identified areas which reduced the sediment concentration by 34% and 84% respectively.

Sharda and Mandal (2018) tried to build up a strategy to implement management and conservation practices in the northern Himalayan region by classifying erosion threat areas and prioritizing them on the basis of erosion rates with targeted soil loss value (T-value). The maximum priority was given for the area where there is a larger difference exists between erosion rate and T value, so that efficient utilization of financial resources could be possible. The classification revealed that 25% of the watershed area was under severe erosion risk categories. The perception of prioritization of erosion prone areas and their treatment with suitable management measures was validated using the field data collected from the representative watersheds.

# **MATERIALS AND METHODS**

## CHAPTER III

### MATERIALS AND METHODS

This chapter illustrates the description of the study area, soil erosion models and methodology adopted for the study. Different factors required for the assessment of soil erosion are identified and detailed. Revised Universal Soil Erosion Model (RUSLE) and Morgan, Morgan and Finney (MMF) model were selected for the study and their performance in assessment of soil erosion was evaluated. Satellite imageries were used as the basic data to determine the effect of vegetation on spatial variation of soil erosion in the particular sub-basin. Land use changes were approved with the strong support of the NDVI maps.

#### 3.1 DESCRIPTION OF THE STUDY AREA

Kunthippuzha sub-basin of Bharatahpuzha river basin was selected for the study. Kunthippuzha river joins the river 'Thutha' which is one among the four main tributaries of Bharathappuzha (largest river basin in Kerala). The location map of the selected sub-basin is shown in Fig. 3.1. The sub-basin is located at the topmost part of the Bharathappuzha river basin (North-East direction). The total catchment area of Bharathappuzha is 6400 km<sup>2</sup>, out of that 15.8% of the area is occupied by the Kunthippuzha sub-basin with an areal extent of 1015.7 km<sup>2</sup> (CWRDM, 1974). The selected watershed is located in between the Latitude-Longitude range of 10° 53' North, 76° 04' East and 11° 14' North, 76° 41' East. The elevation of the sub-basin changes from 20 m to 2300 m. The Kunthippuzha sub-basin spreads in two districts, namely, Palakkad and Malappuram. Major portion of the catchment lies in Palakkad district (Tejaswini and Sathian, 2018).

Kunthippuzha sub-basin falls under humid tropical climatic region. The rainfall distribution in the catchment varies seasonally. Average annual rainfall is about 2300 mm. About 80% of the rainfall is received during monsoon, 15% during post-

monsoon and remaining 5% is received during winter and summer. The mean temperature of the watershed is 27.3°C. The soil type and land use pattern varies spatially within the catchment (Tejaswini and Sathian, 2018)

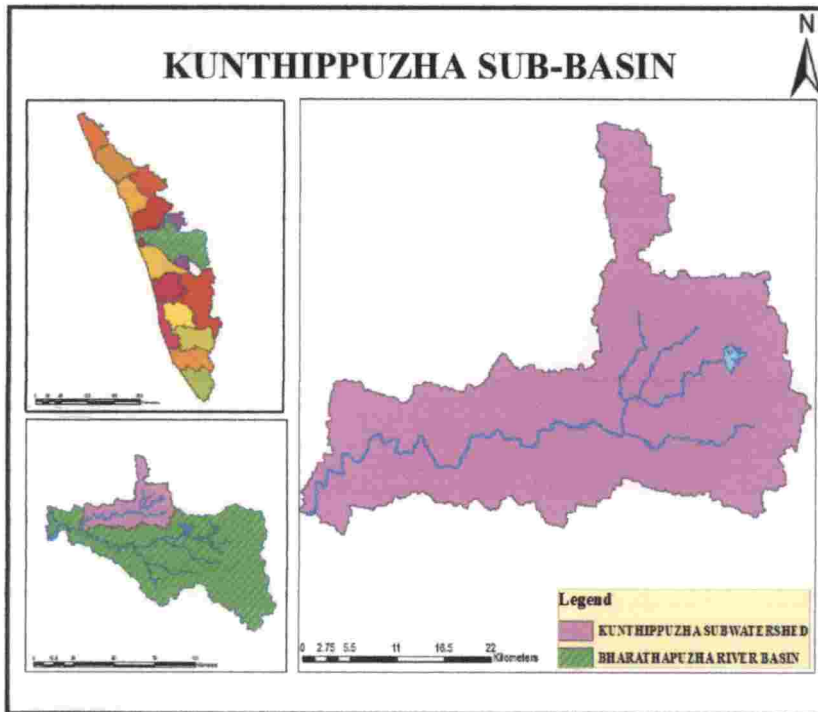


**Fig. 3.1 Location of the study area**

## **3.2. SOFTWARE AND TOOLS USED**

The software and tools used for the study is described below. The study was carried out in GIS environment.

### **3.2.1. ArcGIS 10.3.1**

ArcGIS is a proprietary Geographic Information System (GIS) software, which was developed by Environmental System Research Institute (ESRI). ArcGIS 10.3.1 available at geo-spatial division of KCAET, Tavanur was used in this study. This

particular version was released during 2015. The GIS software has the capability to handle geospatial data (comprising spatial and attribute data) which makes the software more popular from other information systems. It is possible and easy to perform the spatial analysis and temporal analysis of data in GIS environment. In addition to in-built GIS tools, ArcHydro tool, spatial analyst tool and hydrology tool were used. Hydrology tool is used to demarcate the boundary of the particular sub-basin. The ArcHydro tool is used to calculate the slope length factor by identifying the flow accumulation, flow direction and fill sinks in the entire watershed (Zerihun *et al.*, 2018).

### **3.2.2 Collection of Remote Sensing Data**

The satellite imageries, digital elevation models, soil data including structural and textural details, rainfall data (daily and monthly rainfall amount) were collected for the study area. The important data sources used for the particular study are described below.

#### **3.2.2.1 USGS Earth Explorer**

Satellite imageries for the preparation of the land use land cover (LULC) map of the study area are downloaded from the Earth Explorer. USGS Earth Explorer provides imageries from various satellites like ISRO Resourcesat, Landsat, Sentinel, RADAR etc. Furthermore, it provides digital elevation models (DEM) like ASTER global DEM, SRTM DEM, LIDAR, EDNA, IFSAR Alaska etc. It is the user interface system which lets online data search through interactive and query capabilities. The system has provisions to give search criteria including coordinates of the location, predefined area, shape file and year range of the required data. Additional to these criteria, it has the provisions to adjust cloud cover percentage in the data search. It facilitates to see the footprint of the scene and provides the metadata of the searched data which comprises Landsat product identifier, Landsat



scene identifier, acquisition date, details of band, datum used, grid cell size and ground control points.

For the current study related to soil erosion, required satellite imageries of the study location for the year 2000 and 2013 were downloaded from the USGS Earth Explorer. Satellite image of the year 2000 and 2013 were obtained from the dataset of Landsat 7 Enhanced Thematic Mapper (ETM) plus level 1 and Landsat 8 ETM+ level 1. The imageries with little scanned error and no cloud cover is selected for the study. The user interface of the USGS Earth Explorer is shown in Fig. 3.2.

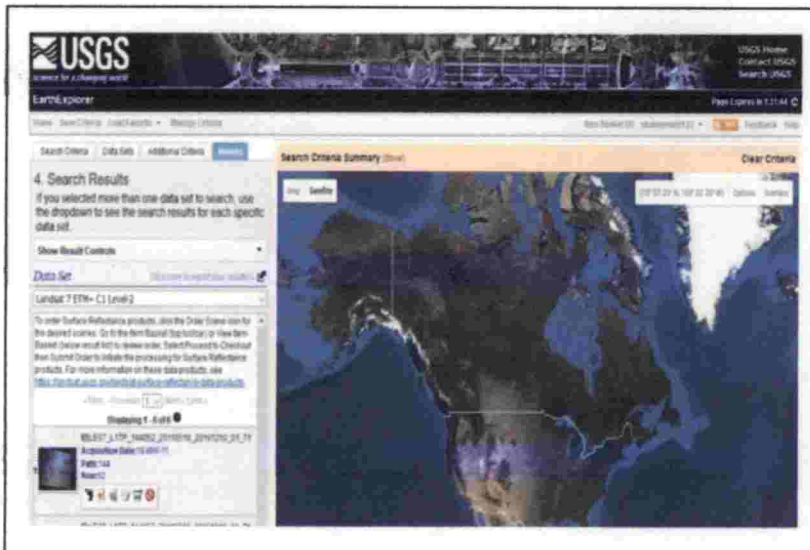


**Fig. 3.2 USGS Earth Explorer user interface**

The USGS Earth Explorer provides the DEM. The DEM of the study area for the year 2013 with 30 m resolution is downloaded from the SRTM (Shuttle Radar Topography Mission) dataset provided in the Earth Explorer.

### **3.2.2.2. OpenTopography**

The DEM of the study location for the year 2000 is downloaded from the Open Topography. SRTM DEM with raster resolution of 30 m is used for the study. The user interface of the OpenTopography is shown in Fig. 3.3.



**Fig. 3.3 User interface of OpenTopography**

### **3.2.2.3 Open Street Map**

Open street map is a user interface system, which provides editable and geo-referenced road networks of the world. Road network data incorporated with land use map and compared with those obtained from the satellite imageries. Data were downloaded for the study area in 'osm' format which is converted into shape file in GIS environment. The user interface of the open street map is shown in Fig. 3.4.

### **3.2.2.4 Bhuvan**

LISS III satellite imageries having resolution 23.5 m for the year 2013 were downloaded from the Bhuvan, an Indian Geo-platform developed by ISRO. The downloaded image was used to check the range of NDVI value of the study area obtained from the Landsat imageries. Five tiles of imageries were required to fix complete study area. Imageries with minimum cloud cover were selected. The downloaded imageries were pan sharpened in ArcGIS. The user interface of the Bhuvan is shown in Fig. 3.5.

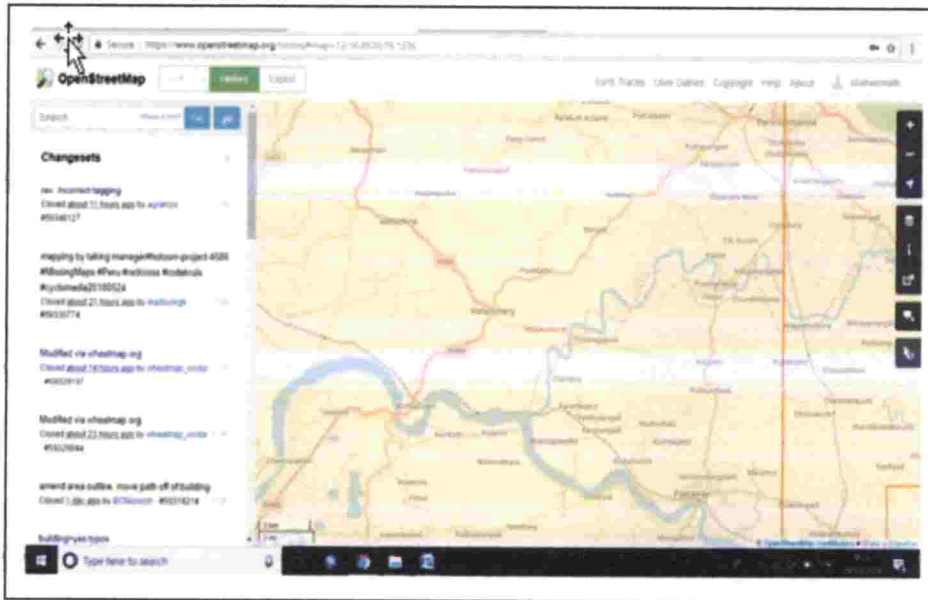


**Fig. 3.4 User interface of open street map**

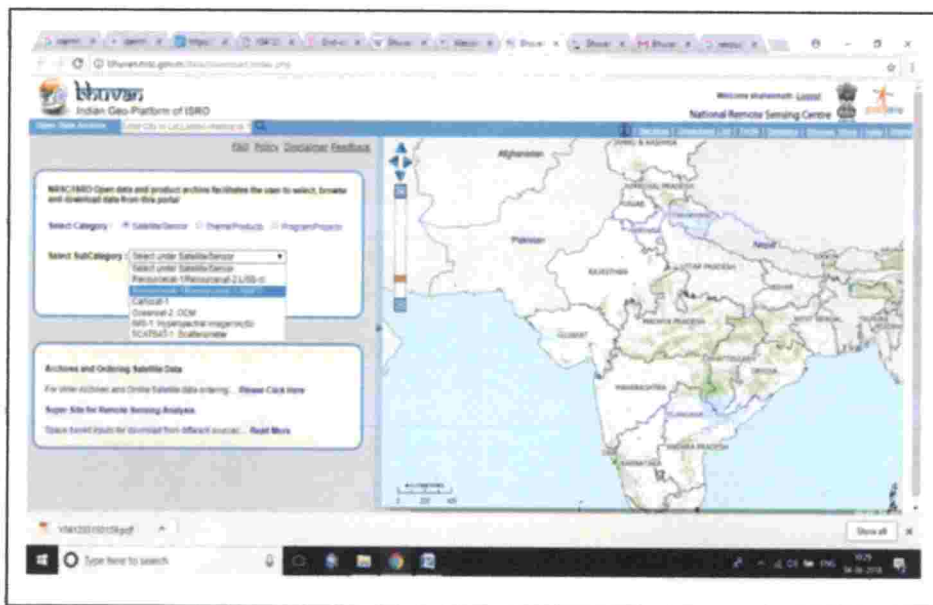


**Fig. 3.5 User interface of Bhuvan**

### 3.3 Methodology Adopted

Soil erosion is one of the most tedious land degradation occurring in the study location. In the current data study, RUSLE and MMF models were used to estimate the



annual soil erosion rate. Among the two models RUSLE is an empirical model whereas the other is a semi-empirical one. Using these soil erosion models, annual average soil loss rate were estimated for the year 2000 and 2013. Spatial variations in land use and corresponding changes in NDVI value were identified using both the models. Impacts of land use change on soil erosion were assessed in GIS environment. The soil erosion prone areas were identified based on zonal scoring techniques (Haregeweyn *et al.*, 2017). The section 3.3 describes the methodologies and parameters confined in these two soil loss estimation models.

### 3.3.1 RUSLE Model

It is the revised version of USLE. The RUSLE model had been widely used, tested and well proven for many years in many locations. It actually estimates annual average erosion rate of soil by incorporating various factors like climate, soil, topography and vegetation (Renard *et al.*, 1997). The fundamental formula for RUSLE and USLE are same, which is given as:

$$A = R * K * LS * C * P \quad (3.1)$$

Where, A is the annual soil loss ( $t \text{ ha}^{-1} \text{ y}^{-1}$ ); R is the erosivity factor ( $\text{MJ mm ha}^{-1} \text{ h}^{-1} \text{ y}^{-1}$ ); K is the soil erodibility factor ( $t \text{ ha h}^{-1} \text{ ha}^{-1} \text{ MJ}^{-1} \text{ mm}^{-1}$ ); LS is the topographic factor; C is the cover and management factor and P is the conservation practice factor. The value ranges of these parameters were clearly mentioned in the chapter II.

### 3.3.2 MMF Model

This particular model was developed by Morgan *et al.* (1984) which comprises two phases namely water and sediment. Number of input data required for this model is quite higher compared to RUSLE model. In water phase, energy of rainfall and depth of overland flow were calculated. The rainfall energy, E ( $\text{J/m}^2$ ) for tropical climate can be computed by using the equation 3.2 (Morgan, 2005);

$$E = R * [29.8 - (127.5/I)] \quad (3.2)$$

Where, R is the annual rainfall (mm) and I is the intensity of erosive rain (mm/h). The intensity of erosive rain was usually taken as 11 for temperate climates, 25 for tropical climates and 30 for strongly seasonal climates. The depth of overland flow (Q, mm) by the rainfall and runoff was estimated by,

$$Q = R * \text{EXP}^{(-R_c/R_o)} \quad (3.3)$$

Where,  $R_c$  is the soil moisture storage capacity under land cover (mm) and  $R_o$  is the mean rain per day (mm). The  $R_c$  is computed considering the soil moisture content at field capacity (MS, % w/w), bulk density of the soil (BD,  $\text{Mg/m}^3$ ), effective hydrologic soil depth (EHD, m) and the ratio of actual to potential evapotranspiration ( $E_t/E_o$ ) as given in the equation 3.4.

$$R_c = 1000 * \text{MS} * \text{BD} * \text{EHD} * (E_t/E_o)^{0.5} \quad (3.4)$$

Where,  $R_o = R/R_n$ ;  $R_n$  is the number of rainy days in a year.

In the sediment phase, soil detachment by rainfall or rate of splash detachment ( $F$ ,  $\text{kg/m}^2$ ) was computed by,

$$F = K * E * \text{EXP}(-0.05 A) * 10^{-3} \quad (3.5)$$

Where, K is the soil detachability index (g/J) defined as the weight of soil detached from the soil mass per unit of rainfall energy and runoff and A is the percentage rainfall contributing to permanent interception and stem flow. The transport capacity of overland flow ( $G$ ,  $\text{kg/m}^2$ ) was estimated by:

$$G = C * Q^2 * \sin S * 10^{-3} \quad (3.6)$$

Where, C is the crop cover management factor and S is the sin of slope angle in degree. Minimum value of the F and G was considered as soil erosion rate.

### 3.4 DELINEATION OF SUB-BASIN BOUNDARY

Hydrology tool in ArcGIS is used for digital demarcation of the watershed boundary. DEM of the study area for the year 2000 (resolution 30 m) were loaded in ArcGIS window. Hydrology tool was obtained by expanding the spatial analyst tool in main window. The process of delineation using hydrology tool comprises the creation of fill sink raster, flow direction raster, flow accumulation raster and watershed raster. DEM of the study area was given as the input raster for the preparation of the fill sink raster, which will help to avoid the imperfections of the DEM chosen. The fill sink raster prepared was selected to get flow direction raster, which highlights the direction of the flow. Flow accumulation raster was created using flow direction raster. Finally watershed raster was prepared from the flow accumulation raster. The prepared watershed raster were then converted into polygon using conversion tool. From the obtained polygon features, polygon feature corresponding to the study location was selected, clipped out and saved as shape file for further activities as shown in the Fig. 3.6.

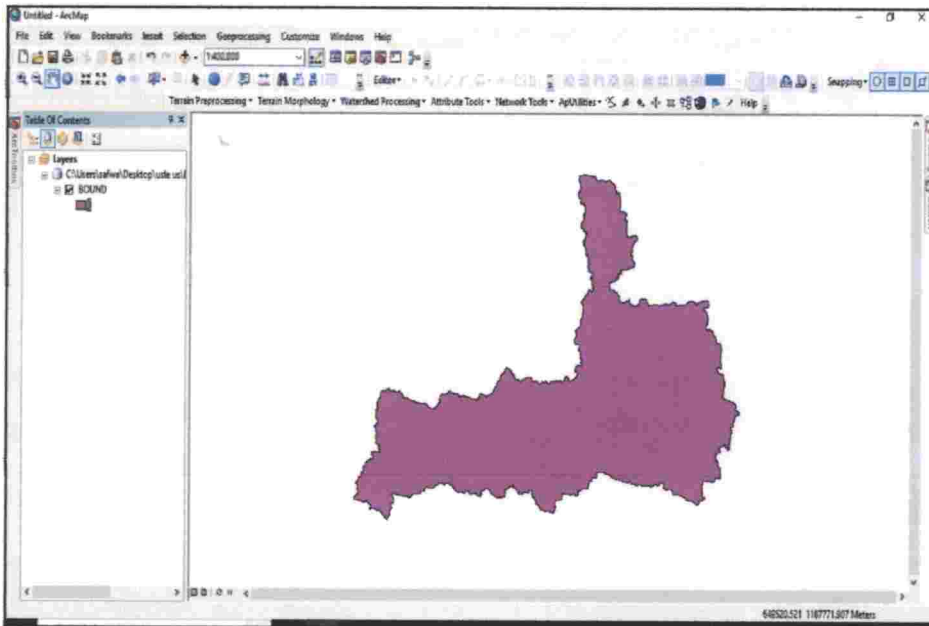


Fig. 3.6 The delineated boundary of the study area (*'Bound.shp'*)

All the operations were performed after projecting the DEM to the projected coordinate system with datum WGS\_1984\_UTM\_43\_N using raster projection tool.

### **3.5 CREATION OF MAP LAYERS FOR RUSLE MODEL**

The assessment of soil erosion using erosion model in GIS environment basically requires input map layers, which were prepared separately and clubbed to form final soil erosion map. The important map layers required were erosivity map or R factor map, erodibility map or K factor map, topographic factor map, C factor map and P factor map (Haregeweyn *et al.*, 2017). Each map was prepared for both the year 2000 and 2013. The following section describes the methods and ways chosen for the preparation of the above mentioned thematic map layers.

#### **3.5.1 Preparation of R Factor Layer**

The factor 'R' notates the effect of rainfall especially its impact to cause erosion. It quantifies the fraction of erosion which is linked to the storm events. This factor greatly depends on the intensity of the rainfall and duration. Usually in RUSLE model, EI<sub>30</sub> index method is considered as most appropriate way to calculate the R factor (Rawat *et al.*, 2013). But the intensity data could not be obtained as the study area and nearby watershed are lacking the recording type rain gauge station. So, daily rainfall data were collected from the RARS Pattambi and Mannarkad rain gauge station for the year 2000 and 2013. Among these two stations, one is located inside the study area and other outside the study location.

In general, not all the storm events are responsible for soil erosion. The erosive events are considered as causative storm events and the criteria which differentiate the erosive events put some thresholds. The storm events with rainfall amount greater than 12 mm was considered as erosive events (Xie *et al.*, 2002). For this particular study area, storm event data could not be possible to get so that the cumulative daily rainfall data was collected and eliminated all the daily rainfall data

carrying the value less than 12 mm to enhance the accuracy of calculation. To estimate the R factor modified Arnoldus (1980) equation were used, which is given below in the equation 3.7.

$$R = \sum_{i=1}^{12} 17.35 \times (1.5 \log_{10} (P_i^2 / P) - 0.08188) \quad (3.7)$$

Where, R is the rainfall erosivity factor ( $\text{MJ mm ha}^{-1} \text{ h}^{-1} \text{ y}^{-1}$ ),  $P_i$  is the monthly rainfall (mm), and P is the annual rainfall (mm). The calculation is completed in Microsoft Excel spread sheet. The isoerodent map was prepared in ArcGIS 10.3.1 software by giving the location (latitude and longitude) of the rain gauge station and erosivity index obtained at each station as input. The calculation of R factor from the daily rainfall data were shown in Appendix I (a-b). The prepared excel sheet comprising latitude and longitude values of the rain gauge station and erosivity index value (as given in Appendix II) was directly added to ArcGIS window.

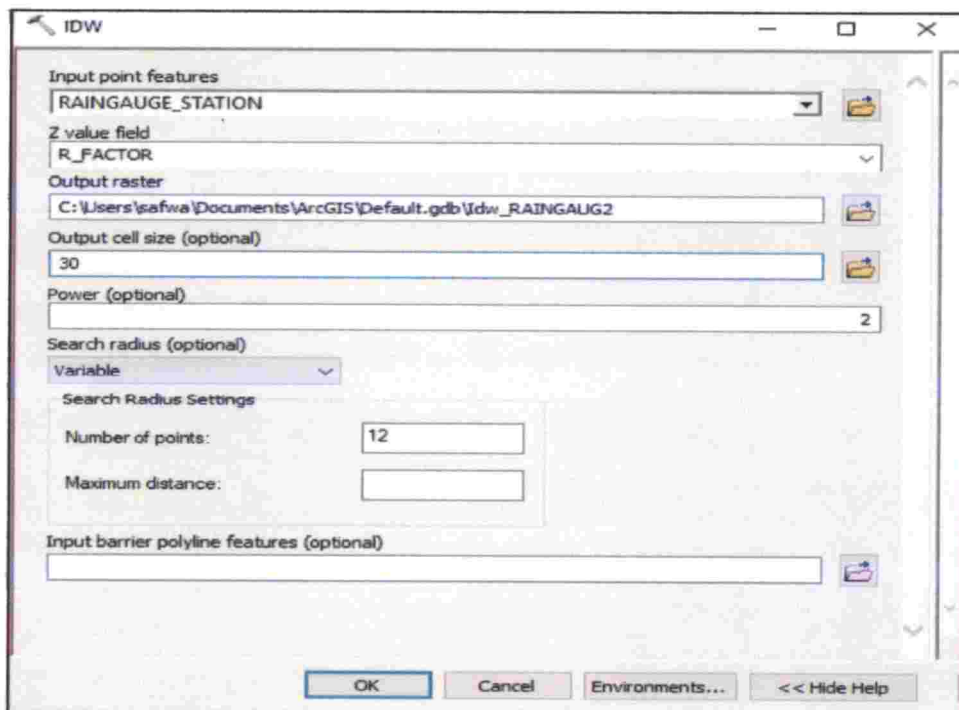


**Fig. 3.7 GIS interface for IDW interpolation**



The Inverse Distance Weighted (IDW) interpolation tool in ArcGIS was used to interpolate the erosivity index value throughout the watershed as suggested by Prasannakumar *et al.* (2011a). The prepared '*Bound.shp*' was given as the process extent for the interpolation. The procedure was repeated for the year 2013 also. The prepared maps were named as '*R2000*' and '*R2013*'. The GIS interface of IDW interpolation tool is shown in Fig. 3.7.

### 3.5.2 Preparation of K Factor Map

K factor or erodibility factor refers to the propensity of the soil to get erode. The factors like soil structure, particle size distribution, organic matters contained in the soil, permeability etc influence the erodibility of the soil. In the particular study soil association map of the Bharathappuzha river basin were collected from the Department of Soil Survey and Soil Conservation. The same soil map was used for both the years 2000 and 2013. The original soil association map was obtained as hard copy along with detailed description of each soil. The description contains soil name, colour, depth of different horizons, taxonomic classes, drainage and permeability, vegetation details, land capability and land irrigability class, fertility status of the soil, particle size distribution containing percentage values of gravel, very coarse sand, coarse sand, fine sand, medium coarse sand, very fine sand, silt and clay and also contains the values of pH, electric conductivity, cation exchange capacity and exchangeable acidity.

The K factor was calculated using Microsoft Excel for each series using the equation 3.8.

$$K = \{2.1 \times M^{1.14} \times 10^{-4} \times (12-a) + 3.25 \times (b-2) + 2.5 \times (c-3)\} / 100 \quad (3.8)$$

In the equation,  $M = (\% \text{ of silt} + \% \text{ of very fine sand}) \times (100 - \% \text{ of clay})$ , 'a' is the % of organic matter content in the soil, 'b' indicates value corresponding to structural classes and 'c' indicates the value corresponding to the permeability class. The b

value varies as follows: 1 for very fine granular; 2 for fine granular; 3 for medium or coarse granular and 4 for blocky, platy or massive structure. Variation of c value is as follows: 1 for rapid; 2 for moderate to rapid; 3 for moderate; 4 for slow to moderate; 5 for slow and 6 for very slow permeability rate. The series with highest K factor was selected from each soil association group. The accuracy of the calculated K factor was checked using nomograph for USLE K factor (Wischmeier and smith, 1978). The soil map used for the study and digitization of the soil map are shown in the Fig. 3.8 and Fig. 3.9 respectively.

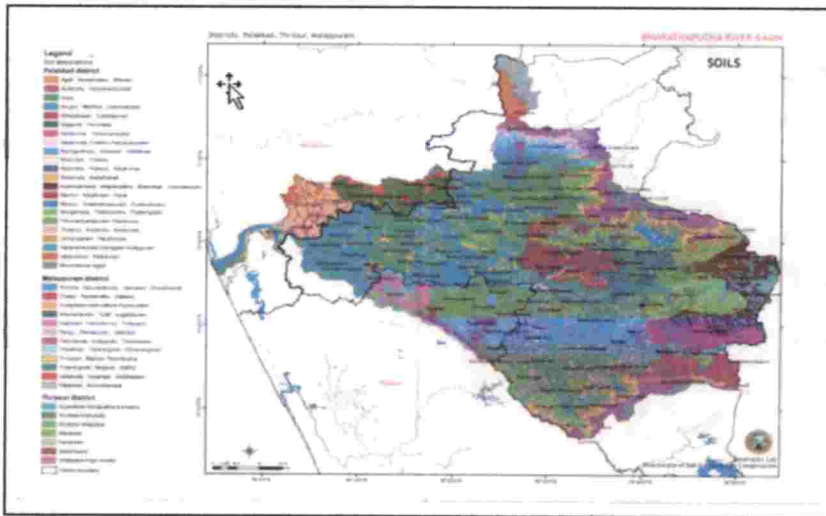


**Fig. 3.8 Soil map of the Bharathapuzha river basin**

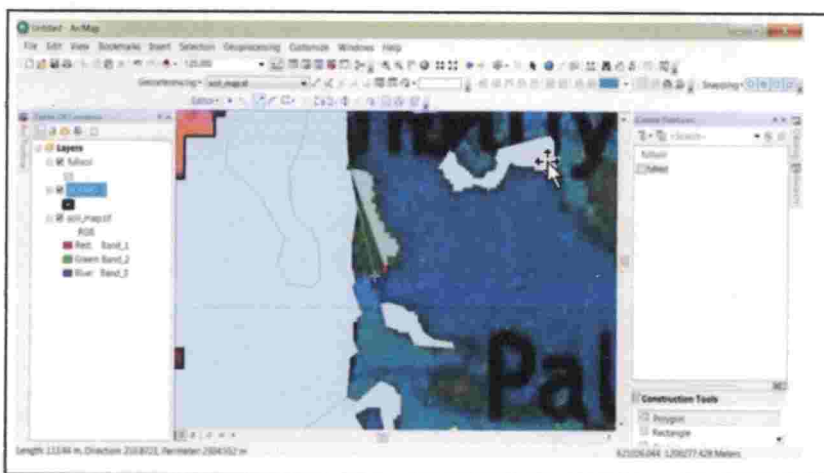


**Fig. 3.9 Digitization of the soil map of the study area**

The hard copy of the map was first scanned and georeferenced in ArcGIS environment. The soil map for the study location was clipped out from georeferenced soil map of the Bharathappuzha river basin using the 'Bound.shp' and digitized using editor tool in ArcGIS. The digitized map was projected into WGS\_1984\_UTM\_43\_N coordinate system. The K value for each series was added in the attribute table. Finally K factor map 'K\_soil' for the study area was prepared. The calculation of K factor value corresponding to each soil group was shown in Appendix III.

### 3.5.3 Preparation of LS Factor Map

It is the combination of the slope length factor (L) and slope steepness factor (S). The topographic factor was derived from the DEM. SRTM DEM with spatial resolution of 30 m downloaded from the USGS earth explorer and OpenTopography for 2013 and 2000 respectively were selected for the study. SRTM DEM was chosen for the study as it found better DEM for the study area (Tejaswini, 2017). Calculation was done using equation 3.9 explained below.

$$LS = \left( \frac{\text{Flow accumulation} * \text{Cell size}}{22.13} \right)^{0.4} \times \left( \frac{\sin \text{slope}}{0.0896} \right)^{1.3} \quad (3.9)$$

Where, slope in degree was considered for calculation.

The LS factor was derived from DEM in ArcGIS environment using ArcHydro tool. The generation of LS factor map for the year 2000 was done by preparing L and S map separately and clubbed to form final topographical factor map. The derivation of slope length was completed as follows:

- The selected SRTM DEM was loaded in ArcGIS window and transformed to projected co-ordinate system (WGS\_1984\_UTM\_43\_N) using raster projection option. The projected DEM was clipped to the study boundary and named as 'dem2000'.

- The 'dem2000' was loaded in Arc window by using the function called 'data management and terrain preprocessing' under terrain preprocessing in the Arc Hydro tool. DEM manipulation was performed by selecting fill sinks to make assurance about the continuous flow of water. The filled hydro DEM was named as "fill2000".
- The 'fill2000' was used for the generation of flow direction map by selecting flow direction option under terrain preprocessing and the prepared map was named as 'fdr2000'.
- Finally flow accumulation map 'fac2000' was prepared from flow direction map. The flow accumulation map basically acts as the input map layer for the generation of slope length map.

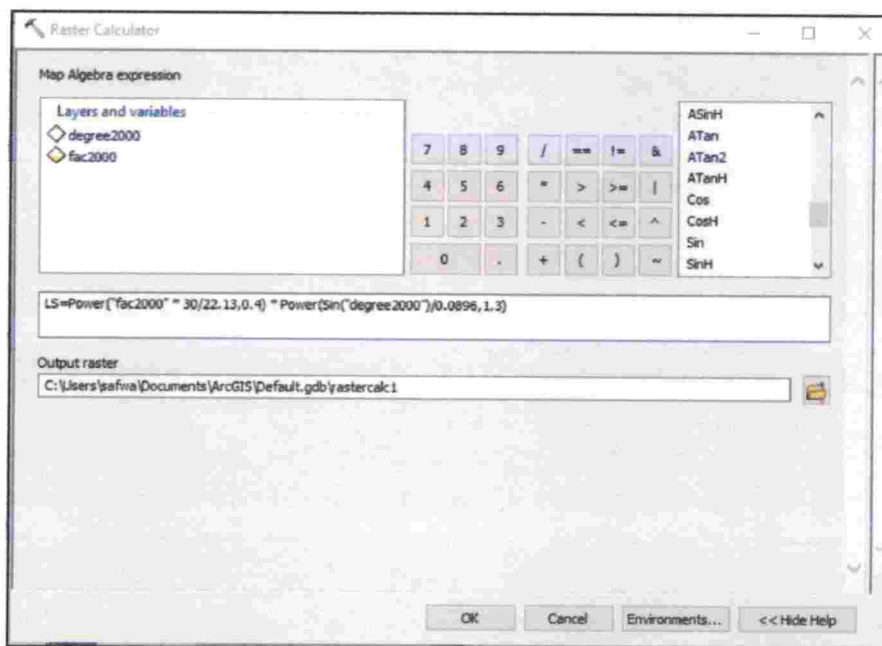


**Fig. 3.10 ArcGIS interface for raster calculator**

The slope function under the spatial analyst tool was used to derive slope steepness factor. The 'Dem2000' was given as input and map was prepared in both degree and percentage by choosing options under output measurement icon. Finally raster calculator function of map algebra under spatial analyst tool were selected

SA

which uses equation 3.9 as input function to calculate LS factor. The methodology adopted for the derivation of LS factor map is shown in Fig. 3.11 below. The same procedures were repeated to generate LS factor map layer for the year 2013 also. The prepared maps were named as ‘LS2000’ and ‘LS2013’. The user interface for raster calculator along with LS factor formula is shown in Fig. 3.10.

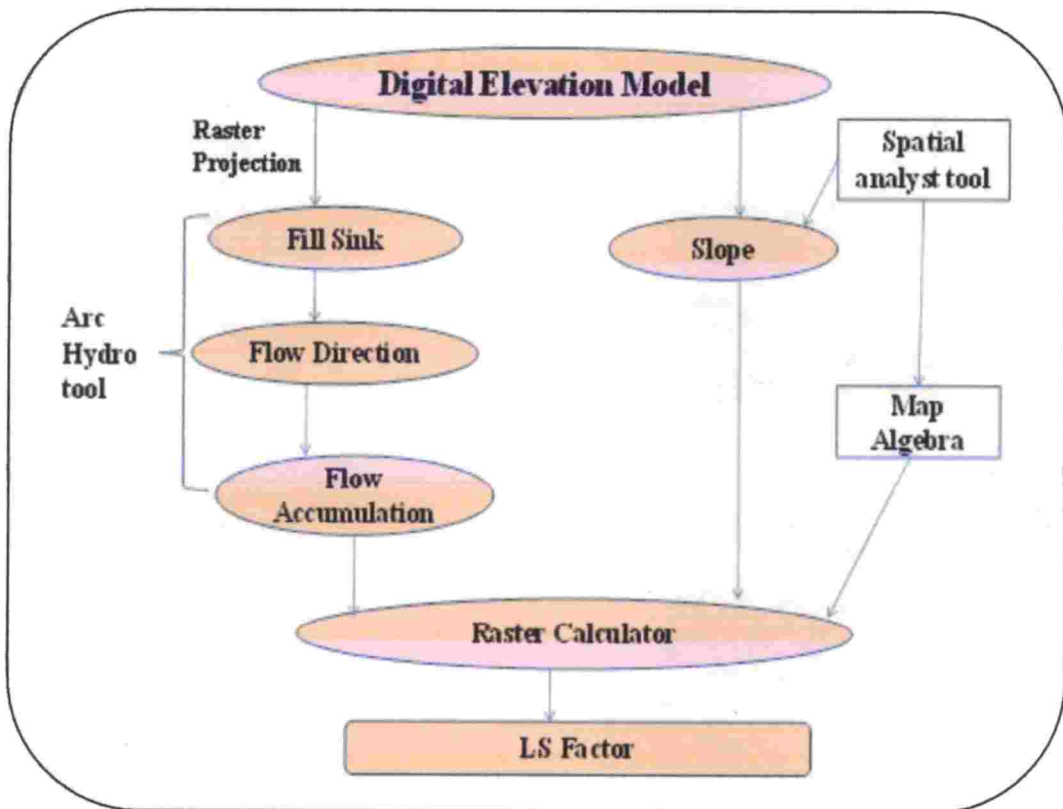


**Fig. 3.11 Flow chart for LS factor determination**

### 3.5.4 Preparation of C Factor Map

The cover management factor or C factor is one of the most important parameter among the RUSLE factors since the effective control in C factor may reduce the soil erosion. The kind of vegetation, its growth stage and canopy cover are the factors strongly affects the C factor. So, derivation of C factor from appropriate vegetation related parameter will be very accurate. NDVI method is the

most suitable and widely accepted method to generate C factor from the remote sensing data like satellite imageries (Kouli *et al.*, 2008). The calculation requires values of red and near infrared band reflectance and the relation is given in equation 3.10.

$$NDVI = \frac{NIR-RED}{NIR+RED} \quad (3.10)$$

The Landsat 7 ETM<sup>+</sup> image for the year 2000 and Landsat 8 ETM<sup>+</sup> image for the year 2013 downloaded from USGS Earth Explorer were taken for the NDVI calculation. NDVI map was generated in ArcGIS using image analysis option. Out of 8 bands obtained with Landsat 7 ETM<sup>+</sup> image, band 3 indicates red band and band 4 indicates NIR band. Similarly, in the case of Landsat 8 ETM<sup>+</sup>, band 4 indicates red band and band 5 stands for NIR. NDVI layer was prepared by selecting NDVI option under image analysis window. The NDVI map for the year 2013 was prepared from the LISS III image for the NDVI range comparison. The generated NDVI maps were named as *NDVI2000.tif* and *NDVI2013.tif* respectively for the year 2000 and 2013. The image analysis tool along with LISS III image clipped for the study area is shown in Fig. 3.12.

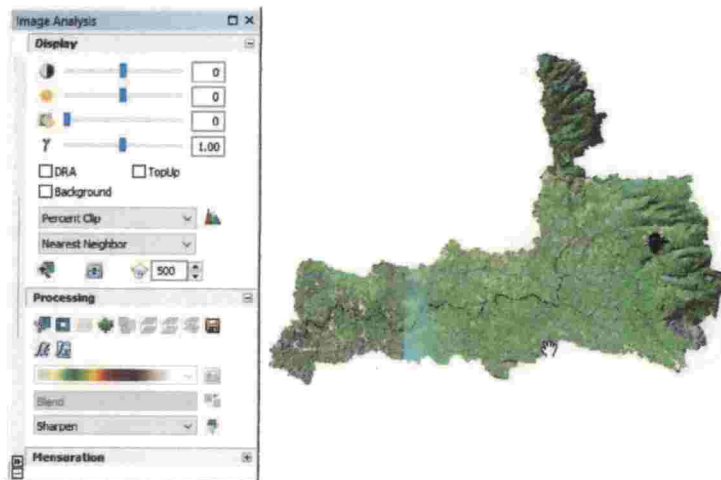


**Fig. 3.12** Image analysis tool with LISS III image clipped for the study area

The C factor map layer was generated from the NDVI map prepared using the equation 3.11.

$$C = \text{EXP} \left( \frac{-2\text{NDVI}}{1-\text{NDVI}} \right) \quad (3.11)$$

The calculation was performed in ArcGIS 10.3.1 using raster calculator for both year 2000 and 2013. The prepared maps were named as ‘C2000’ and ‘C2013’.

### 3.5.5 Preparation of P Factor Map

The P factor or conservation practice factor is mainly influenced by the conservation measures implemented or adopted in the field. The conservation measures increases the time of concentration of water and thereby decreases the soil loss. In usual practices, conservation measures are implemented in the field mainly based on the slope and land use. In the current study the P factor values proposed by the Wischmeier and Smith (1978) based on the land use and field slope in percentage (as given in Table 3.1) was adopted.

**Table 3.1 Variation of P factor with respect to land use and land slope**

Land use	Land slope, %	P factor
Agriculture	0-5	0.10
	5-10	0.12
	10-20	0.14
	20-30	0.19
	30-50	0.25
	50-100	0.33
	>100	0.35
All other land use		1.00

To adopt this method, LULC map is essential. Using the satellite image data downloaded for each year, land use map was prepared in ArcGIS. Maximum likelihood classification was selected under the image classification and preparation of LULC map was done. Pixels corresponding to the different land use categories were identified according to the Landsat chart and idea obtained from the base map. The prepared raster maps for 2000 and 2013 were named as '*Finallandcover2000.tif*' and '*Finallandcover2013.tif*' respectively. The road networks downloaded from the Open street map were added into the prepared land use maps. Ground truth verification was done to check the correctness of the land use maps prepared. Fig. 3.13 and 3.14 show the clipped satellite images of the year 2000 and 2013 respectively.

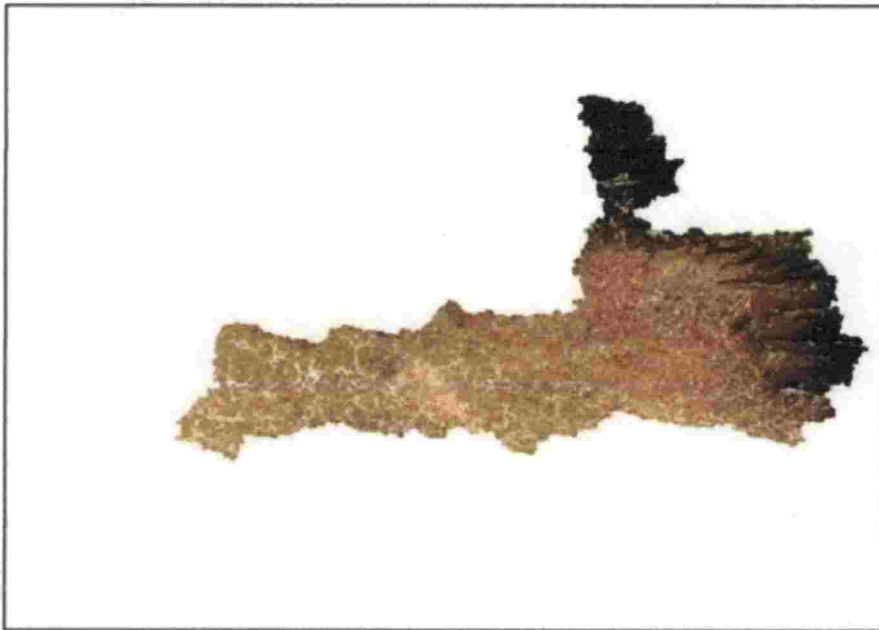


**Fig. 3.13 Clipped Landsat image of the year 2000**

The slope percentage map layer of the year 2000 and corresponding land use map were combined using 'union' option in ArcGIS. Similarly, the slope percentage map layer of the year 2013 and corresponding land use map were combined. The P



factor map layer was prepared through the attribute data management. The prepared maps were named as 'P2000' and 'P2013'.

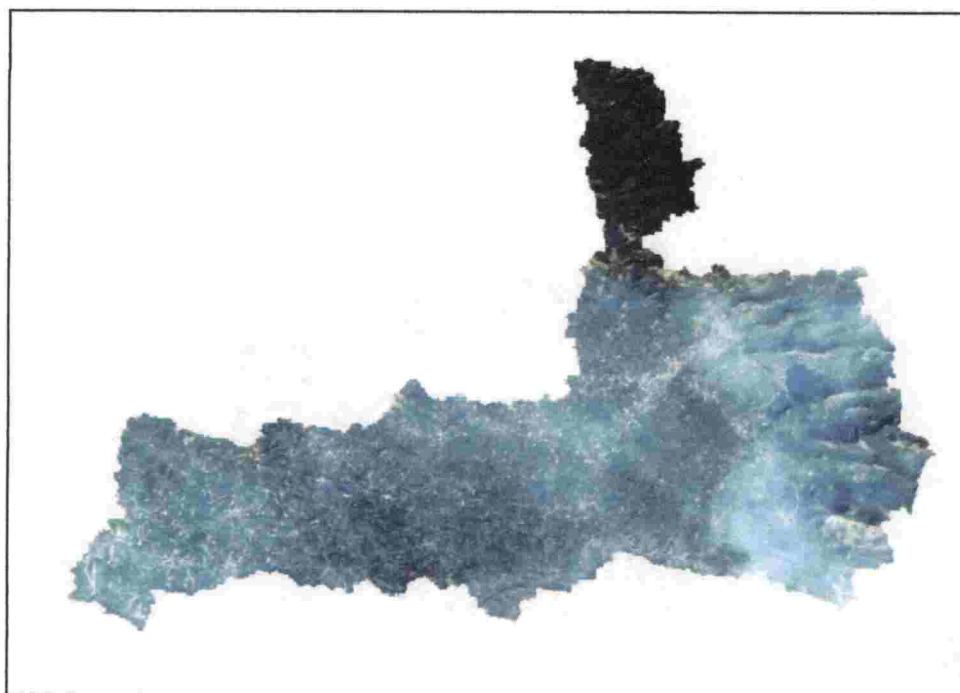


**Fig. 3.14 Clipped Landsat image of the year 2013**

### **3.6 PREPARATION OF SOIL EROSION MAP USING RUSLE**

Final erosion rate for the year 2000 was calculated by applying the RUSLE model, multiplying each map layers such as 'R2000', 'K\_Soil', 'LS2000', 'C2000' and 'P2000' having cell size 30 m using raster calculator. After running the model, final soil erosion map for the year 2000 was obtained. Similarly soil erosion map for the year 2013 also prepared using the respective raster layers of year 2013. All the map layers were prepared in WGS\_1984\_UTM\_43N coordinate system with transverse Mercator projection. The prepared soil erosion maps for the year 2000 and 2013 were analyzed and compared. The Flow chart of the steps adopted in the RUSLE model is shown in the Fig. 3.15.

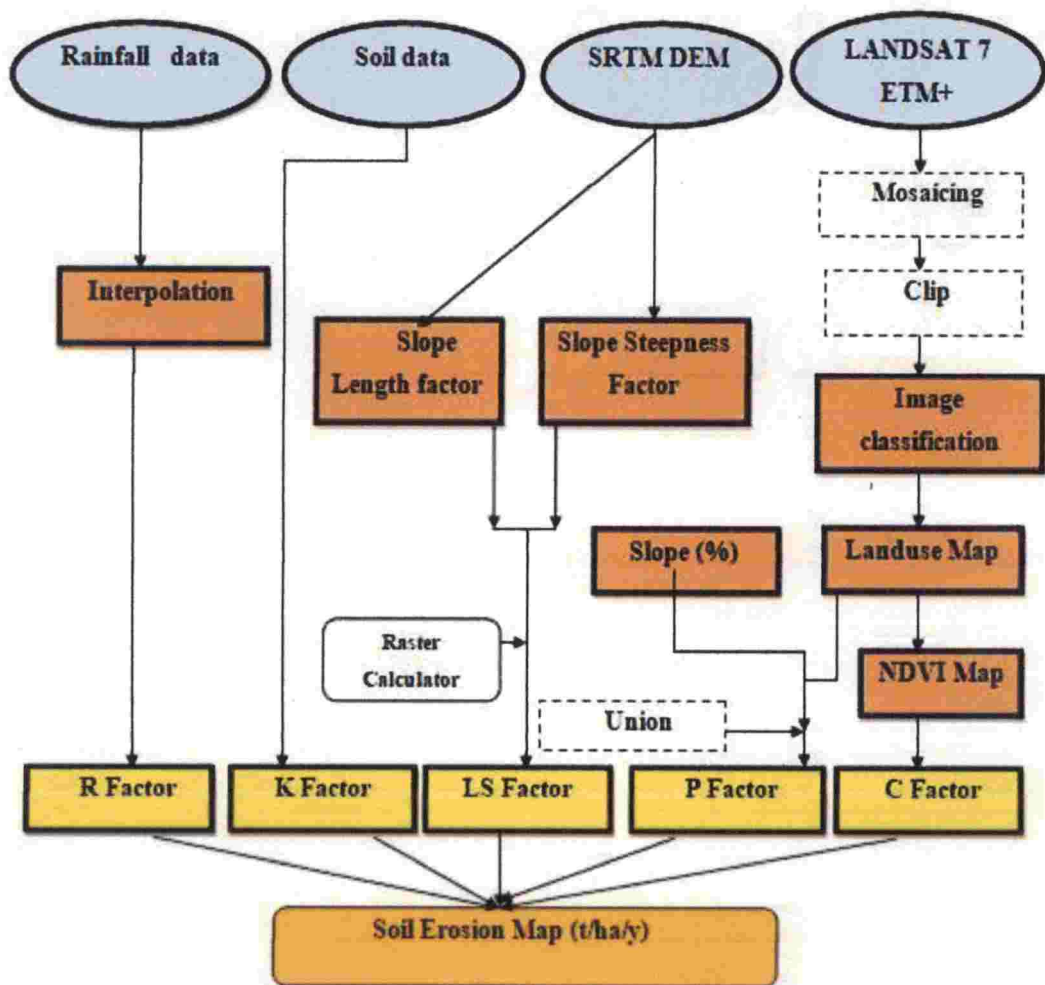


Fig. 3.15 Methodological framework adopted in RUSLE model

### 3.7 CREATION OF MAP LAYERS FOR MMF MODEL

Same base maps including soil map, land use map and slope map prepared in the RUSLE model were used in the MMF model also. The final erosion map was obtained after the attribute data management using the base maps in GIS environment. Detailed procedures adopted in this study are described in this section.

### 3.7.1 Calculation of Input Factors for MMF

As per the equation 3.3, to compute the depth of overland flow in the watershed, data like moisture storage capacity of the soil, annual rainfall amount, mean rain per day etc are required. The average annual rainfall,  $R$  (mm) calculated using the rainfall data obtained from the two rain gauge stations were separately interpolated using IDW interpolation tool. Similarly mean rain per day ( $R_0$ ) value for the year 2000 and 2013 also separately interpolated, which was actually calculated by dividing the average annual rainfall by number of rainy days.

For the calculation of moisture storage capacity, values like MS, BD, EHD and  $E_t/E_0$  are needed. The other required inputs to calculate each MMF parameters are  $K$ ,  $C$  and  $A$  value. Among these parameters MS and BD values were taken from the standard table suggested by Morgan (2005), where the variation of these parameters with respect to soil texture was given. The EHD value for the entire watershed was directly taken from soil association map obtained from the Department of Soil Survey and Soil Conservation.

The texture of each soil series was calculated using online USDA soil texture calculator (Fig. 3.17) and output were validated by comparing the result obtained from the soil texture triangle (Fig. 3.16). Major soil textures found in the watershed are clay, clay loam, sandy loam, sandy clay and sandy clay loam. The soil parameters like MS and BD required for the MMF model are given in Table 3.2. The same soil detachability index ( $K$ ) used in the RUSLE model was applied in this model also. The obtained  $K$ , MS, BD and EHD values were added in the attribute table of the digitized soil map. To prepare separate map of each of these parameters, polygon map was converted into raster by selecting appropriate value field as shown in Fig. 3.18.

The land use land cover parameters in the MMF model include crop cover management factor ( $C$ ),  $E_t/E_0$  and  $A$  as described in the section. The  $C$  factor is the

combined parameter of the RUSLE C and P factor. The C<sub>mmf</sub> maps for the year 2000 and 2013 were prepared by combining obtained RUSLE C and P factor maps ('C2000' and 'P2000' for 2000) for the respective year using map algebra option in ArcGIS spatial analyst tool.

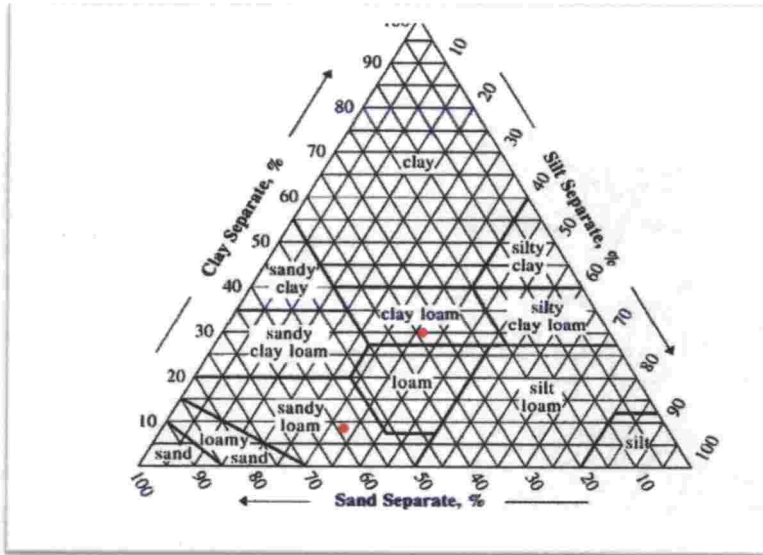


Fig. 3.16 Texture triangle

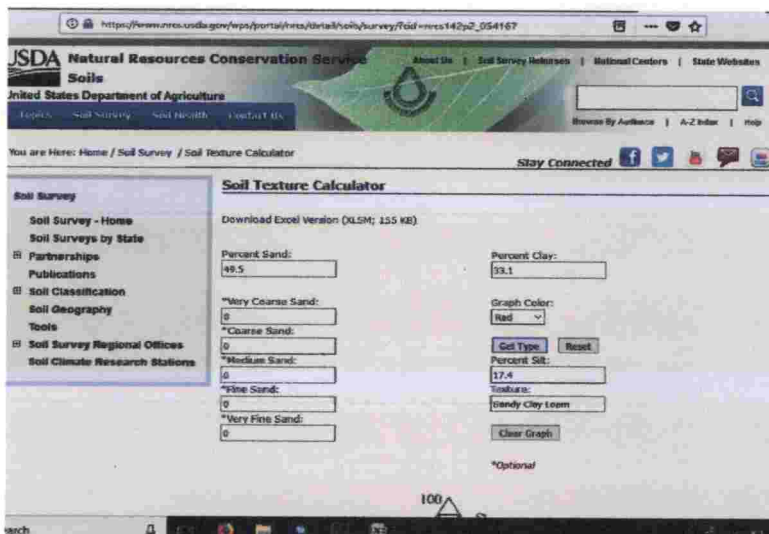
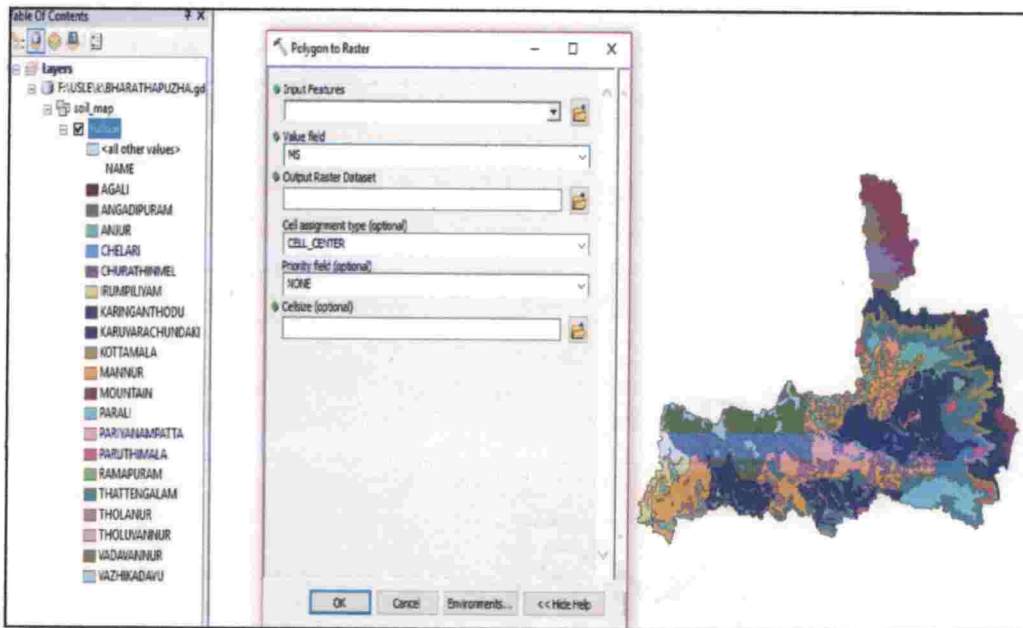


Fig. 3.17 USDA soil texture calculator

**Table 3.2 Soil parameters for MMF model**

Soil texture	MS, % w/w	BD, Mg/m <sup>3</sup>
Clay	0.45	1.1
Clay loam	0.40	1.3
Sandy clay loam	0.38	1.4
Sandy loam	0.28	1.2
Sandy clay	0.28	1.4



**Fig. 3.18 ArcGIS polygon to raster tool with selected value field 'BD'**

The  $E_t/E_0$  and A values corresponding to obtained land use classes were taken from the standard table recommended by the Morgan (2001), which is given in Table 3.3 below. The  $E_t/E_0$  and A factor map were prepared for both the year in ArcGIS by using polygon to raster option. Fig. 3.19 shows the attribute data management of the plant parameters chosen for the MMF model.

**Table 3.3 Plant parameters for MMF model**

Sl. No	Land use	A	$E_t/E_0$
1	Water body	0	0.00
2	Scrub	25	0.80
3	Rubber	30	0.90
4	Paddy	43	1.35
5	Mixed crop	35	0.85
6	Grass land	40	0.95
7	Forest	35	0.95
8	Built-up + barren land	0	0.00
9	Banana	35	0.77
10	Coconut	20	0.85

OBJECTID *	Shape *	NAME	A	Et_Eo
1	Polygon	WATERBODIES	0	0
2	Polygon	BUILD UP LAND	0	0.05
3	Polygon	RUBBER	30	0.9
5	Polygon	PADDY	43	1.35
6	Polygon	BANANA	35	0.77
7	Polygon	COCONUT	20	0.85
8	Polygon	SCRUB	25	0.8
9	Polygon	MIXED CROP	35	0.85
10	Polygon	GRASS LAND	40	0.85
11	Polygon	FOREST	35	0.95

**Fig. 3.19 Attribute data management of the plant parameters for the MMF model**

### 3.7.2 Determination of Factors in Water Phase

As described in the section 3.32, two important factors namely kinetic energy of the rainfall and the depth of overland flow were calculated.

### **3.7.2.1 Calculation of Kinetic Energy of Rainfall**

For the calculation of kinetic energy of rainfall for the year 2000, rainfall data of the year 2000 were collected from RARS Pattambi and Mannarkad rain gauge station. Kinetic energy of rainfall was calculated by using the equation 3.2, where intensity of the rainfall was taken as 25 mm/h as the location is coming under tropical climate (Morgan, 2001). Similarly, to compute the E factor for the year 2013, rainfall data of the year 2013 were considered. E factor calculation from rainfall data was done using Microsoft Excel (Appendix II) and data were interpolated throughout the watershed using IDW interpolation tool in ArcGIS. The prepared maps for the year 2000 and 2013 were named as '*E2000*' and '*E2013*' respectively.

### **3.7.2.2 Calculation of Depth of Overland Flow**

For the computation of the depth of overland flow, it is necessary to compute the moisture storage capacity of the soil, for that the prepared map layers for the year 2000 such as '*MS\_Soil*', '*BD\_Soil*', '*EHD\_Soil*', '*E<sub>v</sub>/E<sub>0</sub>2000*' etc were used. Equation 3.3 was used for the computation and the calculation which was performed using map algebra option in spatial analyst tool of ArcGIS. Finally '*Rc2000*' map of the study area was obtained. Similarly, '*Rc2013*' map was also prepared by following same operation using appropriate input layers of that particular year 2013. Applying the Equation 3.3 in raster calculator using maps of respective year, map showing the depth of overland flow was prepared for both the years ('*Q2000*' and '*Q2013*').

### **3.7.3 Determination of Factors in Sediment Phase**

In the sediment phase of the model, two components such as detachment capacity of the rainfall and runoff (F) and the transport capacity of overland flow were considered (G). According to the MMF model, the average rate of soil erosion is considered as the minimum of F and G. For the preparation of F map for the years

2000 and 2013, raster layers of K, E and A of respective years were considered. The computation was performed using raster calculator in ArcGIS window by applying the Equation 3.5.

In preparation of the transport capacity of the overland flow, slope steepness map for the year 2000 and 2013 were prepared from the SRTM DEM with 30 m resolution of the year 2000 and 2013 respectively. G factor was calculated using Equation 3.6. For the spatial calculation of G factor, raster calculator was used as done earlier.

### 3.8 AVERAGE ANNUAL SOIL EROSION RATE

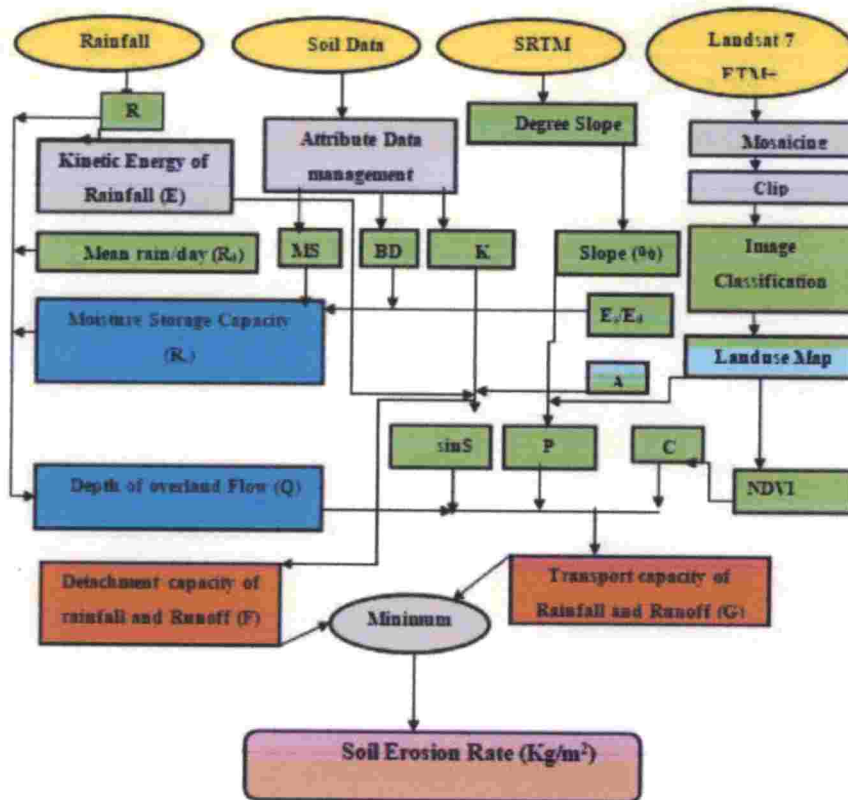
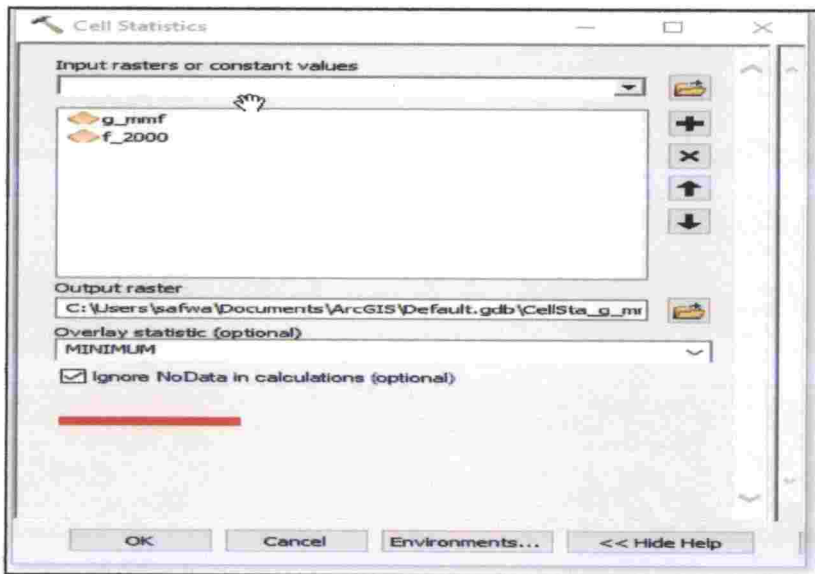


Fig. 3.20 Methodological framework adopted in MMF model



For the preparation of the final soil erosion map, detachment capacity map (F) and transport capacity of overland flow map (G) were compared. The minimum value of these two was considered as the annual soil erosion rate. Considering this fact, final soil erosion map of the study area for the year 2000 and 2013 were prepared using cell statistics option in ArcGIS as shown in Fig. 3.21. The methodological framework adopted in the MMF is shown in the Fig. 3.20.



**Fig. 3.21 Cell statistics tool in ArcGIS**

### **3.9 IDENTIFYING EROSION PRONE AREAS**

To identify the erosion prone areas of the Kunthippuzha sub-basin, the final soil erosion map obtained by RUSLE as well as MMF model for the year 2013 were used. Erosion prone areas were identified using both RUSLE and MMF model and the results were compared with priority details obtained from the soil survey department, Palakkad.

Even though, cell based quantitative assessment of soil erosion are scientifically approved, it needs not give proper and appropriate information about the dominating

factor required to control most. Factorial scoring technique based on the quantitative estimation and qualitative parameters were adopted in this study. Erosion severity zones were identified through the zonal statistical analysis. The steps involved are described below:

- Four parameters (annual rainfall, soil texture, percentage slope and land use) were used for applying factorial scoring technique. So that, respective map layers were prepared showing the spatial distribution of each factors.
- Mean soil loss from the entire study area was noted.
- A mean soil loss value for each zone in each layer was derived from the soil erosion map obtained for the year 2013.
- Mean soil loss of each zone was calculated along with its area. Mean soil loss score were assigned for each zone; for that scores were calculated for each zone by dividing its mean soil erosion value by the mean soil loss value for the entire study area. These permitted to identify most influencing zone over soil erosion.
- With the help of assigned soil loss scores, score map for each factors were prepared.
- All the score map layers were added using raster calculator to obtain total score value carried by each cells of the raster map. Based on the result, the area was divided into five erosion severity score classes: very slight (0-1.5), slight (1.5-3), moderate (3-4.5), severe (4.5-6) and very severe (> 6).

The derived maps showing erosion prone areas were verified using the priority maps referred from the Department of Soil Survey and Soil Conservation.

### **3.10 ESTIMATION OF SEDIMENT YEILD**

The soil erosion models like RUSLE and MMF give a clear indication about the extent of soil erosion but it does not give the details about the quantity of the eroded

soil reaching the outlet as well as where it is really deposited. To check how much quantity of soil reaching the outlet, Sediment Delivery Ratio (SDR) was calculated. For that the entire sub-basin was divided into 16 hydrological units. The sub-basin is having a gauging station at outlet named Pulamanthole gauging station (10° 53' 57" N and 76° 11' 50" E). The discharge and sediment data were collected from Central Water Commission, Kochi for the year 2000 and 2013. The sediment yield for the year 2000 and 2013 were calculated using the equation 3.12.

$$\text{Sediment Yield (SY), kg} = 3600 * 24 * \sum Q * S \quad (3.12)$$

Where, Q is the stream discharge (m<sup>3</sup>/s) and S is the sediment concentration at the outlet (g/l).

Mean soil erosion and areal extent of the hydrological unit was calculated to obtain net quantity of soil eroded. The sediment delivery ratio was calculated using the equation 3.13.

$$\text{SDR} = \text{SY} / \text{E} \quad (3.13)$$

Where, E is the gross erosion in kg.

### **3.11 ANALYSIS OF EFFECT OF LAND USE-LAND COVER ON SOIL EROSION**

To identify the influence of land use and land cover on soil erosion, soil erosion loss map of the study area obtained by the RUSLE and MMF model for the year 2000 and 2013 were analysed. With the integration of corresponding NDVI map prepared from the satellite images, variation of vegetation indices with land use was analysed. Spatial variation of soil erosion with respect to land use in the year 2000 and 2013 was noted in the analysis of soil erosion map along with land use map by considering zonal statistical parameters (Artun *et al.*, 2017).

## **RESULTS AND DISCUSSION**

## CHAPTER IV

### RESULTS AND DISCUSSION

This study was aimed to assess the soil erosion in Kunthippuzha sub-basin by classifying the entire sub-basin area based on the erosion severity classes. The study also analysed the effect of spatial and temporal changes in land use - land cover on the erosion. The results obtained from the study are discussed in this chapter.

#### 4.1 PREPARATION OF INPUT MAP LAYERS FOR RUSLE

##### 4.1.1 Rainfall Erosivity Factor (R Factor)

Soil erosion is very sensitive to distribution of rainfall and thereby erosivity as described by Jain *et al.* (2001). As the watershed area lacks rainfall intensity data, erosivity index factor was estimated from the daily rainfall amount. The R factor for the years 2000 and 2013 were estimated using Modified Fournier Index (MFI) value, since profound correlation is shown between MFI and R factor in the study conducted by the Kouli *et al.* (2008) in North-western Crete, Greece. Spatial variation of erosivity index was identified through mapping with the help of geospatial techniques. The estimated value of R factor ranged between 176.4 and 208.4 with the mean of  $198.3 \text{ MJ mm ha}^{-1} \text{ h}^{-1} \text{ y}^{-1}$  for the year 2000 where as for the year 2013, erosivity varied between 219.28 and 265.3  $\text{MJ mm ha}^{-1} \text{ h}^{-1} \text{ y}^{-1}$ . The mean erosivity index estimated during the year 2013 was  $250.7 \text{ MJ mm ha}^{-1} \text{ h}^{-1} \text{ y}^{-1}$ . The result is in close agreement with the findings of Kumar *et al.* (2014), in which they received an erosivity factor ranging between 150 to 450  $\text{MJ mm ha}^{-1} \text{ h}^{-1} \text{ y}^{-1}$  for the area lying closer to the present study area.

The R factor maps prepared for the years 2000 and 2013 are shown in the Fig. 4.1 and Fig. 4.2 respectively. The erosivity values vary spatially from pixel to pixel, i.e., the points at higher elevation shows higher erosivity values compared to the downstream points in both the maps, more specifically, erosivity decreases as slope

changes from steep to gentle. The high erosivity value is obtained for Mannarkad region. From 2000 to 2013, mean erosivity increased from 198.3 to 250.7 MJ mm ha<sup>-1</sup> h<sup>-1</sup> y<sup>-1</sup> as the rainfall depth increased. The estimated R factor values were compared with several studies, which were estimated by applying the same erosivity model in different parts of the Western Ghats, Kerala (Prasannakumar *et al.*, 2011b; Kumar *et al.*, 2014 and Thomas *et al.*, 2017a) which indicates the reliability of the model adopted. The erosivity factor observed by Kumar *et al.* (2014) in Nilgiri taluk was in the range of 150-450 MJ mm ha<sup>-1</sup> h<sup>-1</sup> y<sup>-1</sup> where as R factor estimated by the Prasannakumar *et al.* (2011b) in Munnar region was 98.67 MJ mm ha<sup>-1</sup> h<sup>-1</sup> y<sup>-1</sup> with standard deviation 69.78 MJ mm ha<sup>-1</sup> h<sup>-1</sup> y<sup>-1</sup>.

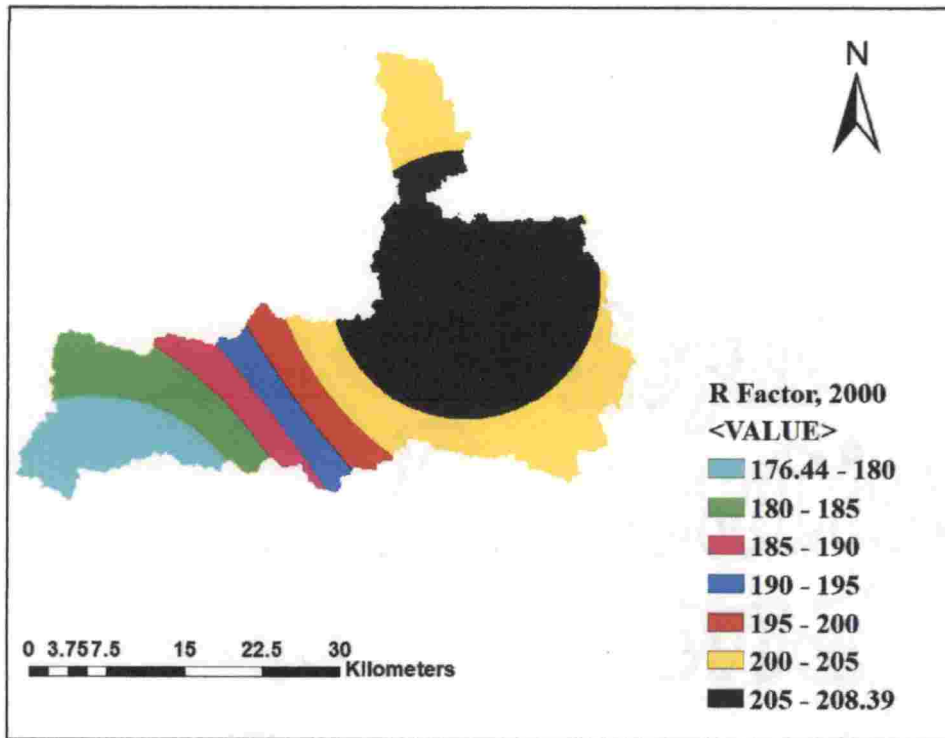


**Fig. 4.1 Spatial distribution of R factor in the year 2000 (*R2000*)**

The computed erosivity values were strongly depending on the depth of rainfall and number of rainy days. More rainfall depth received within comparatively less rainy days carries higher erosivity indices. In this study, the erosivity index of

about 265.26 MJ mm ha<sup>-1</sup> h<sup>-1</sup> y<sup>-1</sup> was obtained from the cumulative rainfall depth of 2529.1 mm on 76 days in Mannarkad region. The result was comparable with the R factor value obtained in Siruvani watershed area by Prasannakumar *et al.* (2011a), which was about 36 MJ mm ha<sup>-1</sup> h<sup>-1</sup> y<sup>-1</sup> calculated from the 1241 mm rainfall received in 79 days.

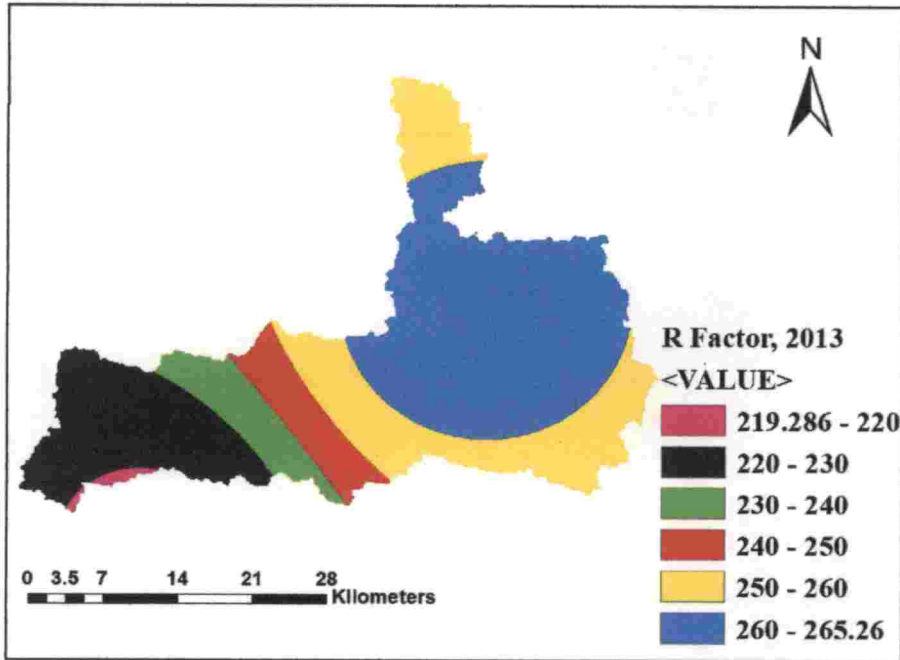
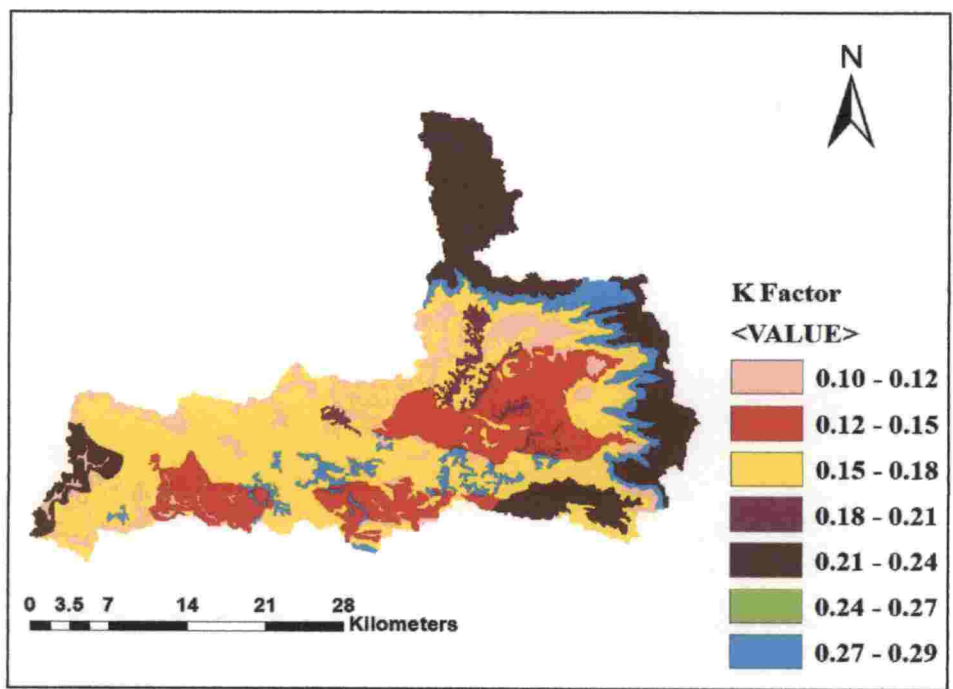


Fig. 4.2 Spatial distribution of R factor in the year 2013 (R2013)

#### 4.1.2 Soil Erodibility Factor (K)

The erosion vulnerability of the soil is greatly described by the soil erodibility factor (K). In this study, soil map prepared by the Department of Soil Survey and Soil Conservation was used for the extraction of all the soil characteristics, as the field determination of all those features requires several years of time. Five textural groups like sandy clay loam, clay loam, sandy loam, sandy clay and clay were identified in the Kunthippuzha sub-basin using textural calculator and USDA nomograph.

As stated by Wischmeier and Smith (1978), the K values vary with respect to the sticky and less sticky characteristics of the soil, where less sticky soils are more erodible compared to that of sticky soil. The computed K values from this study justifies with the statement given by the Wischmeier and Smith (1978). The soil with less fraction of clay compared to sand and silt possess higher K value, where as soil with higher clay content resulted in lesser K value. It is not a worth practice to assign K factor values according to the texture only as coarse sand is not having greater importance in determining K factor as in textural calculation.



**Fig. 4.3 Spatial distribution of K factor ( $K_{soil}$ )**

In the present study, erodibility index was found low in soil with higher clay content as reported by Belasri and Lakhouili (2016). The spatial distribution of K factor is shown in Fig. 4.3. The result shows that K factor for the study area varies from 0.10 to 0.29 t ha h ha<sup>-1</sup> MJ<sup>-1</sup> mm<sup>-1</sup>.



### 4.1.3 LS Factor

The LS factor generated for the years 2000 and 2013 are shown in Fig. 4.4 and 4.5 respectively. For the year 2000, the value of LS factor ranged from 0.001 to 31, with mean and standard deviation of 1.46 and 3.48 respectively. Similarly, for the year 2013, the value of LS factor ranged from 0.0015 to 32.6, with mean and standard deviation of 1.90 and 4.5 respectively. Higher elevation pixels carry high LS factors. The result obtained shows consistency with the results reported by Prasannakumar *et al.* (2011b) in Munnar forest division, where LS factor was in the range of 0 to 32 with mean 5.32 and standard deviation 4.63. In both the studies, LS factor was estimated by the same formula.

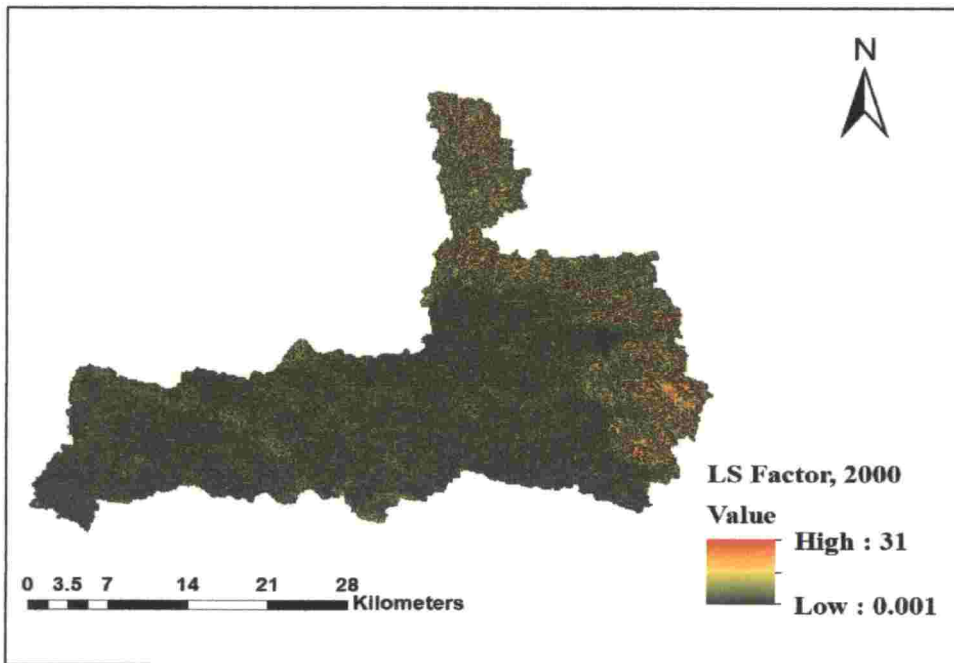


**Fig. 4.4 Spatial distribution of LS factor in the year 2000 (LS2000)**

Further, the estimated LS values were comparable with several other erosion studies conducted in different parts of Kerala which include LS ranges of 0.07 to 58.6 by Thomas *et al.* (2017a) in Muthirappuzha sub basin, 0.07 to 58.8 by Thomas *et al.* (2017b) in Pamba river basin, 19.4 by Pradeep *et al.* (2014) in Meenachil sub-

watershed and 2.028 for the year 2005 by Prasannakumar *et al.* (2011a) in Attappady region. The authenticity of the obtained LS factor map can be validated by these studies conducted in different parts of Kerala with similar terrain feature. The mean topographical factor showed an increase of 0.44 from 2000 to 2013.

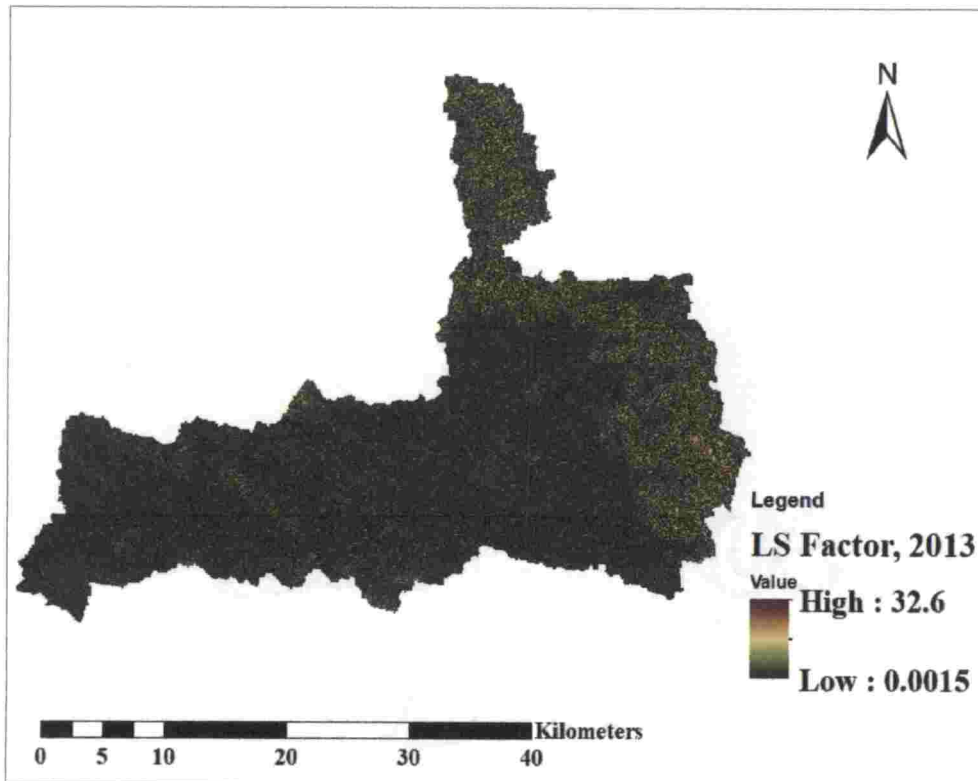


**Fig. 4.5 Spatial distribution of LS factor in the year 2013 (LS2013)**

#### 4.1.4 C Factor Map

The C factor or cover management factor very much depends on the extent of vegetation/canopy cover in the field. Considering the urbanization and notable vegetation changes in the field, the NDVI maps generated from the Landsat imageries were used to generate the C factor values for the year 2000 and 2013. In the present study, the calculated C factor through exponential scaling methods ranges from 0.0001 to 2.05 and 0.0004 to 2.15 for the year 2000 and 2013 respectively. The

higher C factor is obtained for water bodies as well as built-up plus barren lands. The obtained results were in agreement with those derived by the Bayramov *et al.* (2013) and Thomas *et al.* (2017a). The derived C factor maps for the years 2000 and 2013 are shown in Fig. 4.6 and 4.7 respectively.

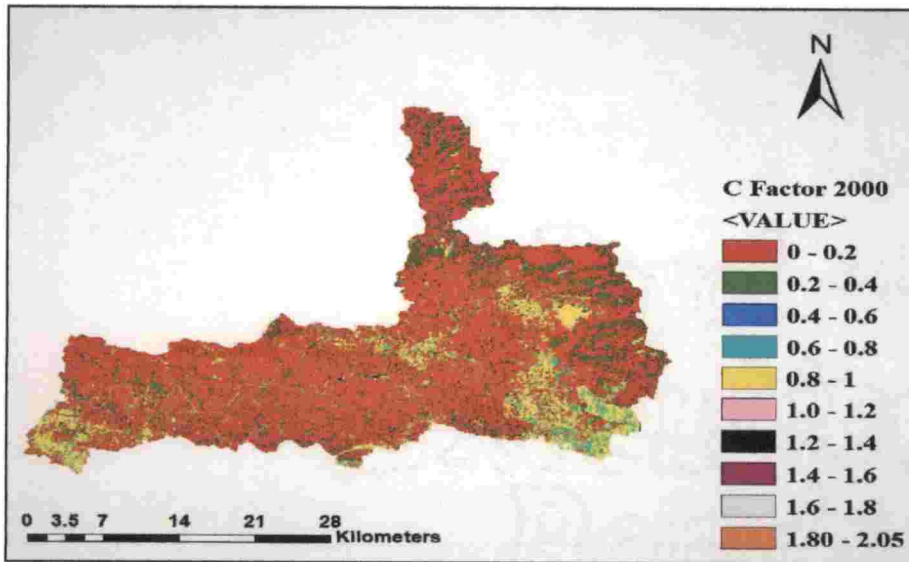


**Fig. 4.6 Spatial distribution of C factor in the year 2000 (C2000)**

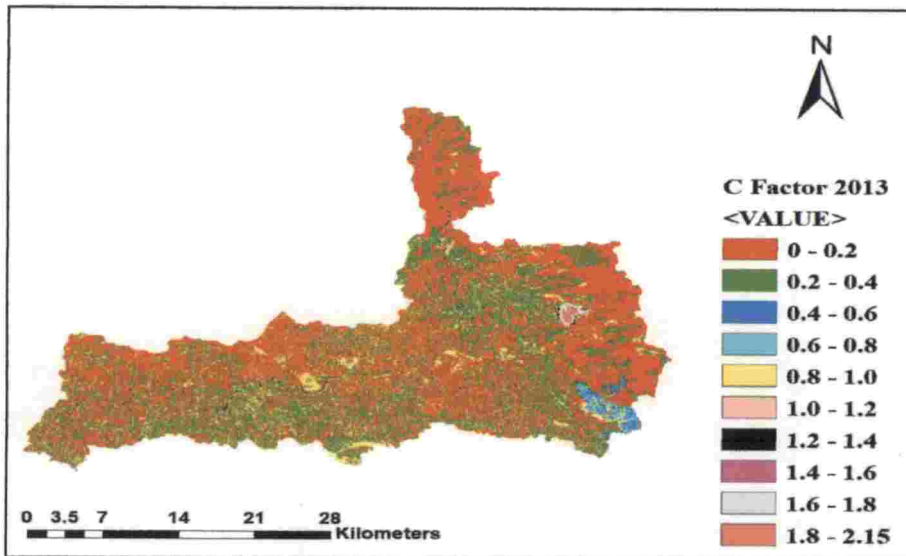


**Fig. 4.7 Spatial distribution of C factor in the year 2013 (C2013)**

The variation of mean C factor with respect to land use in the years 2000 and 2013 are shown in Fig. 4.8.

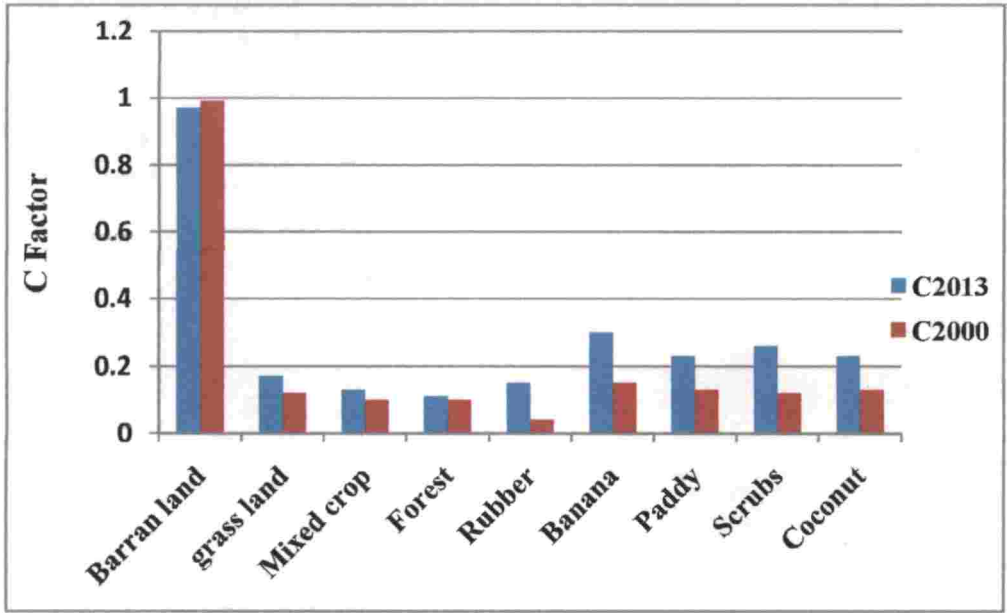


**Fig. 4.8 Spatial variation of C factor in the years 2000 and 2013**

Small variation ranging from 0 to 0.15 was observed in C factor values corresponding to the land use. The C factor value increased from the 2000 to 2013. It may be due to the decrease in the thickness of canopy as same amount of variation is not observed in the case of built-up plus barren lands (Singh and Panda, 2017). Highest C factor value observed for built-up plus barren lands in both the years as it carries less NDVI values. Lands with vegetation carries less C factor compared to built-up plus barren lands. The variation of average C factor with respect to land use for the years 2000 and 2013 are given in Appendix IV.

**4.1.5 P Factor Map**

Most of the previous studies related to RUSLE model assigned P value for the entire watershed as '1' (Shiono *et al.*, 2002; Alexakis *et al.*, 2013). The present study may be considered to be more accurate compared to above mentioned previous

108

studies as this study considered slope and land use factors for assigning the P factor, as suggested by the Wischmeier and Smith (1978). The prepared P factor maps for the years 2000 and 2013 are shown in the Fig. 4.9 and 4.10 respectively. Controlling of the erosion can be accomplished by the modification of P factor. By varying the P factor, it is possible to identify to what extent the erosion can reduce (Adedji *et al.*, 2010).

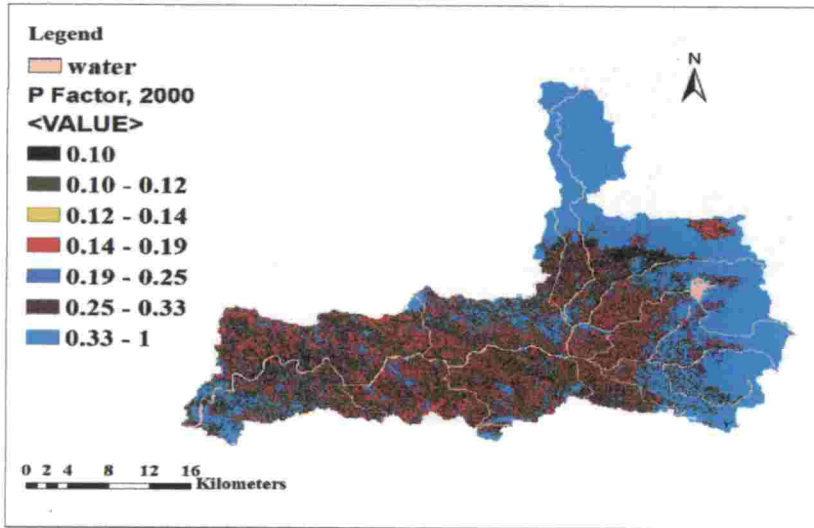


**Fig. 4.9 Spatial distribution of P factor in the year 2000 (*P2000*)**

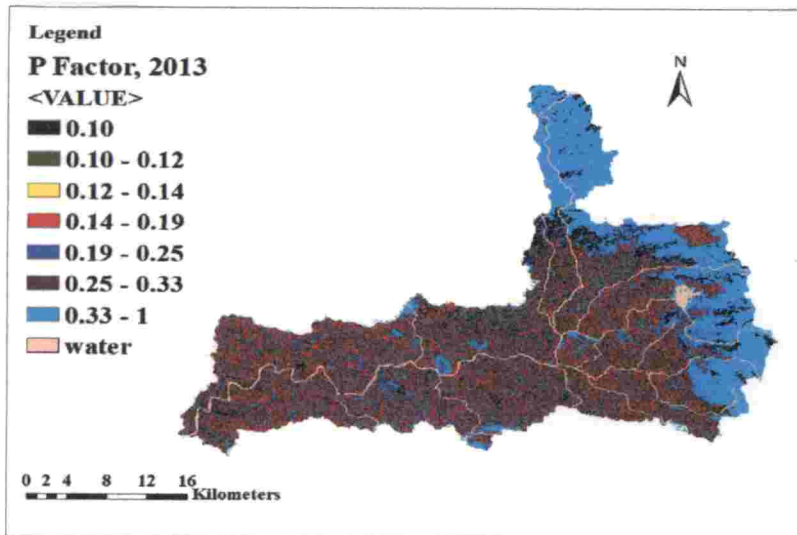


**Fig. 4.10 Spatial distribution of P factor in the year 2013 (*P2013*)**

## 4.2 PREPARATION OF INPUT MAP LAYERS OF MMF MODEL

The number of thematic map layers required for the MMF model was comparatively higher when considered to RUSLE model. Among the number of thematic maps required in this model, the detachability index map (K) for the study area prepared for RUSLE model was used in this model also. Furthermore, the RUSLE P and C factor multiplied and applied as a substitute for the MMF crop cover management factor C. The details about all prepared input map layers for the MMF model were described in this section.

The plant parameters like  $E_t/E_0$  and A value, the soil parameters like MS and BD were assigned for each land use types and soil textures respectively using the values suggested by Morgan (2005). The similar method was followed by Barman *et al.* (2013) and Tesfahunegn *et al.* (2014) also. The EHD maps were prepared by assigning the value obtained with soil map instead of following Morgan (2005), which enhances the accuracy of the preparation of EHD layer. The maps related to soil textures like MS and BD are shown in Fig. 4.11 and Fig. 4.12 respectively. In Fig. 4.13, spatial distribution of EHD values are shown. Similarly, the 'A' values for the years 2000 and 2013 are shown in Fig. 14 and Fig. 15 respectively. The  $E_t/E_0$  map prepared for the years 2000 and 2013 are shown in Fig. 16 and Fig. 17.

The factor C in MMF model is same as the combined form of C and P factors in RUSLE model. While applying the equation to calculate transport capacity (G) of rainfall and runoff, the RUSLE C and P factor were substituted instead of adopting Morgan (1984) C values as done by Barman *et al.* (2013). The derivation of MMF C factor from RUSLE C and P was done according to Tesfahunegn *et al.* (2014), which increased the calculation accuracy.

The slope maps derived from the SRTM DEM were used and sin of the angle values was calculated. The slope factor estimated for the years 2000 and 2013 are

shown in Fig. 18 and Fig. 19 respectively. The mean steepness of the slope for the year 2000 was 0.17, which changed to 0.19 during the year 2013.

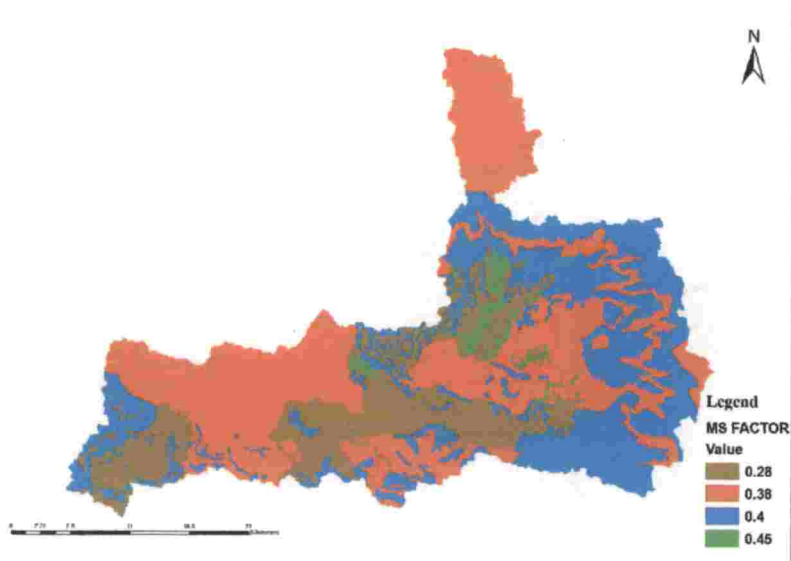


**Fig. 4.11** Spatial distribution of MS values (*MS<sub>soil</sub>*)

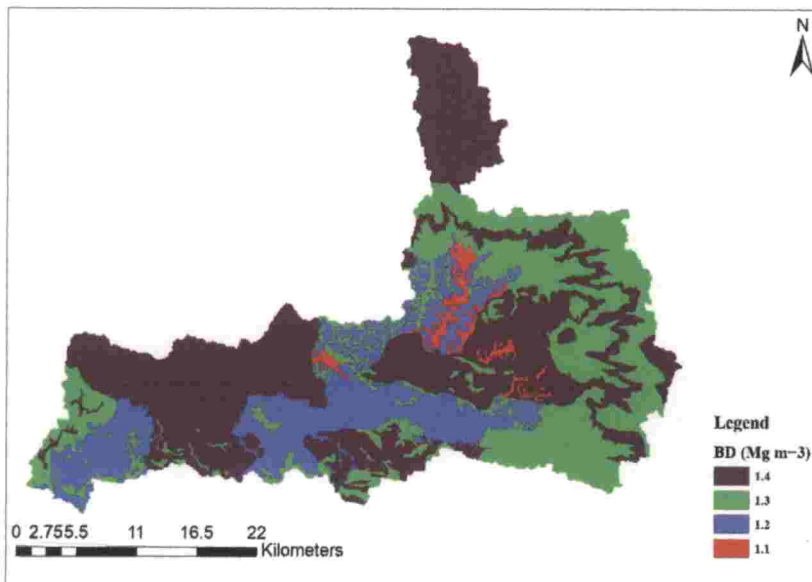


**Fig. 4.12** Spatial distribution of BD values (*BD<sub>soil</sub>*)

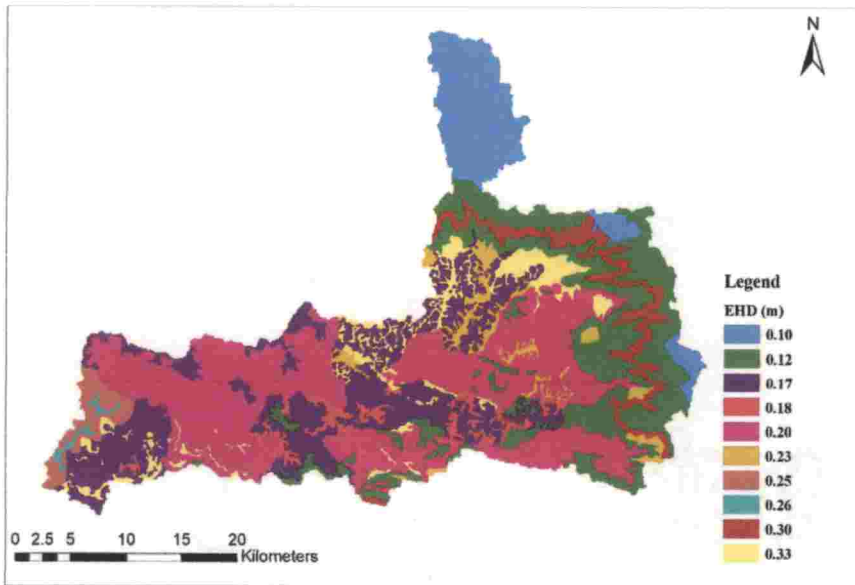


Fig. 4.13 Spatial distribution of EHD values (*EHD<sub>soil</sub>*)

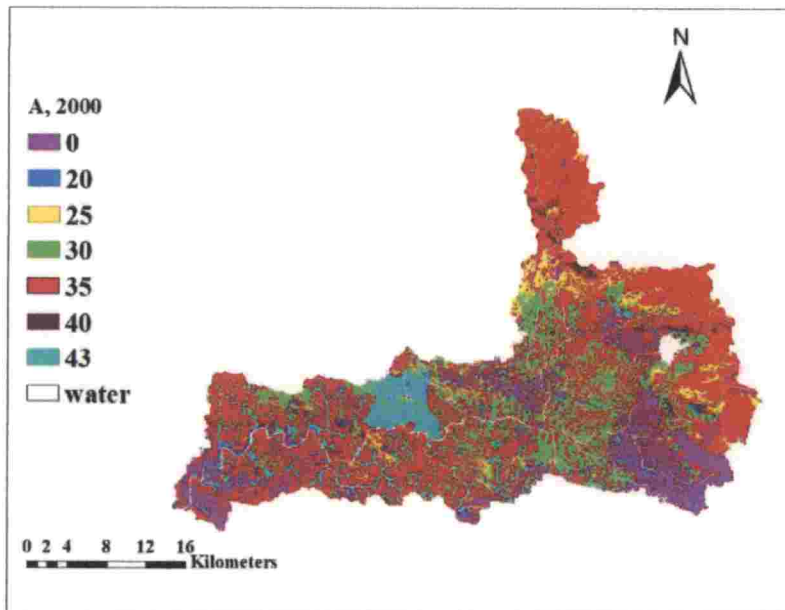


Fig. 4.14 Spatial distribution of 'A' values of the year 2000 (*A<sub>2000</sub>*)



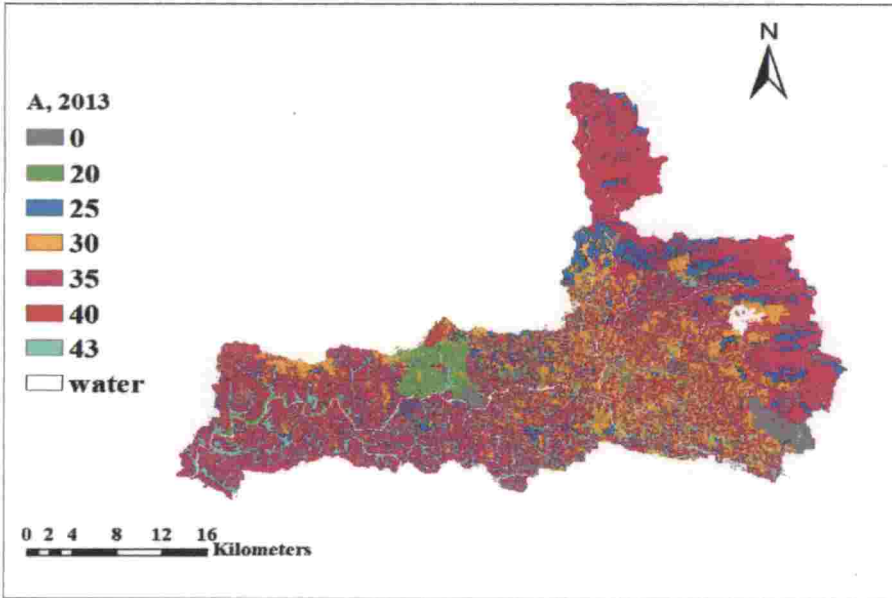


Fig. 4.15 Spatial distribution of 'A' values of the year 2013 ( $A_{2013}$ )

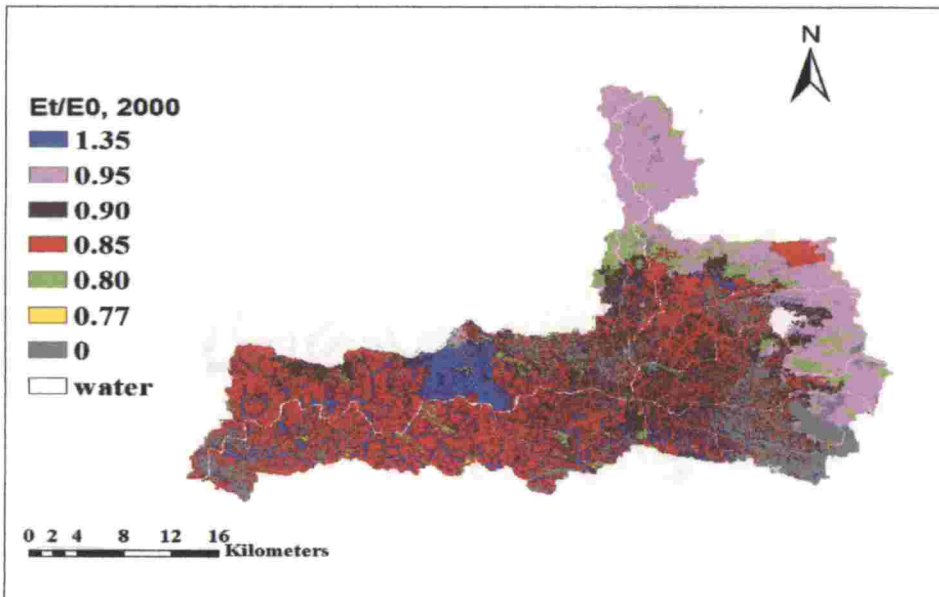
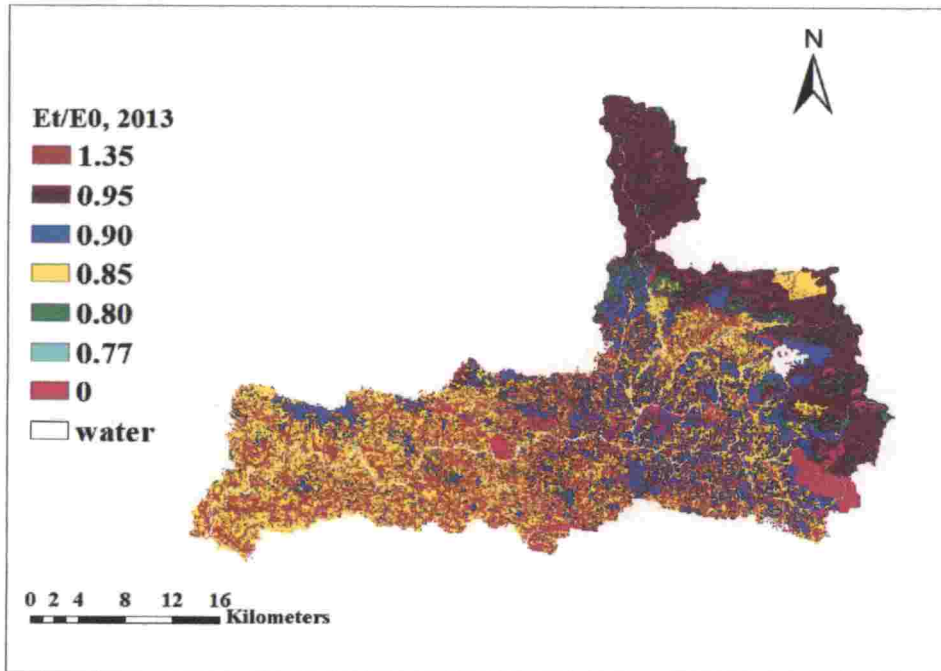
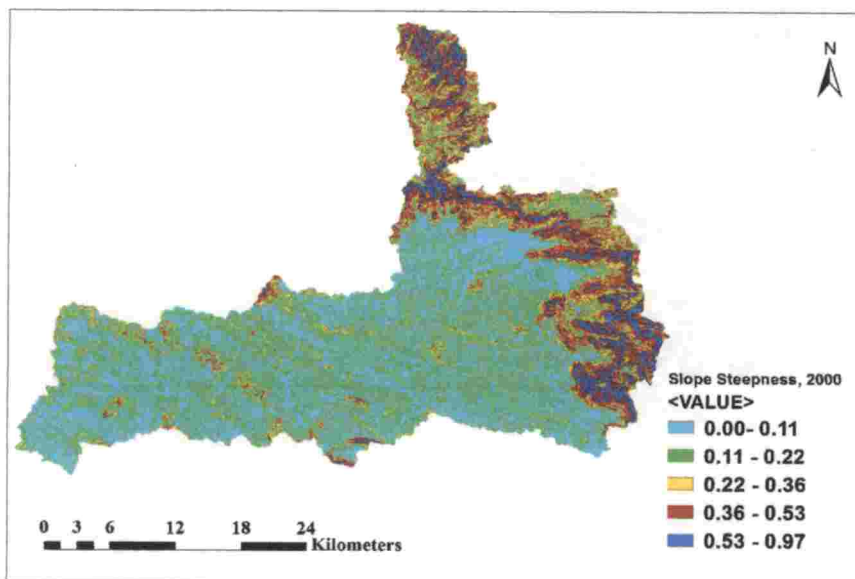


Fig. 4.16 Spatial distribution of  $E_t/E_0$  values of the year 2000 ( $E_t/E_0_{2000}$ )



**Fig. 4.17 Spatial distribution of  $E_t/E_0$  values of the year 2013 ( $E_t/E_0_{2013}$ )**



**Fig. 4.18 Slope steepness map of the year 2000 ( $S_{2000}$ )**

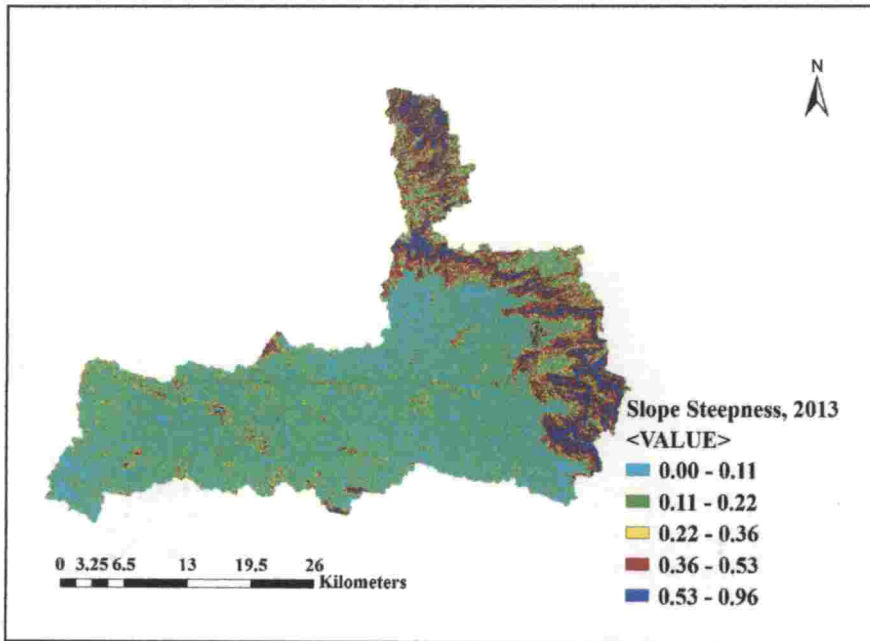


**Fig. 4.19 Slope steepness map of the year 2013 (S2013)**

The calculation of MMF factors was performed in two phases as described in the chapter III.

#### **4.2.1 Determination of Factors in Water Phase**

##### **4.2.1.1 Kinetic Energy of Rainfall Map (E)**

To prepare the kinetic energy of rainfall map, the annual rainfall depth (mm) for the years 2000 and 2013 obtained from Pattambi and Mannarkad rain gauge stations were interpolated using IDW interpolation tool as done to prepare erosivity map for the study area (Prasannakumar *et al.*, 2011b). The annual rainfall obtained at Pattambi rain gauge station during the year 2000 and 2013 were 1674.6 mm (in 52 days) and 2417.3 mm (in 76 days) respectively. Similarly, the rainfall obtained at Mannarkad rain gauge station were 2047 mm (in 67 days) and 2529.1 mm (in 76 days) respectively for the same years.

The kinetic energy factor was determined using the equation suggested by the Morgan (2005) specifically for tropical climates. Intensity of rainfall was taken as 25 mm/h as done by Morgan (2001) and Barman *et al.* (2013) for tropical climates. The lack of intensity data affects the overall accuracy of this model. The kinetic energy maps generated for the years 2000 and 2013 are shown in Fig. 4.20 and 4.21 respectively. The mean kinetic energy of rainfall obtained for the year 2000 was 47742.4 J/m<sup>2</sup>. The E value increased to 61622.7 J/m<sup>2</sup> in the year 2013 as the rainfall depth increased. The generated E value for the Kunthippuzha sub-basin resembles with the E value found at Majuli island of Assam by Barman *et al.* (2013), where it was 49294.1 J/m<sup>2</sup>. The E value will vary linearly with the rainfall distribution, since they are positively correlated. Bhaware (2006) obtained E value of about 22979.7 J/m<sup>2</sup> in Doon valley, Dehradun from annual rainfall of 954.68 mm, which was in proportional to the obtained E factor in this study.

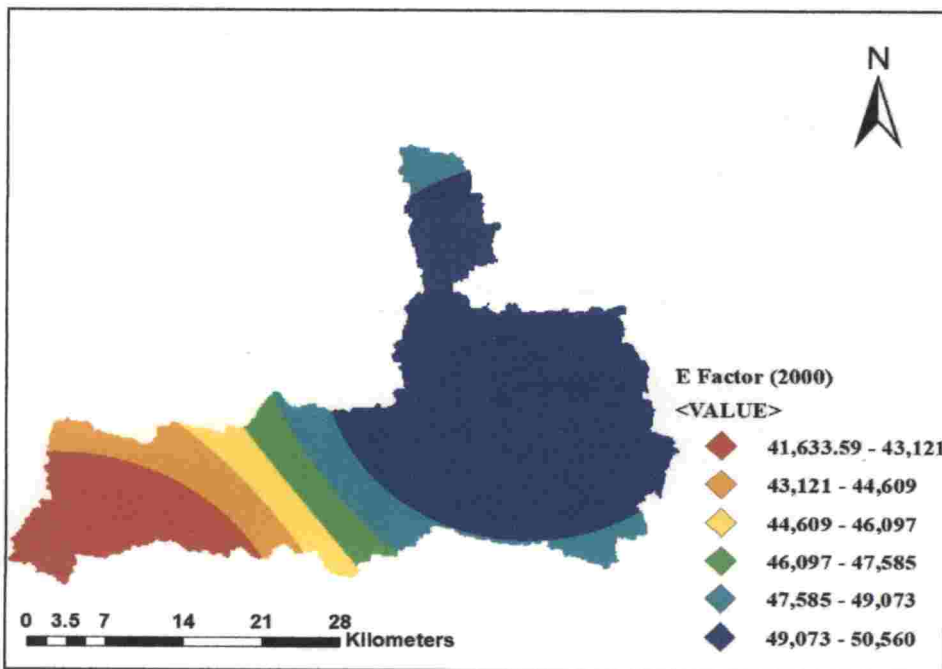


**Fig. 4.20** Spatial distribution of E factor in the year 2000 (*E*2000)

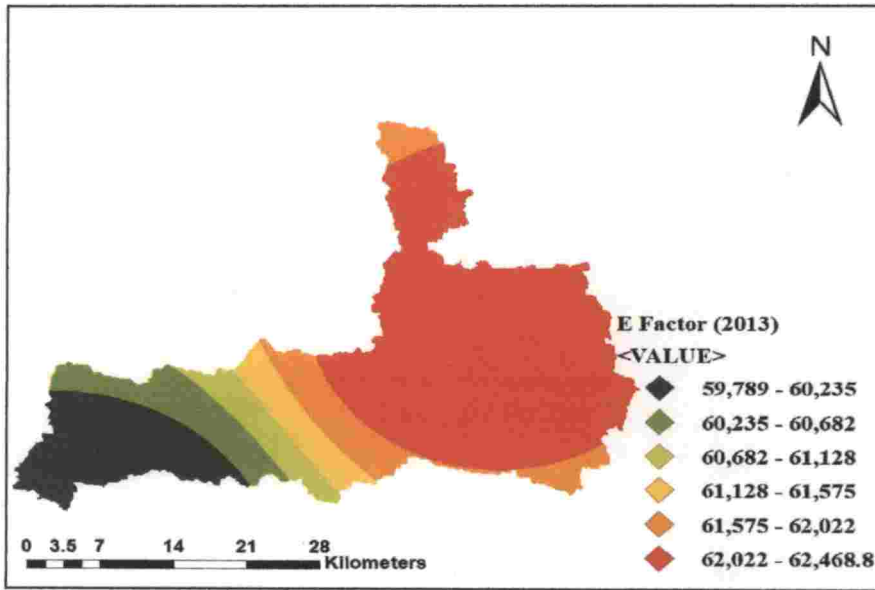


**Fig. 4.21 Spatial distribution of E factor in the year 2013 (*E*2013)**

As the kinetic energy factor depends mainly on the rainfall distribution, spatial variation of E factor shows similar trend as the rainfall distribution. In both the year 2000 and 2013, the E factor values increases towards north eastern part of the sub-basin as the elevation of the terrain showed similar trend. The maximum kinetic energy was observed around Mannarkad region as it received maximum rainfall in both the year (Thlakma *et al.*, 2018).

#### 4.2.1.2 Depth of Overland Flow (*Q*)

To calculate the depth of overland flow (*Q*, mm), interpolated rainfall depth data, moisture storage capacity of the soil ( $R_c$ , mm) and interpolated mean rain depth per day map were used for both the years 2000 and 2013. Mean rainy depth/day for the years 2000 and 2013 were 31 mm and 32.8 mm respectively. The moisture storage capacity ( $R_c$ ) of the soil was calculated as a function of MS, BD, EHD, and  $E_v/E_0$ . The spatial variation of  $R_c$  factor for the years 2000 and 2013 are shown in Fig. 4.22 and Fig. 4.23 respectively. In the year 2000, the mean moisture storage capacity of the soil was 70.3 mm which reduced to 66.1 mm by the year 2013, which

indicated the increased runoff capacity with the reduction of vegetation cover (Tesfahunegn *et al.*, 2014).

The analysis of  $R_c$  map with soil texture showed that the highest  $R_c$  value was found to be in clay soil in the year 2000 which was about 93.6 mm and least value was found in sandy loam soil (45.5 mm). Similar trend was found in the year 2013 also. These results were in agreement with the general characteristics of different textures of the soil (Wischmeier and Smith, 1978).

The depth of overland flow ( $Q$ , mm) by rainfall and runoff obtained in the year 2000 varied from 2.9 mm to 2047 mm with the mean of 500.4 mm whereas in the year 2013 it was in the range of 4.6 mm to 2529.1 mm with the mean of 748.1 mm. The increase in  $Q$  value increases the chances of rise in erosion rate in the sub-basin (Tesfahunagn *et al.*, 2014). The  $Q$  factor map generated for the years 2000 and 2013 are shown in the Fig. 4.24 and Fig. 4.25 respectively.

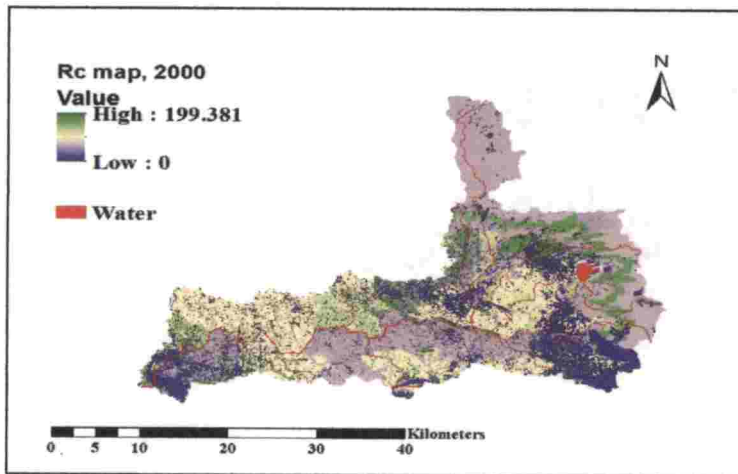


**Fig. 4.22 Spatial distribution of  $R_c$  factor in the year 2000 ( $R_c$  2000)**

The  $Q$  value highly depends on the rainfall distribution and soil parameters as described by Morgan (2005). The generated  $Q$  factor map shows that in the year 2013, sandy loam soil experiences more  $Q$  value as it had obtained the mean rainfall of 2483.6 mm. Even though clay soil obtained higher mean value of rainfall as well

as lesser interception, it experienced lesser Q value which proves the influence of the textural properties over the overland flow and thereby on soil erosion.

In the year 2000, very less fraction of interception was performed over the sandy clay soil; it was clearly visible in its mean Q value as it experiences highest Q among others.

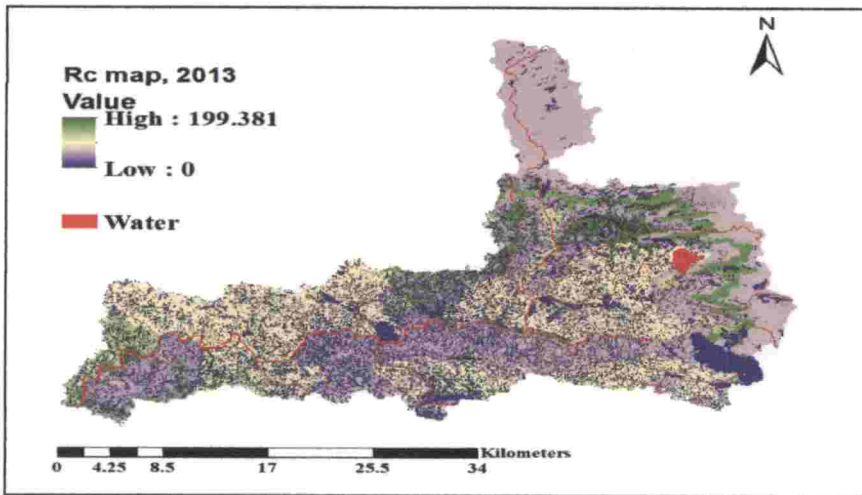


Fig. 4.23 Spatial distribution of  $R_c$  factor in the year 2013 ( $R_c$  2013)

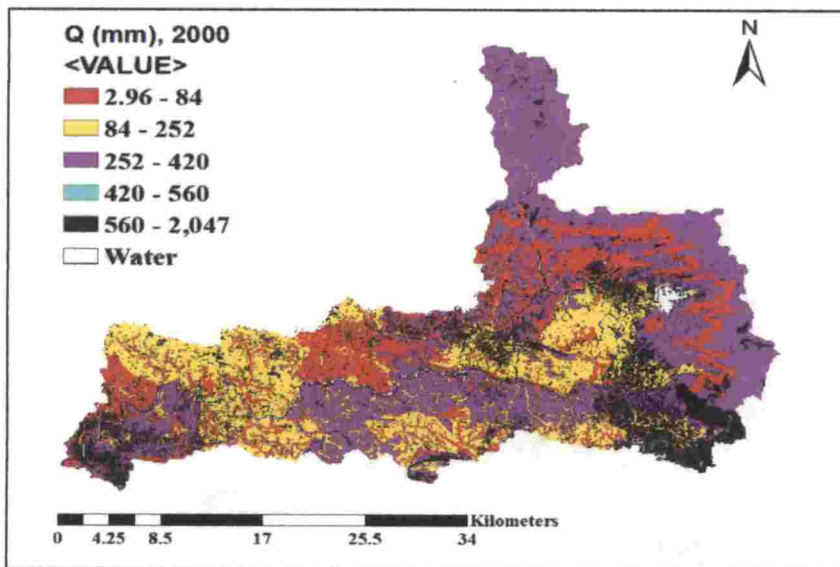
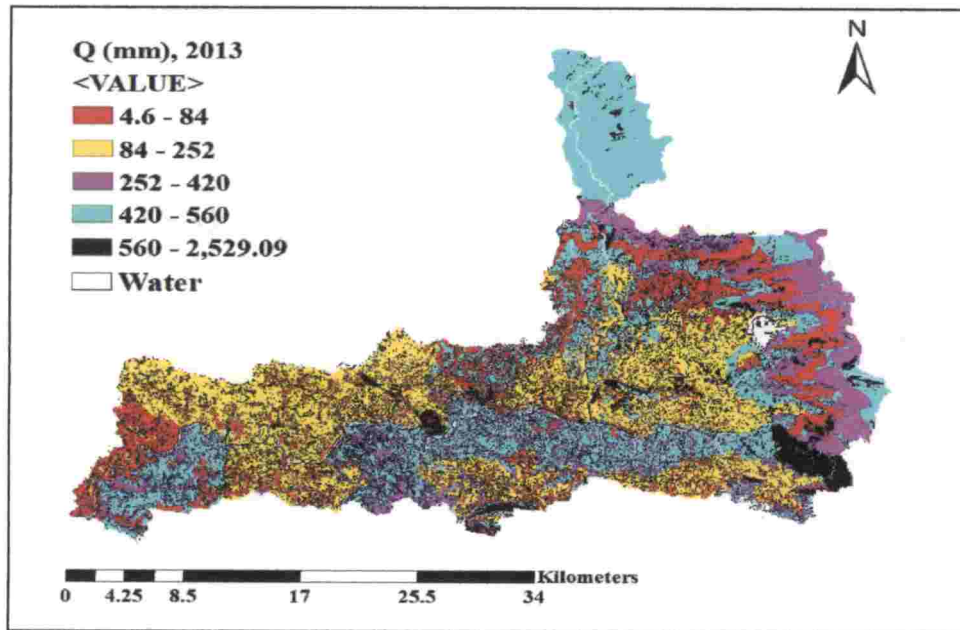


Fig. 4.24 Spatial distribution of Q factor in the year 2000 ( $Q_{2000}$ )



**Fig. 4.25 Spatial distribution of Q factor in the year 2013 (Q2013)**

#### 4.2.2 Determination of Factor in Sediment Phase

According to MMF model, minimum of the transport capacity of the rainfall and runoff and the rate of soil detachment is considered as soil erosion rate as described in the chapter III. The transport capacity of rainfall and runoff (G) was estimated for the years 2000 and 2013. In 2000, it was found to be in the range of  $9.8 \times 10^{-9}$  to  $3866.1 \text{ kg/m}^2$  with mean 97.6 whereas in the year 2013, it was in the range of  $6.1 \times 10^{-8}$  to  $6049.4 \text{ kg/m}^2$  with mean of  $220.3 \text{ kg/m}^2$ . The result was in agreement with the result obtained by Barman *et al.* (2013) at Majuli island of Assam. The slope steepness (S), changes in land use, urbanization in many parts of the study area and higher amount of precipitation contributing to raise depth of overland flow leads to transport more soil from its original location. The transport capacity map (G) prepared for the year 2000 and 2013 are shown in Fig. 4.27 and Fig. 4.28.

The rate of soil detachment (F) by rainfall and runoff was calculated by considering soil detachability index (K), kinetic energy of rainfall and fraction of



interception contributing evapo-transpiration and stem flow (A). The analysis of the map generated showed that the areas with less vegetal cover compared to other areas experience more soil loss even though they were obtaining similar amount of rainfall. The result was in agreement to the Tesfahunegn *et al.* (2014).

In the year 2000, the F value generated for the study area was ranging from 0.49 kg/m<sup>2</sup> to 14.59 kg/m<sup>2</sup> with the mean of 2.85 kg/m<sup>2</sup>. Similarly in the year 2013, it was in the range of 0.69 kg/m<sup>2</sup> to 18.09 kg/m<sup>2</sup> with mean about 4.03 kg/m<sup>2</sup>. The soil detachment rate map derived for the Kunthippuzha sub-basin of the years 2000 and 2013 are shown in the Fig. 4.29 and Fig. 4.30 respectively.

The analysis of the F map shows that in the years 2000 and 2013, maximum mean value of rainfall obtained over clay soil whereas least over the sandy clay because of the terrain feature they are located at. In the year 2000, the least interception (mean) value experienced with the soil texture sandy clay where more on clay and sandy clay loam. Combining the overall influence of the soil parameters, E values and interception, clay loam soil experienced more splash detachment (F) where sandy clay experiences lesser in the year 2000. Similarly, in the year 2013, sandy clay soil obtained least rainfall distribution as well as maximum interception. So, it showed least F value among all textures.

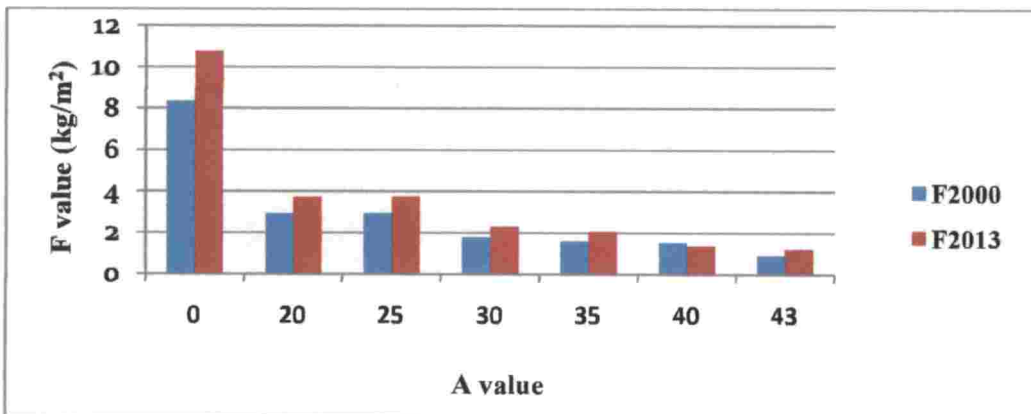


**Fig. 26 Variation F values with A factor for the year 2000 and 2013**

The variation of F value with respect to 'A' factor clearly shows the effect of vegetation for controlling soil erosion. Fig. 26 shows the variation F values corresponding to A value in the year 2000 and 2013. The mean values of R, Q, F, rainfall and A experienced over each soil texture were given in the Appendix V.

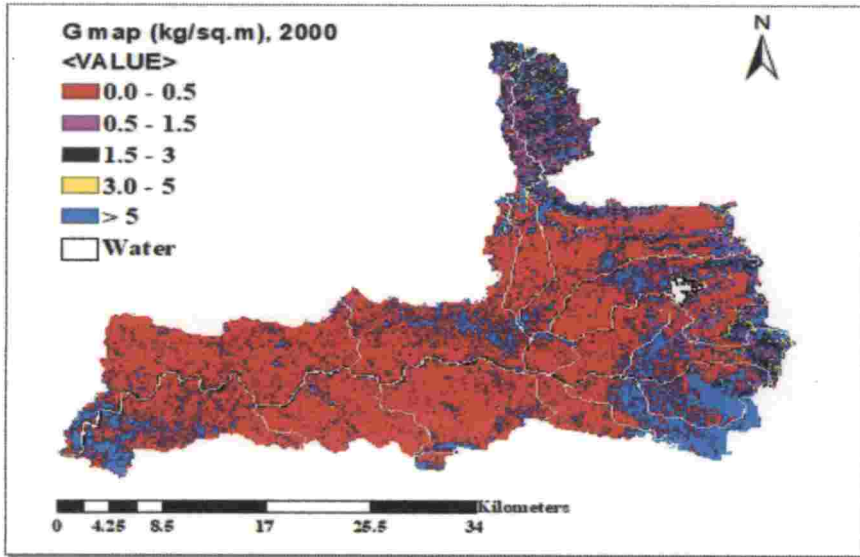


**Fig. 4.27 Spatial distribution of 'G' factor in the year 2000 (*G2000*)**

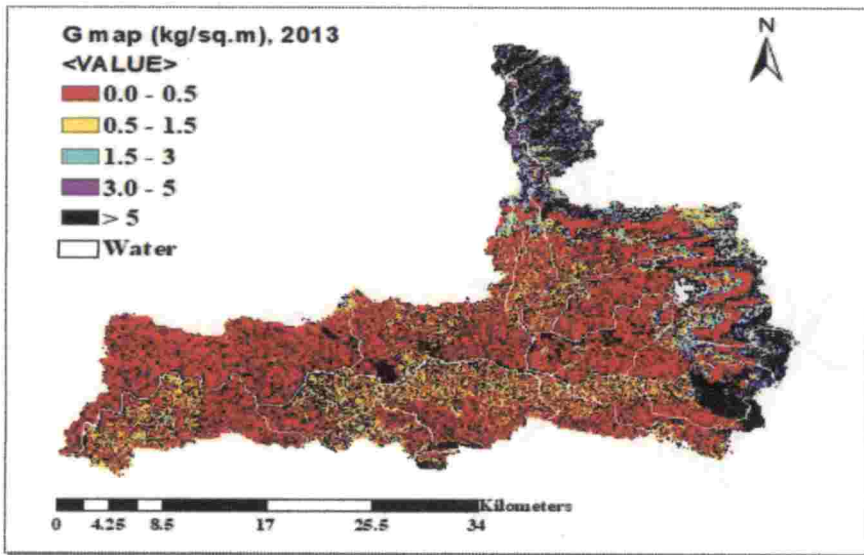


**Fig. 4.28 Spatial distribution of 'G' factor in the year 2013 (*G2013*)**

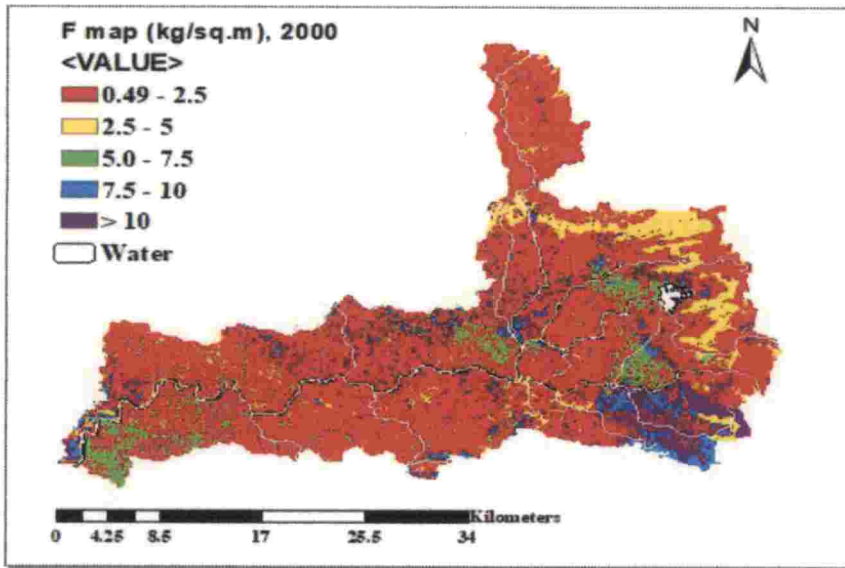


**Fig. 4.29** Spatial distribution of 'F' factor in the year 2000 (*F2000*)

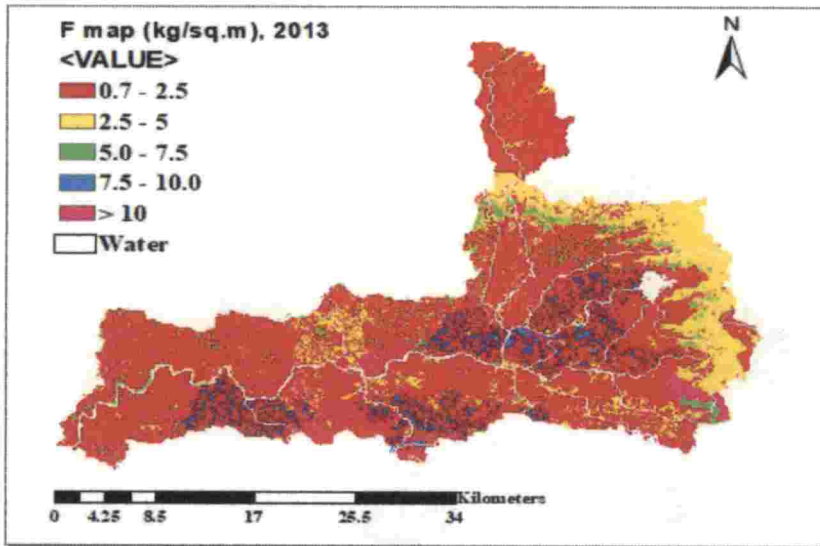


**Fig. 4.30** Spatial distribution of 'F' factor in the year 2013 (*F2013*)

### 4.3 Spatial Distribution of Soil Loss by Different Models

The spatial distribution of soil loss in the year 2000 and 2013 is described in this section. The soil erosion map for the year 2000 by RUSLE is shown in the Fig.

123

4.31. The mean soil erosion was found to be about 20.58 t/ha/y. The total quantity of soil eroded was 2056804 t/y. The obtained soil erosion was in agreement with the different studies performed in various places of Kerala having tropical climate with mountainous terrain. The north-east portion of the sub-basin is prone to more erosion. It may be due to the higher precipitation and steeper slope.

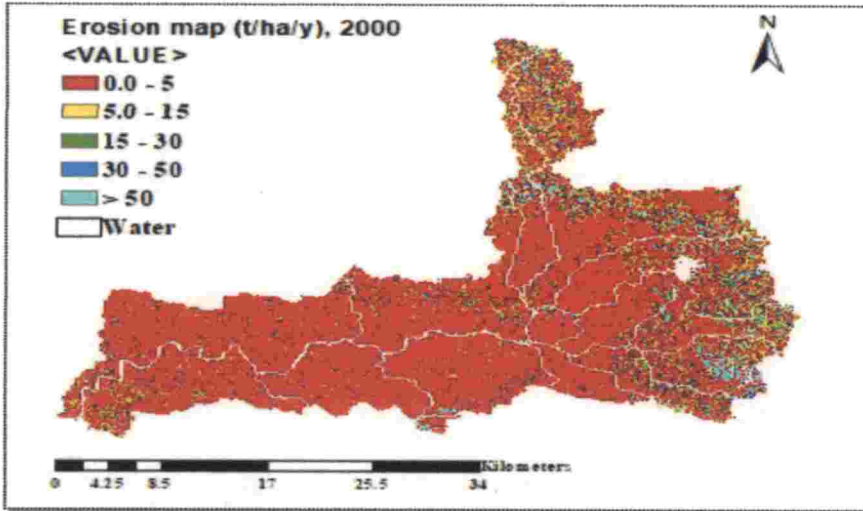


**Fig. 4.31 Spatial distribution of soil erosion by RUSLE (2000)**

Similarly, in the year 2013, soil erosion rate was increased upto 35.1 t/ha/y with net amount of 3508451 t/y. The spatial distribution of soil erosion map obtained by RUSLE model in the year 2013 is shown in the Fig. 4.32. The maps obtained in 2013 shows similar trend as obtained during 2000 but it varies quantitatively. The change identified in both maps was mainly due to the increased rainfall distribution as well as drastic changes in the land use pattern in the study area.

On comparison with several studies performed in the Western Ghats, relatively similar and comparable result was obtained in Kunthippuzha sub-basin (Prasannakumar *et al.*, 2011a; Prasannakumar *et al.*, 2011b; Prasannakumar *et al.*, 2012; Pradeep *et al.*, 2014 and Thomas *et al.*, 2017a). The relatively lesser variation in soil loss observed in these studies is mainly due to the difference in rainfall distribution as well as land use characteristics.

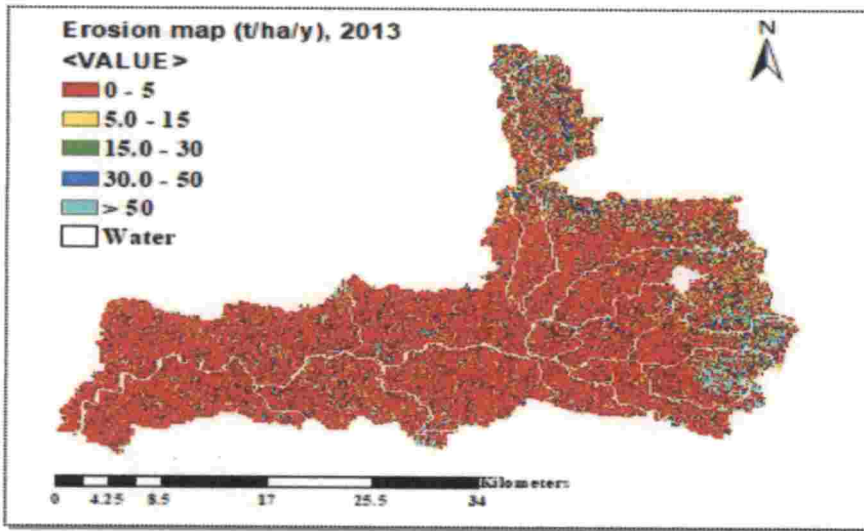


**Fig. 4.32 Spatial distribution of soil erosion by RUSLE (2013)**

The generated soil erosion map by MMF model for the year 2000 is shown in Fig. 4.33. The mean soil erosion rate was found about 18.3 t/ha/y with net quantity of 1829758 t/y. The estimated erosion was similar to those obtained by RUSLE model, the rate being a little less than that.

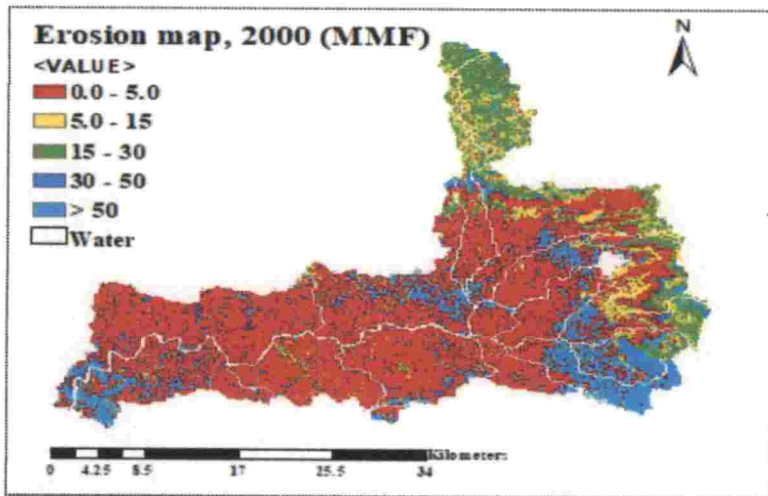


**Fig. 4.33 Spatial distribution of soil erosion by MMF (2000)**

The estimated value increased quantitatively in the year 2013. The mean average soil erosion found by this model was 32.78 t/ha/y. The Fig. 4.34 shows the

174472



spatial variation of soil loss in the year 2013. Net quantity of soil eroded was 3276332 t/y.

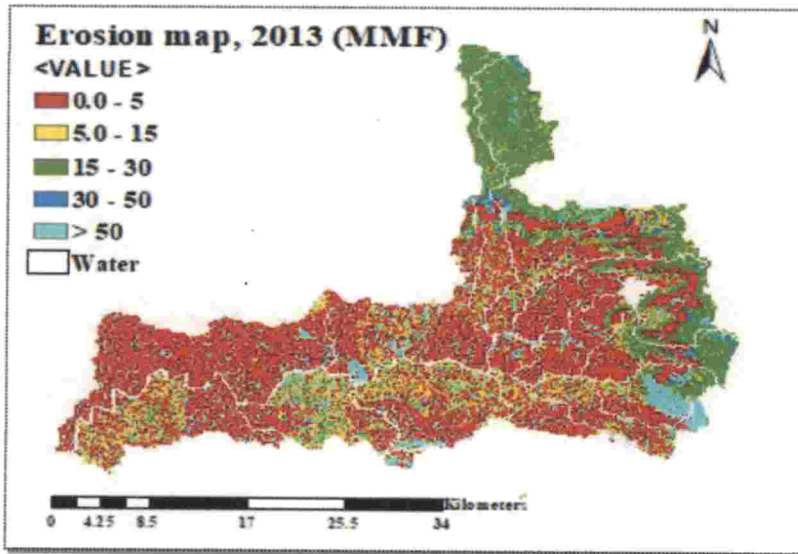


**Fig. 4.34 Spatial distribution of soil erosion by MMF (2013)**

#### **4.4 Estimation of Sediment Delivery Ratio (SDR)**

The sub-basin with 16 micro-watersheds is shown in Fig. 4.35

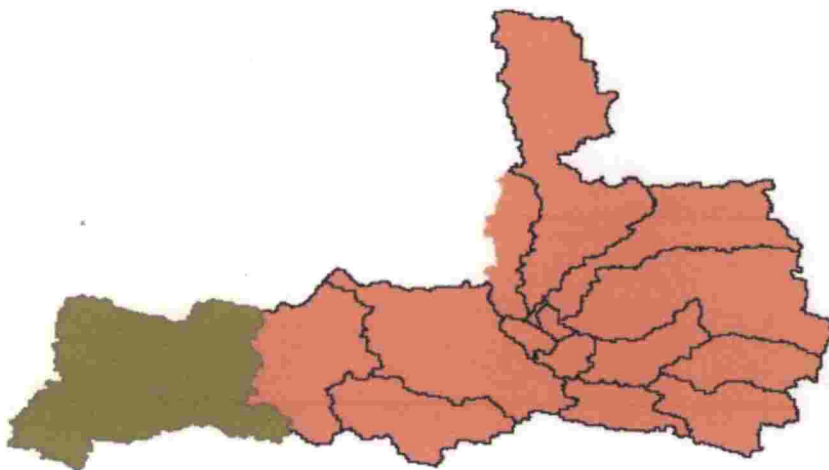


**Fig. 4.35 Kunthippuzha sub-basin with 16 micro-watersheds**

Erosion from the 822 km<sup>2</sup> area with Pulamanthole station as outlet was considered. The SDR values calculated for the years 2000 and 2013 are given in Table 4.1.

**Table 4.1. Sediment delivery ratio calculation**

Model	YEAR	Contributing area	Gross erosion (tonnes)	Sediment yield (tonnes)	SDR
RUSLE	2000	Sub-basin area for the outlet	1907439	42097.327	0.022
	2013	Sub-basin area for the outlet	3222682	106472.273	0.033
MMF	2000	Sub-basin area for the outlet	1493618	42097.327	0.028
	2013	Sub-basin area for the outlet	2707101	106472.273	0.039

Considering the SDR obtained using RUSLE in the year 2013, the average SDR calculated for the whole watershed is 0.033. The result is in agreement with the findings of Singh and Panda (2017) who calculated the SDR value in Kapgiri watershed, India.

The SDR obtained for the entire watershed was very low which indicate that even if more amount of soil gets eroded from the Kunthippuzha sub-basin, it gets deposited at intermediate locations before reaching the Pulamanthole outlet. It may be due to the trapping of eroded soil in paddy fields before reaching urban areas as in the case of Kapgiri watershed (Singh and Panda, 2017). These conclusions are based on logical assumptions that the impact of land use land cover on SDR value is influenced by many factors like topography, land use land cover, soil characteristics, transport system as well as their complex interactions (Walling, 1983; Richard, 1993).

The result obtained from the present study is also in agreement with the findings of Zhou and Wu (2008) who explained that the sediments are more prone to deposition. Zhou and Wu (2008) calculated SDR values in Chaobaihe catchment, North China. The calculated SDR values from the 6 hydrological stations were 0.001, 0.038, 0.159, 0, 0.012 and 0.036. The result showed that the SDR obtained at downstream outlet was less, as a result of increase in area.

The SDR value also highlights the inefficiencies of the conventional methods to quantify soil erosion through sediment trapping, as it does not consider the trapping of sediments in the intermediate locations inside the watershed. So, assessment of soil erosion using soil erosion models with the integration of GIS and remote sensing provides cell based details which can overcome the demerits of the conventional techniques.

#### **4.5 Erosion Severity Maps Based On Erosion Scores for the Year 2013 to Identify the Erosion Prone Areas**

This study adopted factor related scoring techniques based on the zonal statistics to prioritize the Kunthippuzha sub-basin based on erosion severity classes. For the development of hydrologic response zones, the land use maps, soil texture maps, reclassified rainfall distribution maps and reclassified slope maps were taken (Haregeweyn *et al.*, 2017). Zonal mean soil losses were derived for each layer from the obtained soil erosion maps by RUSLE and MMF models. Fig. 4.36 to 4.38 shows the zonal elements of slope, rainfall, soil texture and land use layers and their corresponding obtained average soil losses by RUSLE as well as MMF models.

Among different ranges of rainfall distribution, by MMF model 74.2% of erosion occurred within the range of rainfall > 2500 mm which accounted for 61% of the study area. Lesser contribution observed under the 2460-2480 mm range, which was about 5.9% accounted for 6.1% of the study area. Similarly, in the case of RUSLE model, it showed similar trend, but it varied quantitatively. The highest



fraction of soil loss was 78.7% and lowest was 4.7%. The mean soil erosion corresponding to each range and its areal distribution is given in the Appendix. VI.

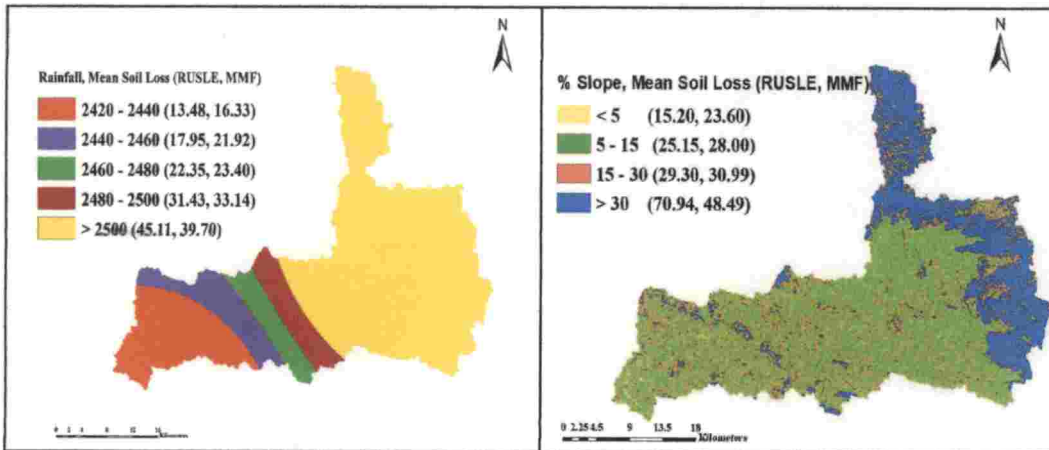


Fig. 4.36 Zonal elements of rainfall and slope with their corresponding mean soil erosion by RUSLE and MMF

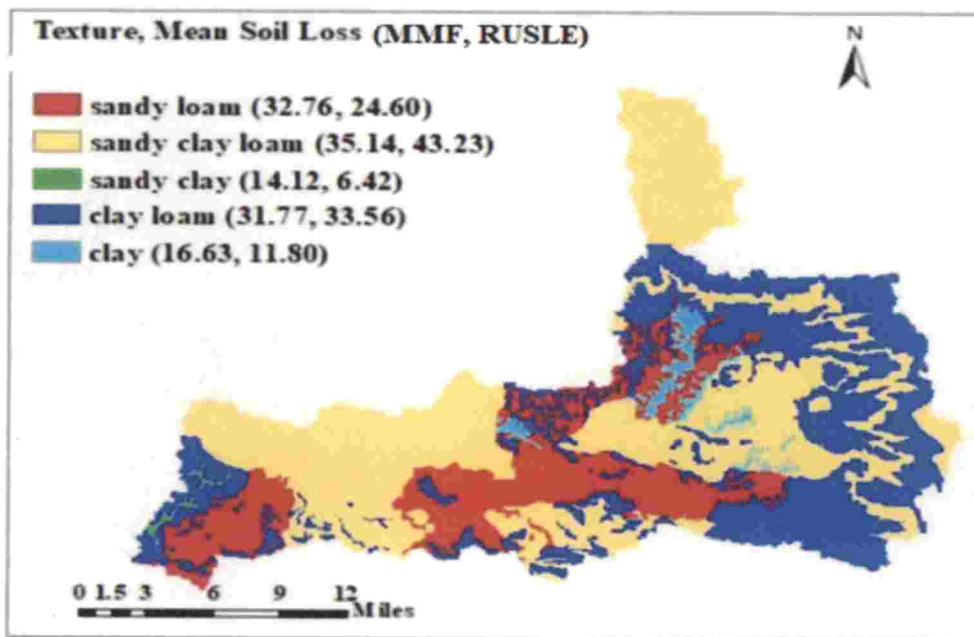
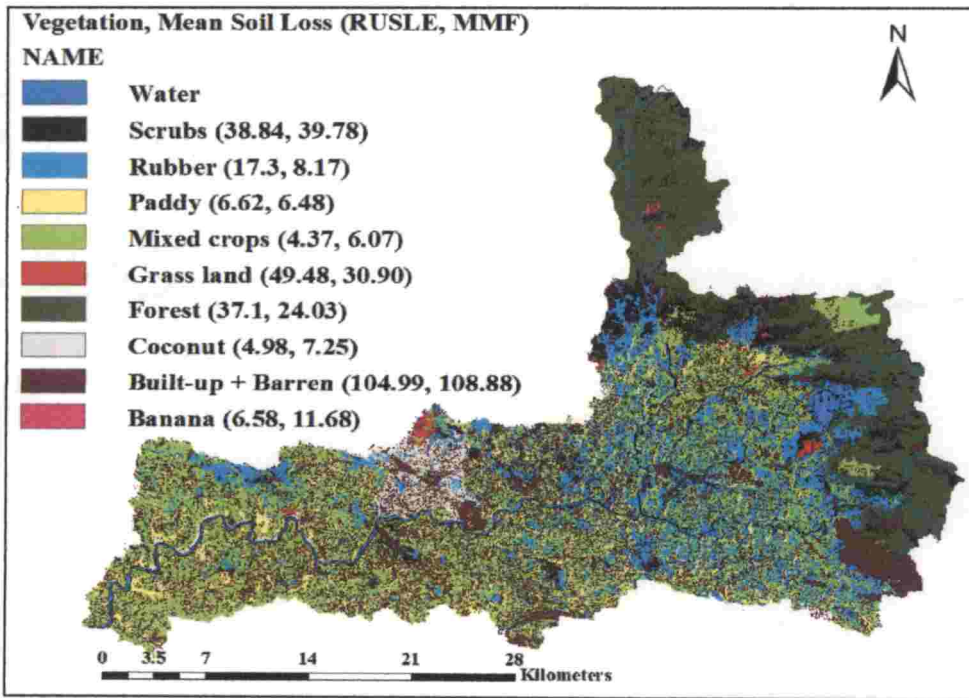


Fig. 4.37 Zonal elements of soil with mean soil erosion by RUSLE and MMF



**Fig. 4.38 Zonal elements of vegetation with mean soil erosion by RUSLE and MMF**

Among the slope classes, by MMF model, very gentle slope lands accounted for 7.3% (10.14% of area), gently sloping lands for 34.73% (40.71% of area), steeply sloping lands for 26.21% (27.73% of area) and very steep slopes for 31.76% (21.4% of area) of the soil losses. By RUSLE model, it was 4.4, 28.06, 23.12 and 43.37% respectively. Maximum soil erosion was observed at very steeper slope in both the models (Appendix VIII).

Among the soil textures, highest mean soil erosion was observed in the case of sandy clay loam in both the models. The mean values, total erosion and areal distribution corresponding to each soil texture are given in Appendix VII. Among land uses, by MMF model, high average soil losses of about 108.9 t/ha was experienced under built-up plus barren land whereas least was about 6.1 t/ha under

mixed crop. Similarly by RUSLE model, the values was 104.9 and 4.4 t/ha respectively for built-up plus barren land and mixed crop (Appendix IX).

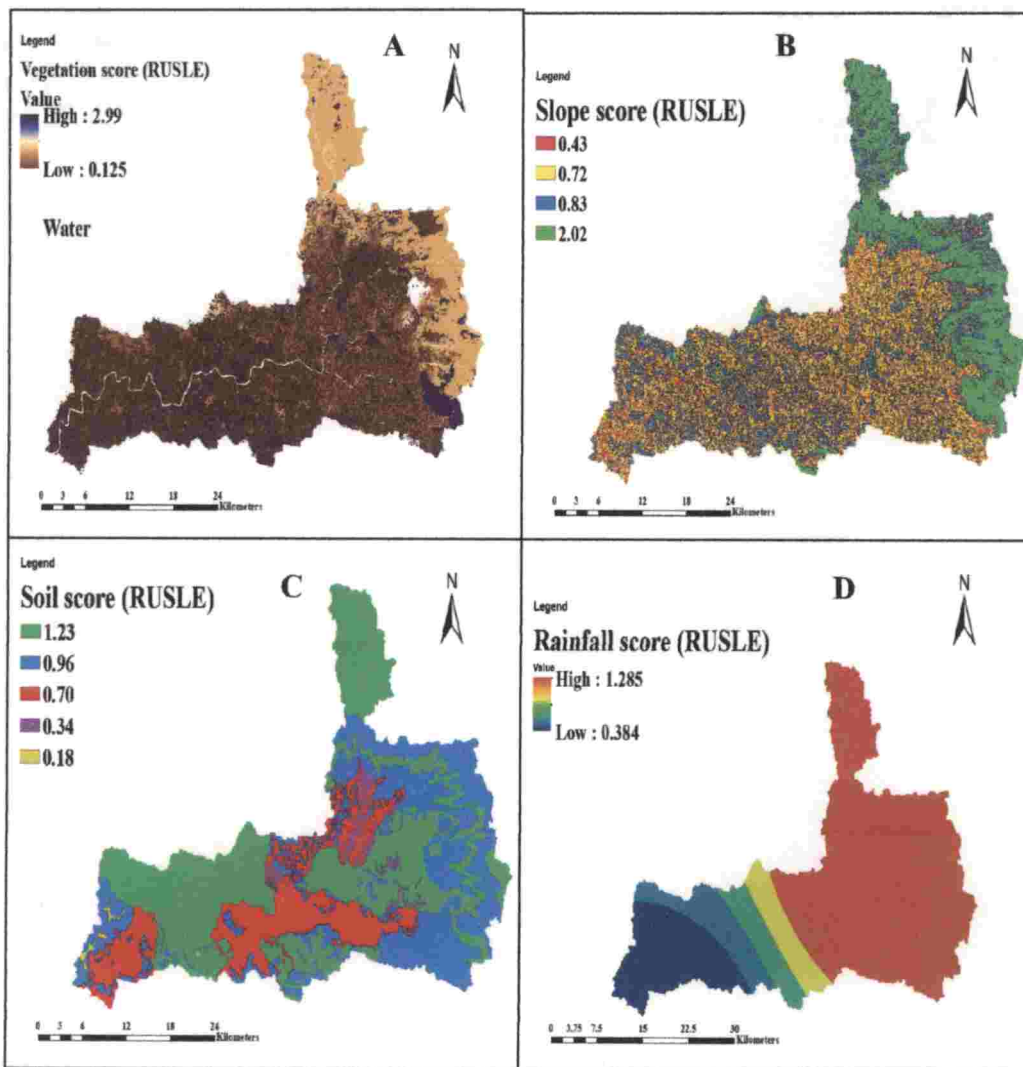


**Fig. 4.39 Soil loss scores for major soil loss factor layers: (a) land use score (b) slope score (c) soil score (d) rainfall score (RUSLE)**

In accordance with the zonal analysis results, mean rate of soil erosion as well as the relative scores were calculated for each layer. The scores corresponding to each layer are given in Appendix (V-IX). The score maps related to land use, slope, soil and rainfall were generated from RUSLE and MMF model which are shown

respectively in Fig. 4.39 and Fig. 4.40. Combining the relative scores of each maps, total score map of the Kunthippuzha sub-basin was generated. As explained in the chapter III, the scores were divided into the five classes. The final soil erosion risk maps with severity classes generated using RUSLE and MMF model is shown in Fig 4.41 (A-B) respectively.

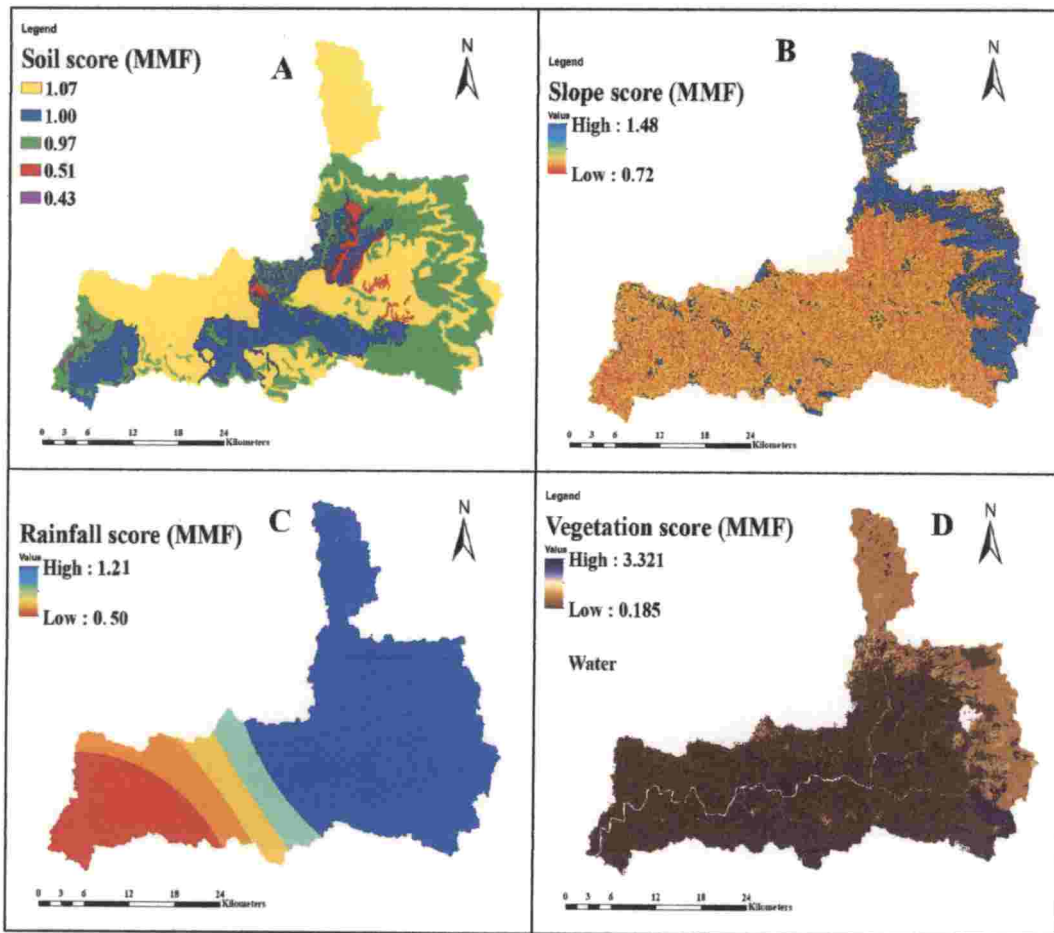


**Fig. 4.40 Soil loss scores for major soil loss factor layers: (a) soil score (b) slope score (c) rainfall score (d) and land use score (MMF)**

The Erosion prone areas were identified and they are categorized as very slight, slight, moderate, severe and very severe erosion affecting areas. The range of erosion classes with its areal extent are given in Table 4.2.

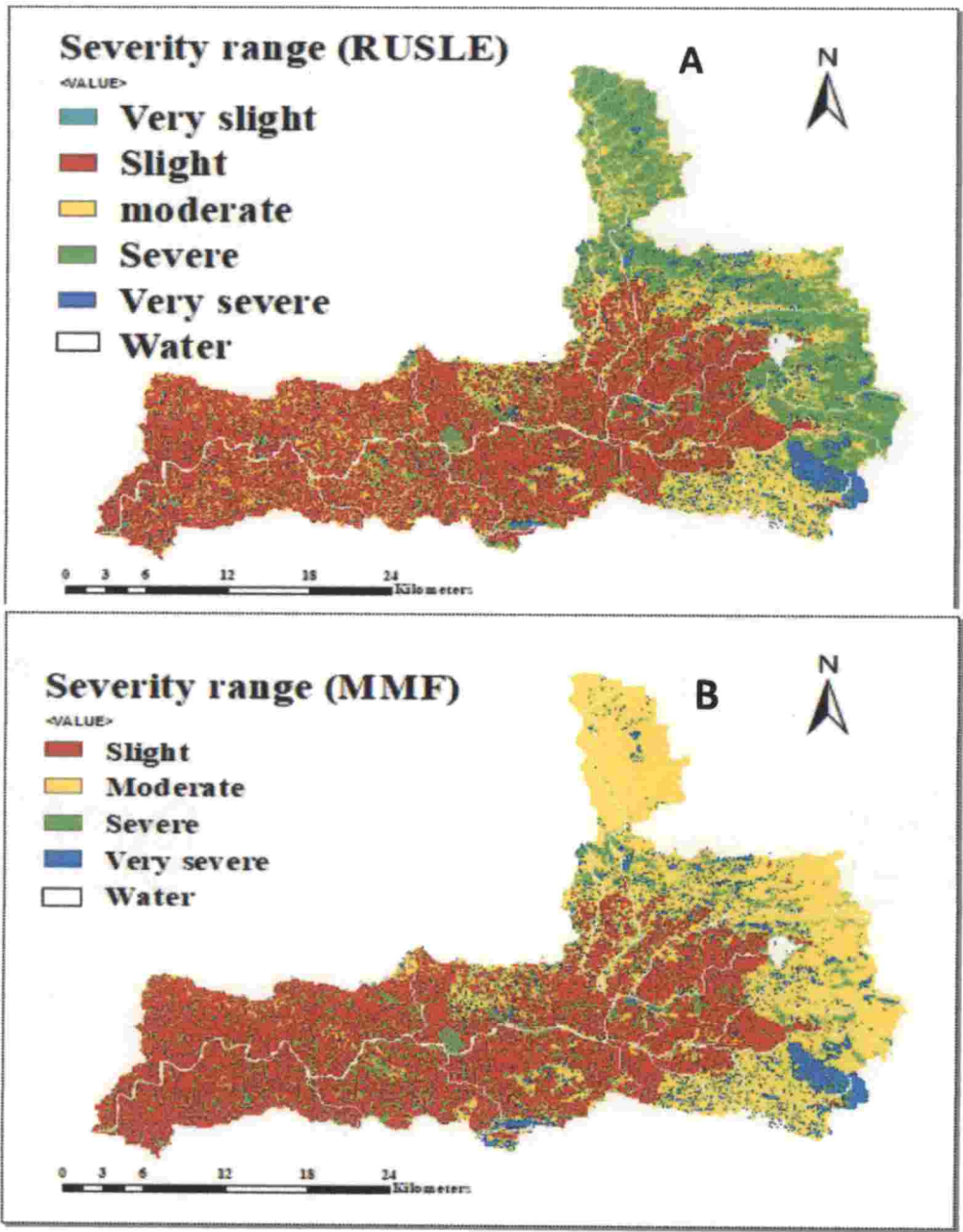


Fig. 4.41 Soil erosion map with severity ranges A) RUSLE B) MMF

**Table 4.2. Soil erosion severity classes with area covered**

Erosion severity class	Area covered by erosion severity classes			
	RUSLE		MMF	
	km <sup>2</sup>	%	km <sup>2</sup>	%
Very slight	1.56	0.15	0.00	0.00
Slight	413.41	40.70	396.36	39.02
Moderate	292.15	28.76	375.21	36.94
Severe	229.7	22.61	151.59	14.92
Very severe	62.49	6.15	76.15	7.5

From the result obtained in this study, it is visible that the erosion rates estimated by two models differ quantitatively. But in qualitative terms, both models shows similar trend of variation. The result obtained by RUSLE shows that it mainly follows the topography. This finding was in agreement with the result obtained by Svorin (2003). In hilly terrains, higher results are obtained by RUSLE model. The erosion results are sometimes under estimated in MMF model especially in hilly topography with vegetation cover, as this model considers the minimum value of F and G where F value is totally independent of slope. The similar discussion was made by Mondal *et al.* (2016) also. As the Kunthippuzha sub-basin lacks field data on soil loss, the validation of the two models could not be done. So, qualitative comparison instead of quantitative comparison was made between the models. The erosion severity areas (very severe areas) were similar in both the maps (Fig. 4.40). Those points were checked with the priority details in watershed atlas from Department of Soil Survey and Soil Conservation, which confirm the correctness of the obtained erosion prone area map by two models.

#### **4.5 Analysis of Effect of Land Use on Erosion**

The NDVI values are the vegetation related indices derived from the multispectral satellite imageries. These are very much dependant on the extent of canopy. As vegetation is one of the most influencing parameter of soil erosion,

assessment of NDVI to correlate the vegetation and thereby soil erosion is very much necessitated. More than crop type, this factor depends on the thickness as well as greenness of the canopy.

The NDVI maps of the Kunthippuzha sub-basin for the year 2000 and 2013 were generated from the satellite imageries Landsat 7 and Landsat 8 respectively, which are shown in Fig. 4.42.

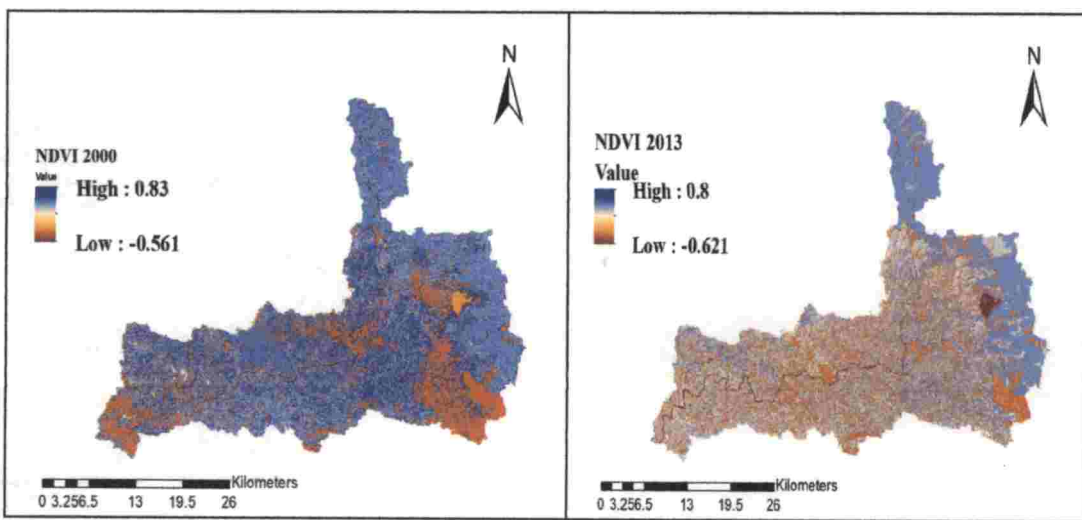


**Fig. 4.42 NDVI maps for the years 2000 and 2013**

The NDVI values obtained of the Kunthippuzha sub-basin in the year 2000 was ranging from -0.561 to 0.83 where as in the year 2013, it was -0.621 to 0.8. The range of NDVI map obtained in the year was validated using NDVI map prepared by the LISS III satellite image downloaded from the Bhuvan. Very little variation was observed between the maps prepared from Landsat 8 and LISS III image which can be attributed to difference in the resolution of the image.

To analyse the NDVI values with the spatial and temporal variation of land use, land use maps for the years 2000 and 2013 were prepared from Landsat imageries. Ten predominant land use types were identified. The land covered with more types of crops was named as 'mixed crop'. Other land uses identify in the

watershed was barren + built-up land, water bodies, rubber, coconut, paddy, grass land, banana, scrubs and forest. Some of the land uses generated from satellite data were verified by ground truthing with GPS. The landuse maps prepared for the study area in the year 2000 and 2013 are shown in Fig.4.43 (A-B).

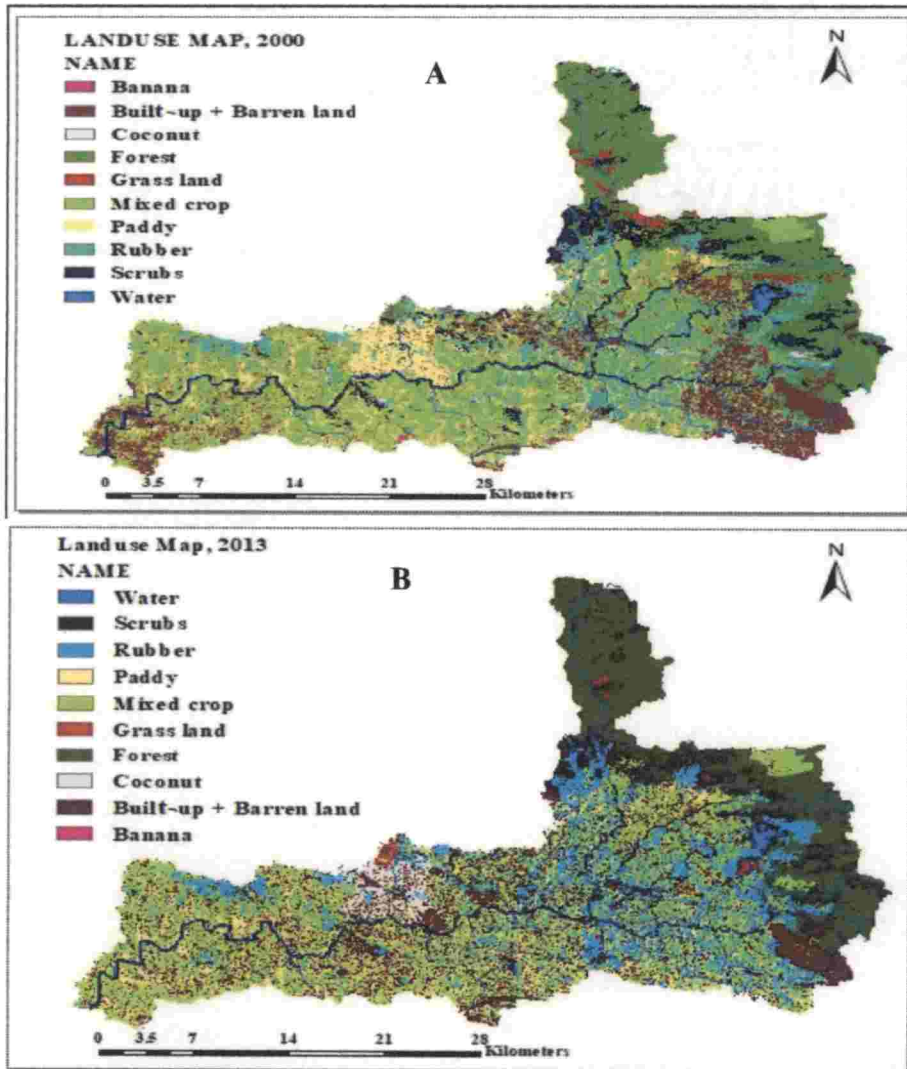


**Fig. 4.43 Land use maps generated for Kunthippuzha sub-basin for the year a) 2000 b) 2013**

Field photographs taken during the ground truthing are shown in Plate 4.1.





**Plate 4.1. Field photographs of the study area**

The analysis of NDVI maps with land use shows that it depends mainly over vegetation canopy rather than the crop type. The mean NDVI values corresponding to different land uses and its variation in the year 2000 and 2013 are given in Table 4.3.

The NDVI maps generated for the year 2000 and 2013 shows that higher NDVI values are located in the north-east side of the Kunthippuzha sub-basin, especially corresponding to forest land. Similarly, lesser range of NDVI values obtained corresponding to water bodies. The result obtained was in agreement with the Sharma (2010) who conducted similar study at Maithon catchment, Jharkhand.

The comparison of the NDVI maps of the years 2000 and 2013 proved the occurrence of some drastic variation in the spatial distribution of NDVI values. The count of pixels (30 m x 30 m) with NDVI greater than 0.5 was decreased in the year 2013, which are the clear demarcation of the decrease in the vegetation extent as well as the density of canopy by the year 2013. The NDVI ranges and corresponding count of pixels for the years 2000 and 2013 are shown in Fig. 4.44.

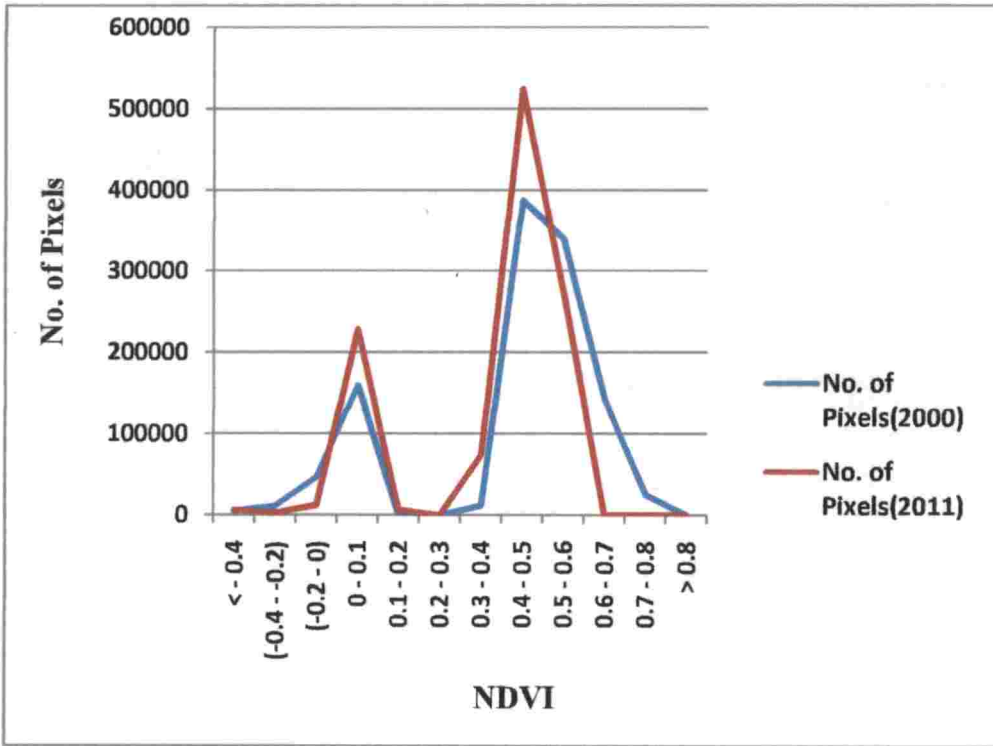


**Fig. 4.44 Variation of pixel count with NDVI values**

The land use pattern varies spatially as well as temporally within the watershed and hence erosion. Among all the identified land use types, highest erosion was found by RUSLE and MMF was in the built-up plus barren land in the year 2000 as well as 2013. According to the results obtained from RUSLE and MMF the lesser erosion was experienced under mixed crops in the year 2013, whereas it was under paddy during the year 2000. The variations of area under each land use

class, average NDVI values, mean soil erosion rate (t/ha/y) obtained through the RUSLE as well as MMF model for both the years 2000 and 2013 are given in Table 4.2.

**Table 4.3. Spatial variations in NDVI and mean soil erosion with the changes in land use in the year 2000 and 2013**

Land use type	Area (km <sup>2</sup> )		Average NDVI		Mean soil loss (t/ha/y)			
					RUSLE		MMF	
	2000	2013	2000	2013	2000	2013	2000	2013
Built-up + Barren land	178.03	210.60	0.001	0.02	69.50	104.99	66.11	108.88
Grass Land	8.09	4.49	0.51	0.46	15.31	49.48	10.60	30.90
Mixed crops	311.06	311.23	0.54	0.51	4.34	4.37	3.01	6.07
Forest	180.69	170.79	0.53	0.52	18.15	37.1	11.65	24.03
Rubber	152.20	158.87	0.62	0.48	8.54	17.3	8.30	8.17
Banana	3.08	2.32	0.48	0.38	5.28	6.58	7.84	11.68
Paddy	106.89	72.02	0.49	0.42	1.42	6.62	2.34	6.48
Scrubs	47.81	43.35	0.51	0.40	40.60	38.84	37.68	39.78
coconut	11.44	25.62	0.50	0.42	2.83	4.98	4.90	7.25

Considering the areal distribution of land use, as a result of urbanisation, keeping the land uncultivated as well as deforestation, the areal extent of built-up plus barren land gets increases by 32.57 km<sup>2</sup> from 2000 to 2013, which leads to increase the rate of soil erosion. According to RUSLE model, the increase was about 35.49 t/ha/y whereas by MMF it was 42.77 t/ha/y.

Average erosion rate varies within the sub-basin among various land uses. The analysis with temporal and spatial variation of soil erosion, maximum rate of soil

erosion was found in the built-up land plus barren. In the case of forest land, a decrease in area about 10.1 km<sup>2</sup> by the gap of 13 years, the drastic changes in soil erosion rate was observed, which reveals the importance of conserving forest land. The drastic change was mainly caused by the steeper sloping condition of the terrain of which they are located at. As the soil erosion is the result of complex interaction of many factors. Most of the sediment transport was happened in the water bodies. Implementation of water conservation measures like check dams, gully plugging etc can reduce such kinds of erosion. A small increase of about 0.17 km<sup>2</sup> was observed in the case of 'mixed crops', even though 3.06 t/ha/y increases in erosion was observed by MMF model, this may be mainly due to the effect of increase in rainfall. In these areas, even the occurrence of dramatic changes in rainfall distribution, only small raise in erosion was observed because of the effect of canopy cover. The grasslands are situated in hilly terrain with higher slopes. The areal coverage of grasslands was reduced by 3.60 km<sup>2</sup> by the year 2013. The erosion rate increased according to both methods from 15.30 to 49.48 and 10.60 to 30.90 respectively. This variation indicates the necessity of vegetation cover in controlling the erosion even in the steeper slopes also.

In the case of rubber plantation, the planted area showed an increase of 6.6 km<sup>2</sup>, which reduces the erosion by 0.126 t/ha by the MMF model, but according to RUSLE some deviation in the results was noted. It can be interpreted by the general nature of the RUSLE and MMF model as the former model mainly depends on topography, where splash detachment factor in MMF was totally independent of slopes. The rate of soil erosion increased under the coconut plantation was comparatively lesser as the area under coconut was increased by the 11.44 km<sup>2</sup> to 25.62 km<sup>2</sup>, mainly due to conversion of paddy fields. The soil with more clay content also helps to reduce the erosion.

The analysis of the effect of overall changes in land use over soil erosion clearly revealed the importance of vegetation cover in controlling the erosion. The

analysis showed that even though the vegetation is one of the most influencing parameters, other parameters like soil characteristics, slope and rainfall also play important role in this.

The study can be extended for predicting the future soil erosion by analysing the trend observed during the previous studies. Accurate measurement of different parameters in the field and incorporation of rainfall intensity data can improve the performance of the models. Furthermore, the identification of the most prominent factor affecting soil erosion on pixel basis will help in implementing soil and water conservation measures in sub-basin.

## **SUMMARY AND CONCLUSION**

## CHAPTER V

### SUMMARY AND CONCLUSION

Land and water are the two fundamental natural resources extremely essential for the existence of life. Among all issues associated with land and water, soil erosion is the most common, well-distributed and complex problem experienced mostly in humid and sub-humid mountainous regions. Hence, identification of erosion prone areas for the effective management of these two vital resources is very much necessitated for the overall development of country. This particular study mainly focused to identify the erosion prone areas in Kunthippuzha sub-basin using RUSLE and MMF models and to analyse the effect of spatial and temporal variations of land use and the corresponding effects on the rate of soil erosion with the support of NDVI values. The GIS technology incorporated remote sensing data which can give more reliable prediction was adopted in this study, as the conventional methods to estimate soil erosion rate are very expensive and time consuming. Furthermore, the chance of deposition of detached particles in other parts of the watershed other than outlet is more in case of conventional methods. The estimation was done for two years (2000 and 2013) to analyse the effect of temporal variations of land use – land cover on erosion.

For the execution of RUSLE model, map layers corresponding to R factor, K factor, LS factor, C factor as well as P factor were prepared and analysed for its spatial variation within the watershed. Data corresponding to rainfall, soil, slope as well as vegetation was collected for the years 2000 and 2011. The rainfall data was collected from the Pattambi and Mannarkad rain gauge station and the soil related data was collected from the department of soil survey and soil conservation. The slope and vegetation related parameters were derived from the remote sensing data viz. digital elevation models and satellite imageries. The mean value of R factor estimated using the daily rainfall data of the years 2000 and 2013 were 198.3 and

250.7 MJ mm ha<sup>-1</sup> h<sup>-1</sup> y<sup>-1</sup>. The estimated K factor ranged from 0.10 to 0.29 t ha h ha<sup>-1</sup> MJ<sup>-1</sup> mm<sup>-1</sup>. The average value of LS was found to be 1.46 and 1.90 respectively for the years 2000 and 2013 generated using the digital elevation models. The C factor was estimated using the NDVI values derived from the satellite imageries. The C factor found to be increasing in the study area due to the changes in land use and decrease in the density of canopy. The P factor was estimated by assigning values obtained from the literature according to land use as well as percentage slope.

For the execution of MMF model, the calculation was done in two phases, viz., water and sediment phase. In the water phase, the kinetic energy of rainfall (E) as well as depth of overland flow (Q) were determined for both years 2000 and 2013. The kinetic energy of rainfall (E) increased towards the north-east side of the watershed and the rainfall distribution also showed the similar trend. The estimated average E value for the years 2000 and 2013 were 47742.44 J/m<sup>2</sup> and 61622.75 J/m<sup>2</sup> respectively. The depth of overland flow showed profound correlation with the soil texture and rainfall distribution and was 500.4 mm and 748.1 mm for the years 2000 and 2013 respectively. The value was less in clay textured soil for both the years. The RUSLE map viz. K factor map, C factor map and P factor map were used in the MMF model also. In the sediment phase, detachment capacity of rainfall (F) and transport capacity of the runoff (G) were estimated. The minimum value among the two (F and G) based on pixel value was taken as the soil erosion rate. Among these two factors, F factor is totally independent of slope and strongly depended on soil parameters, where as C factor varies with vegetation as well as slope.

The mean soil erosion estimated for the year 2000 by MMF and RUSLE model were 18.30 t/ha/y and 20.58 t/ha/y respectively. Similarly in the year 2013, it was 32.78 t/ha/y and 35.1 t/ha/y respectively. Analysis using both the models showed that the north-east side of the watershed experienced more erosion. Both the models gave spatial variation of soil erosion with the integration of GIS. The erosion results are sometimes under estimated in MMF model especially in steep slope areas



as the F factor in MMF model completely independent of slope, Results obtained from both models were quantitatively different, but were similar qualitatively.

Sediment Delivery Ratio was calculated for the entire watershed. The SDR obtained for entire watershed was less which indicates that most of the eroded sediments get deposited at intermediate locations before reaching the outlet, as intermediate locations contains more paddy fields and plain areas. The SDR calculation enhances the importance of adopting GIS technology.

In order to find the erosion prone areas in the sub-basin, quantitative assessment along with qualitative ranking using factorial scoring method was adopted. Pixel based scoring was done based on mean soil erosion value obtained under each zone of rainfall, slope, soil and vegetation. The score raster corresponding to land use, rainfall, slope and topography were added and combined score map was obtained. From the study based on the RUSLE model, 0.15% of the area experienced very low erosion, 40.70% was under slight erosion and 28.76% area under moderate erosion severity class. The percentage under severe erosion range was 22.61% and under very severe erosion range was 6.15%. According to MMF model, about 39.02% of total area of watershed was found under very low risk range of erosion. Around 36.94 per cent of sub-basin lies in slight risk of erosion. 14.92% sub-basin area was under severer range while about 7.50% of area showed very severe risk of soil erosion.

NDVI values corresponding to land use were identified, in which negative NDVI values correspond to water pixels, whereas higher NDVI values represents the thick vegetation. In the year 2000, the NDVI value ranged from -0.561 to 0.83 whereas in the year 2013, it was -0.621 to 0.8. From the analysis of the temporal variation in land use over the NDVI, it was observed that NDVI value decreased by the year 2013 at the points where density of the canopy decreased. The spatial variation of soil erosion varied from pixel to pixel according to the land use pattern. Highest soil

erosion risk was noted for built-up plus barren land. Considering the areal distribution of land use as a result of urbanisation, keeping the land uncultivated as well as under deforestation, the areal extent of built-up plus barren land got increased by 32.57 km<sup>2</sup> from the year 2000 to 2013, which led to the increase the rate of soil erosion. The least temporal variations in soil erosion was observed in the case of mixed crops which was about 0.03 t/ha/y by RUSLE model and 3.05 t/ha/y by MMF model. Furthermore, the analysis showed that the erosion occurrence depends on the overall effect of the complex interactions between the rainfall, slope, vegetation as well as topography.

Analysis of the study showed that in RUSLE model the estimated rate of erosion mainly varied based on changes in topography, whereas in MMF it is highly dependent on vegetation. The performance of the MMF model can be improved if all the parameters involved in the model can be accurately measured in the field.

Considering the results obtained from the two models, it was observed that the output from the models varied quantitatively, but qualitatively they showed similar trend. As Kunthippuzha basin lacks field data corresponding to soil erosion, verification of the two models was not possible.

174472



# **REFERENCES**

## CHAPTER VI

### REFERENCES

- AbdelRahman, M.A.E., Natarajan, A., Srinivasamurthy, C.A., and Hegde, R. 2016. Estimating soil fertility status in physically degraded land using GIS and remote sensing techniques in Chamarajanagar district, Karnataka, India. *Egypt. J. Remote Sens. Space Sci.* 19(1): 95-108.
- Adediji, A., Tukur, A.M., and Adepoju, K.A. 2010. Assessment of revised universal soil loss equation (RUSLE) in Katsina area, Katsina state of Nigeria using remote sensing (RS) and geographic information system (GIS). *Iran. J. Energy Environ.* 1(3): 255-264.
- Adeogun, G.A., Ibitoye, B.A., Salami, A.W., and Ihagh, T.G. 2018. Sustainable management of erosion prone areas of upper watershed of Kainji hydropower dam, Nigeria. *J. King Saud Univ. Eng. Sci.*
- Ahmed, S.I., Rudra, R.P., Gharabaghi, B., Mackenzie, K., and Dickinson, W.T. 2012. Within-storm rainfall distribution effect on soil erosion rate. *Int. Scholarly Res. Network Soil Sci.*
- Alexakis, D.D., Hadjimitsis, D.G., and Agapiou, A. 2013. Integrated use of remote sensing, GIS and precipitation data for the assessment of soil erosion rate in the catchment area of "Yialias" in Cyprus. *Atmos. Res.* 13: 108-124.
- Al-quraishi, A.M.F. 2003. Soil erosion risk prediction with RS and GIS for the northwestern part of Habei province, China. *Pak. J. Appl. Sci.* 3(12): 659-669.
- Amore, E., Modica, C., Nearing, M.A., and Santoro, V.C. 2004. Scale effect in USLE and WEPP application for soil erosion computation from three Sicilian basins. *J. Hydrol.* 293: 100-114.

- Anache, J.A.A., Wendland, E.C., Oliveira, P.T.S., Flanagan, D.C., and Nearing, M.A. 2017. Runoff and soil erosion plot-scale studies under natural rainfall: a meta-analysis of the Brazilian experience. *Catena* 152: 29-39.
- Antal, J., Maderkova, L., Cimo, J., and Drgonova, K. 2015. Analysis of calculation methods for determination of rain erosivity for Slovak Republic. *Acta Sci. Pol. Formatio Circumiectus* 14(4): 5-14.
- Arnoldus, H.M.J. 1980. An approximation of the rainfall factor in the universal soil loss equation. In: Boodt, M.D. and Gabriels, D. (eds.). *Assessment of Soil Erosion*. John Wiley and Sons, Chichester, Gran Bretana, pp.127-132.
- Artun, O., Dinc, A.O., and Satir, O. 2017. Estimation of soil losses using various soil erosion models in a sample plot in Mediterranean part of Turkey. *Fresenius Environ. Bull.* 26(5): 3385-3394.
- Atakora, E.T., Kyei-Baffour, N., Ofori, E., and Antwi, B.O. 2013. Simulation of sediment transport to Sawah rice fields by applying the water erosion prediction project (WEPP) model to a watershed in Ghana. *J. Soil Sci. Environ. Manag.* 4(3): 46-53.
- Auerswald, K., Fischer, F.K., Kistler, M., Treisch, M., Maier, H., and Brandhuber, R. 2018. Behavior of farmers in regard to erosion by water as reflected by their farming practices. *Sci. Total Environ.* 613-614: 1-9.
- Babu, R., Dhyani, B. L., and Kumar, N. 2004. Assessment of erodibility status and refined iso-erodent map of India. *Indian J. Soil Conserv.* 32(2): 171-177.
- Balasubramani, K., Veena, M., Kumaraswamy. K., and Saravanabavan, V. 2015. Estimation of soil erosion in a semi-arid watershed of Tamil Nadu (India) using

revised universal soil loss equation (RUSLE) model through GIS. *Model. Earth Syst. Environ.* 1(10): 1-17.

Ballabio, C., Borrelli, P., Spinoni, J., Meusburger, K., Michaelides, S., Begueria, S., Klik, A., Petan, S., Janecek, M., Olsen, P., Aalto, J., Lakatos, M., Rymaszewicz, A., Dumitrescu, A., Tadic, M.P., Diodato, N., Kostalova, J., Rousseva, S., Banasik, K., Alewell, C., and Panagos, P. 2017. Mapping monthly rainfall erosivity in Europe. *Sci. Total Environ.* 579: 1298-1315.

Barman, S., Aggarwal, S.P., and Dutta, M.K. 2013. Soil erosion due to change in vegetated area in the Majuli island of Assam. *Int.J. Adv. Remote Sens. GIS Geogr.* 1(1): 8-19.

Bayramov, E., Buchroithner, M.F., and Mcgurty, E. 2013. Differences of MMF and USLE models for soil loss prediction along BTC and SCP pipelines. *J. Pipeline Syst. Eng. Pract.* 4: 81-96.

Beasley, D.B., Huggins, L.F., and Monke, E.J. 1981. ANSWERS: A model for watershed planning. *Trans. ASAE* 23(4): 938-944.

Behera, P., Rao, K.H.V.D., and Das, K.K. 2005. Soil erosion modeling using MMF model - a remote sensing and GIS perspective. *J. Indian Soc. Remote Sens.* 33(1): 165-176.

Belasri, A. and Lakhouili, A. 2016. Estimation of soil erosion risk using the universal soil loss equation (USLE) and geo-information technology in Oued El Makhazine watershed, Morocco. *J. Geogr. Inf. Syst.* 8: 98-107.

Bhattacharyya, T., Babu, R., Sarkar, D., Mandal, C., and Dhyani, B.L. 2007. Soil loss and crop productivity model in humid subtropical India. *Curr. Sci.* 93(10): 1397-1403.

- Bhaware, K.O. 2006. Soil erosion risk modeling and current erosion damage assessment using remote sensing and GIS techniques. M.Tech (Ag) thesis, Indian Institute of Remote Sensing, Dehradun, 130p.
- Bilotta, G.S., Grove, M., and Mudd, S.M. 2012. Assessing the significance of soil erosion. *Trans. Inst. Br. Geogr.*
- Biswas, S. 2012. Estimation of soil erosion using remote sensing and GIS and prioritization of catchments. *Int. J. Emerging Technol. Adv. Eng.* 2(7): 124-128.
- Boggs, G., Devonport, C., Evans, K., and Puig, P. 2001. GIS-based rapid assessment of erosion risk in a small catchment in the wet/dry tropics of Australia. *Land Degrad. Develop.* 12: 417-434.
- Bogunovic, I., Pereira, P., Kisic, I., Sajko, K., and Sraka, M. 2018. Tillage management impacts on soil compaction, erosion and crop yield in Stagnosols (Croatia). *Catena* 160: 376-384.
- Bouaziz, M., Leidig, M., and Gloaguen, R. 2011. Optimal parameter selection for qualitative regional erosion risk monitoring: a remote sensing study of SE Ethiopia. *Geosci. Front.* 2(2): 237-245.
- CWRDM (1991). *Water Resources Development of Bharathapuzha Basin*. A status report, Centre for Water Resources Development and Management, Kozhikode, Kerala.
- Devaranavadagi, V.S. and Bosu, S.S. 2014. Estimation of runoff and soil loss in clay soils of Perambalur district, Tamil Nadu. *Karnataka J. Agric. Sci.* 27(4): 503-506.

- Drift, J.W.M.V.D. 1995. The effect of temperature change on soil structure stability. In: Zwerver, S., Rompaey, R.S.A.R.V., Kok, M.T.J., and Berk, M.M. (eds), *Climate Change Research: Evaluation and Policy Implications*. Elsevier Science, pp. 923-930.
- Elangovan, A.B. and Seetharaman, R. 2011. Estimating rainfall erosivity of the revised universal soil loss equation from daily rainfall depth in Krishanagiri watershed region of Tamil Nadu, India. In: *Environmental and Computer Science*. Proceedings of an International Conference, Singapore. Asia-Pacific Chemical, Biological and Environmental Engineering Society, pp. 48-52.
- Fang, N., Shi, Z., Li, L., Guo, Z., Liu, Q., and Ai, L. 2012. The effects of rainfall regimes and land use changes on runoff and soil loss in a small mountainous watershed. *Catena* 99: 1-8.
- FAO [Food and Agriculture Organization]. 1991.
- Fen-Li, Z. 2006. Effect of vegetation changes on soil erosion on the Loess Plateau. *Pedosphere* 16(4): 420-427.
- Ferro, V, Giordano, G., and Iovino, M. 1991. Isoerosivity and erosion risk map for Sicily. *Hydrol. Sci. J.* 36(6): 549-564.
- Ferro, V., Porto, P., and Yu, B. 1999. A comparative study of rainfall erosivity estimation for Southern Italy and South eastern Australia. *Hydrol Sci J.* 44(1): 3-24.
- Franzluebbbers, A.J. 2002. Water infiltration and soil structure related to organic matter and its stratification with depth. *Soil Tillage Res.* 66: 197-205.



- Fraser, A.I., Harrod, T.R., and Haygarth, P.M. 1999. The effect of rainfall intensity on soil erosion and particulate Phosphorus transfer from arable soils. *Water Sci. Technol.* 39(12): 41-45.
- Ganasri, B.P. and Ramesh, H. 2016. Assessment of soil erosion by RUSLE model using remote sensing and GIS - a case study of Nethravathi basin. *Geosci. Front.* 7(6): 953-961.
- Gelagay, H.S. and Minale, A.S. 2016. Soil loss estimation using GIS and remote sensing techniques: a case of Koga watershed, north western Ethiopia. *Int. Soil Water Conserv. Res.* 4: 126-136.
- Gould, B.W., Saupe, W.E., and Klemme, R.M. 1989. Conservation tillage: the role and operator characteristics and the perception of soil erosion. *Land Econ.* 65(2): 167-182.
- Gray, D. 2016. Effect of slope shape on soil erosion. *J. Civil Environ. Eng.* 6(3).
- Gyssels, G., Poesen, J., Bochet, E., and Li, Y. 2005. Impact of plant roots on the resistance of soils to erosion by water: a review. *Prog. Phys. Geogr.* 2: 189-217.
- Hadley, R.F. and Lusby, G.C. 1967. Runoff and hillslope erosion resulting from a high-intensity thunderstorm near Mack, western Colorado. *Water Resour. Res.* 3(1): 139-143.
- Hao, C., Oguchi, T., and Pan, W.U. 2017. Assessment for soil loss by using a scheme of alternative sub-models based on the RUSLE in a Karst basin of southwest China. *J. Integr. Agric.* 16(2): 377-388. [https://doi.org/10.1016/S2095-3119\(16\)61507-1](https://doi.org/10.1016/S2095-3119(16)61507-1).

- Haregeweyn, N., Tsunekawa, A., Poesen, J., Tsubo, M., Meshsha, D.T., Fenta, A.A., Nyssen, J., and Adgo, E. 2017. Comprehensive assessment of soil erosion risk for better land use planning in river basins : case study of the Upper Blue Nile River. *Sci. Total Environ.* 574: 95-108.
- Helming, K. 2001. Wind speed effects on rain erosivity. In: Stott, D.E., Mohtar, R.H., and Steinhardt, G.C. (eds), *Sustaining the Global Farm*. 10<sup>th</sup> international soil conservation organization meeting, Germany. Purdue University and the USDA-ARS, National Soil Erosion Research Laboratory. pp. 771-776.
- Huang, C., Wells, L.K., and Norton, L.D. 1999. Sediment transport capacity and erosion processes: model concepts and reality. *Earth Surf. Processes Landforms* 24: 503-516.
- Hudson, N. 1993. *Field Measurement of Soil Erosion and Runoff*. FAO Soils Bulletin Series No. 68, Food and Agriculture Organization of the United Nations, Rome, 139p.
- Hurni, H. 1985. Erosion-productivity-conservation systems in Ethiopia. In: [anonymous] (eds), *Soil Conservation*. Proceedings of paper presented at the 4<sup>th</sup> international conference, 3-9 November 1985, Maracay, Venezuela.
- Imani, R., Ghasemieh, H., and Mirzavand, M. 2014. Determining and mapping soil erodibility factor (Case study: Yamchi watershed in northwest of Iran). *Open J. Soil Sci.* 4: 168-173.
- Jain, K.S., Kumar, S., and Varghese, J. 2001. Estimation of soil erosion for a Himalayan watershed using GIS technique. *Water Resour. Manag.* 15: 41-54.

- Janecek, M., Kubatova, E., and Tipl, M. 2006. Revised determination of the rainfall-runoff erosivity factor R for application of USLE in the Czech Republic. *Soil Water Res.* 1(2): 65-71.
- Jensen, J.R. 2005. *Introductory Digital Image Processing: A Remote Sensing Perspective*. New jersey, Pearson prentice hall.
- Jinze, M. 1981. The establishment of experimental plots for studying runoff and soil loss in the rolling Loess region of China. In: *Erosion and Sediment Transport Measurement*. Proceedings of the florence symposium, IAHS, pp. 467-477.
- Karthik, P., Lakshumanan, C., and Ramki, P. 2017. Estimation of soil erosion vulnerability in Perambalur taluk, Tamil Nadu using revised universal soil loss equation model (RUSLE) and geo-information technology. *Int. Res. J. Earth Sci.* 5(8): 8-14.
- Karydas, C.G., Petriolis, M., and Manakos, I. 2013. Evaluating alternative methods of soil erodibility mapping in the Mediterranean island of Crete. *Agric.* 3: 362-380.
- Kayet, N., Pathak, K., Chakrabarty, A., and Sahoo, S. 2018. Evaluation of soil loss estimation using the RUSLE model and SCS-CN method in hillslope mining areas. *Int. Soil Water Conserv. Res.* 6(1): 31-42.
- Khan, M.A., Gupta, V.P., and Moharana, P.C. 2001. Watershed prioritization using remote sensing and geographical information system: a case study from Guhiya, India. *J. Arid Environ.* 49: 465-475. <https://doi.org/10.1006/jare.2001.0797>.
- Khanal, A. and Fox, G.A. 2016. Detachment characteristics of root-permeated soils from laboratory jet erosion tests. *Ecol. Eng.*

- King, C. and Delpont, G. 1993. Spatial assessment of erosion: contribution of remote sensing, a review. *Remote Sens. Rev.* 7: 223-232.
- Kinnell, P.C., McGregor, K.J., and Rosewell, C. 1994. The IXEA index as an alternative to the EI30 erosivity index. *Trans. ASAE* 37: 1449-1456.
- Kinneth, G.R., Weesies, F.G.R., and Porter J.P. 1991. Revised universal soil loss equation. *J. Soil Water Conserv.* 46: 30-33.
- Kosmas, C., Gerontidis, S., and Marathianou, M. 2000. The effect of land use change on soils and vegetation over various lithological formations on Lesbos (Greece). *Catena* 40: 51-68.
- Kouli, M., Soupios, P., and Vallianatos, F. 2008. Soil erosion prediction using the revised universal soil loss equation (RUSLE) in a GIS framework, Chania, Northwestern Crete, Greece. *Environ. Geol.* 57: 483-497.
- Kumar, M.K., Annadurai, R., and Ravichandran, P.T. 2014. Assessment of soil erosion susceptibility in Kothagiri taluk using revised universal soil loss equation (RUSLE) and geo-spatial technology. *Int. J. Sci. Res. Publ.* 4(10): 1-13.
- Lal, R.1990. *Soil Erosion in the Tropics: Principles and Management*. McGraw-Hill, New York.
- Li, S., Lobb, D.A., Lindstrom, M.J., Papiernik, S.K., and Farenhorst, A. 2008. Modeling tillage induced redistribution of soil mass and its constituents within different landscapes. *Soil Sci. Soc. Am. J.* 72(1): 167-179.

- Loureiro, N.S. and Coutinho M.A. 2001. A new procedure to estimate the RUSLE  $EI_{30}$  index, based on monthly rainfall data and applied to the Algarve region, Portugal. *J. hydrol.* 250: 12-18.
- Lufafa, A., Tenywa, M.M., Isabirye, M., Majaliwa, M.J.G., and Woomer, P.L. 2003. Prediction of soil erosion in a Lake Victoria basin catchment using a GIS-based universal soil loss model. *Agric. Syst.* 76: 883-894.
- McCool, D.K., Brown, L.C., and Foster, G.R. 1987. Revised slope steepness factor for the USLE. *Trans. ASAE* 30: 1387-1396.
- Mhazo, N., Chivenge, P., and Chaplot, V. 2016. Tillage impact on soil erosion by water: discrepancies due to climate and soil characteristics. *Agric. Ecosyst. Environ.* 230: 231-241.
- Michael and Ojha. 1996. *Principles of Agricultural Engineering, Volume II*. Jain Brothers, 623p.
- Miller, M.F. 1926. Waste through soil erosion. *J. Am. Soc. Agron.* 18: 153-160.
- Mohamadi, M.A. and Kavian, A. 2015. Effects of rainfall patterns on runoff and soil erosion in field plots. *Int. Soil Water Conserv. Res.* 3: 273-281.
- Mondal, A., Khare, D., and Kundu, S. 2016. A comparative study of soil erosion modeling by MMF, USLE, RUSLE. *Geocarto I.*
- Moore, R.R. 1979. Rainfall erosivity in east Africa: Kenya, Tanzania, Uganda. *Phys. Geogr.* 61: 147-156.
- Morgan, R.P.C. 2001. A simple approach to soil loss prediction: a revised Morgan, Morgan and Finney model. *Catena* 44: 305-322.

- Morgan, R.P.C. 2005. *Soil Erosion and Conservation*. Blackwell Publishing, UK, 304p.
- Morgan, R.P.C., Morgan, D.D.V., and Finney, H.J. 1984. A Predictive model for the assessment of soil erosion risk. *J. Agric. Eng. Res.* 30: 245-253.
- Morgan, R.P.C., Quinton, J.N., Smith, R.E., Govers, G., Poesen, J.W.A., Auerswald, K., Chisci, G., Torri, D., and Styczen, M.E. 1998. The European soil erosion model (EUROSEM): a dynamic approach for predicting sediment transport from fields and small catchments. *Earth Surf. Process Landforms* 23: 527-544.
- Nearing, M.A., Page, D.I., Simanton, J.R., and Lane, L.J. 1989. Determining erodibility parameters from rangeland field data for a process-based erosion model. *Trans. ASAE* 32(3): 919-924.
- Nearing, M.A., Pruski, F.F., and O'Neal, M.R. 2004. Expected climate change impacts on soil erosion rates: a review. *J. Soil Water Conserv.* 59(1): 43-50.
- Nigussie, T.A., Fanta, A., Melesse, A.M., and Quraishi, S. 2014. Modeling rainfall erosivity from daily rainfall events, Upper Blue Nile basin, Ethiopia. In: Melesse, A.M. (ed.), *Nile River Basin*. Springer International Publishing Switzerland, pp. 307-336.
- Okorafor, O.O., Akinbile, C.O., Adeyemo, A., and Egwuonwu, C.C. 2017. Determination of rainfall erosivity index (R) for Imo state, Nigeria. *Am. J. Eng. Res.* 6(2): 13-16.
- Ostovari, Y., Ghorbani-dashtaki, S., and Bahrami, H. 2017. Soil loss prediction by an integrated system using RUSLE, GIS and remote sensing in semi-arid region. *Geoderma Regional*. <https://doi.org/10.1016/j.geodrs.2017.06.003>.

- Ouyang, W., Wu, Y., Hao, Z., Zhang, Q., Bu, Q., and Gao, X. 2018. Combined impacts of land use and soil property changes on soil erosion in a mollisol area under long-term agricultural development. *Sci. Total Environ.* 613: 798-809.
- Panagos, P., Ballabio, C., Borrelli, P., Meusburger, K., Klik, A., Rouseva, S., Tadic, M.P., Michaelides, S., Hrabalíkova, M., Olsen, P., Aalto, J., Lakatos, M., Rymaszewicz, A., Dumitrescu, A., Begueria, S., and Alewell, C. 2015. Rainfall erosivity in Europe. *Sci. Total Environ.* 511: 801-814.
- Pandey, A., Chowdary, V.M., and Mal, B.C. 2007. Identification of critical erosion prone areas in the small agricultural watershed using USLE, GIS and remote sensing. *Water Resour. Manag.* 21: 729-746.
- Pandey, A., Mathur, A., Mishra, S.K., and Mal, B.C. 2009. Soil erosion modeling of a Himalayan watershed using RS and GIS. *Environ. Earth Sci.* 59: 399-410.
- Parveen, R. and Kumar, U. 2012. Integrated approach of universal soil loss equation (USLE) and geographical information system (GIS) for soil loss risk assessment in upper south Koel basin, Jharkhand. *J. Geogr. Inf. Syst.* 4: 588-596.
- Petkovsek, G. and Mikos, M. 2004. Estimating the R factor from daily rainfall data in the sub-mediterranean climate of southwest Slovenia. *Hydrol. Sci. J.* 49(5): 869-877.
- Pradeep, G.S., Krishnan, M.V.N., and Vijith, H. 2014. Identification of critical soil erosion prone areas and annual average soil loss in an upland agricultural watershed of Western Ghats, using analytical hierarchy process (AHP) and RUSLE techniques. *Arab. J. Geosci.*

- Prasannakumar, V., Shiny, R., Geetha, N., and Vijith, H. 2011a. Spatial prediction of soil erosion risk by remote sensing, GIS and RUSLE approach: a case study of Siruvani river watershed in Attapady valley, Kerala, India. *Environ. Earth Sci.* 64: 965-972.
- Prasannakumar, V., Vijith, H., Abinod, S., and Geetha, N. 2012. Estimation of soil erosion risk within a small mountainous sub-watershed in Kerala, India, using revised universal soil loss equation (RUSLE) and geo-information technology. *Geosci. Front.* 3(2): 209-215.
- Prasannakumar, V., Vijith, H., Geetha, N., and Shiny, R. 2011b. Regional scale erosion assessment of a sub-tropical highland segment in the western ghats of Kerala. *Water Resour. Manage.* 25: 3715-3727.
- Rahaman, S.A., Aruchamy, S., Jegankumar, R., and Ajeez, S.A. 2015. Estimation of annual average soil loss, based on RUSLE model in Kallar watershed, Bhavani basin, Tamil Nadu, India. In: [anonymous] (eds), *ISPRS Annals of the Photogrammetry, Remote Sensing and Spatial Information Sciences*. Proceedings of joint international geoinformation conference, Kuala Lumpur, Malaysia, pp. 207-214.
- Ramsankaran, R., Kothiyari, U.C., and Ghosh, S.K. 2012. Geospatial based hydrological and soil erosion modeling - a pilot study in Pathri Rao watershed. *Int. J. Water Resour. Environ. Manag.* 3(1): 41-57.
- Rao, Y.P. 1981. Evaluation of cropping management factor in universal soil loss equation under natural rainfall condition of Kharagpur, India. In: [Anonymous] (eds), *Problems of Soil Erosion and Sedimentation*. Proceedings of the south-east Asian regional symposium, Bangkok, pp. 241-254.



- Rawat, J.S., Joshi, R.C., and Mesia, M. 2013. Estimation of erosivity index and soil loss under different land uses in the tropical foothills of Eastern Himalaya (India). *Trop. Ecol.* 54(1): 47-58.
- Renard, K.G. and Ferreira, V.A. 1993. RUSLE model description and database sensitivity. *J. Environ. Qual.* 22: 458-466.
- Renard, K.G. and Freimund, J.R. 1994. Using monthly precipitation data to estimate the R factor in the revised USLE. *J. Hydrol.* 157: 287-306.
- Renard, K.G., Foster, G.R., Weesies, G.A., McCool, D.K., and Yoder, D.C. 1997. *Predicting soil erosion by water: a guide to conservation planning with the Revised Universal Soil Loss Equation (RUSLE)*. Agriculture Handbook No. 703, USDA-ARS.
- Renard, K.G., Foster, G.R., Weesies, G.A., McCool, D.K., and Yoder, D.C. 1996. *Predicting Soil Erosion by Water - A Guide to Conservation Planning with the Revised Universal Soil Loss Equation (RUSLE)*. USDA-ARS Agriculture Handbook No. 703, Ankeny.
- Richard, K. 1993. Sediment delivery and the drainage network. In: *Channel Network Hydrology*. John Wiley and Sons, Chichester, West Sussex, UK, pp. 222-254.
- Romkens, M.J.M., Helming, K., and Prasad, S.N. 2001. Soil erosion under different rainfall intensities, surface roughness and soil water regimes. *Catena* 46:103-123.
- Roose, E.J. 1975. Natural mulch or chemical conditioner for reducing soil erosion in humid tropical areas. *Spec. Publ. Soil Sci. Soc. Am. J.* 7: 131-138.

- Rooseboom, A. and Annandale, G.W. 1981. Techniques applied in determining sediment loads in South African rivers. In: *Erosion and Sediment Transport Measurement*. Proceedings of the Florence symposium, IAHS, pp. 219-224.
- Ryan, K.T. 1981. Sediment measurement techniques used by the soil conservation service of New South Wales, Australia. In: *Erosion and Sediment Transport Measurement*. Proceedings of the Florence symposium, IAHS, pp.151-158.
- Ryken, N., Nest, T.V., Al-barri, B., Blake, W., Taylor, A., Bode, S., Ruyschaert, G., Boeckx, P., and Verdoodt, A. 2018. Soil erosion rates under different tillage practices in central Belgium: new perspectives from a combined approach of rainfall simulations and <sup>7</sup>Be measurements. *Soil Tillage Res.* 179: 29-37. <http://doi.org/10.1016/j.still.2018.01.010>.
- Sadeghi, S.H.R. and Mizuyama, T. 2010. Applicability of the modified universal soil loss equation for prediction of sediment yield in Khanmirza watershed, Iran. *Hydrol. Sci. J.* 52(5): 1068-1075.
- Schwab, G.O., Frevert, R.K., Edminster, T.W., and Barnes, K.K. 1981. *Soil and Water Conservation Engineering*. 3rd Edition, Wiley, New York.
- SCSA [Soil Conservation Society of America].1982.
- Sensoy, H. and Kara, O. 2014. Slope shape effect on runoff and soil erosion under natural rainfall conditions. *iForest* 7: 110-114.
- Sharda, V.N. and Mandal, D. 2018. Prioritization and field validation of erosion risk areas for combating land degradation in North Western Himalayas. *Catena* 164: 71-78. <https://doi.org/10.1016/j.catena.2017.12.037>.

- Sharma, A. 2010. Integrating terrain and vegetation indices for identifying potential soil erosion risk area. *Geo-spatial Inf. Sci.* 13(3): 201-209.
- Shiono, T., Kamimura, K., Okushima, S., and Fukumoto, M. 2002. Soil loss estimation on a local scale for soil conservation planning. *Jpn. Agric. Res. Q.* 36(3): 157-161.
- Sholagberu, A.T., Mustafa, M.R.U., Yusof, K.W., and Ahmad, M.H. 2016. Evaluation of rainfall-runoff erosivity factor for Cameron highlands, Pahang, Malaysia. *J. Ecol. Eng.* 17(3): 1-8.
- Shrestha, D.P. and Jetten, V.G. 2018. Modelling erosion on a daily basis, an adaptation of the MMF approach. *Int. J. Appl. Earth Obs. Geoinf.* 64:117-131.
- Shrestha. 1997. Assessment of soil erosion in the Nepalese Himalaya: a case study in Likhu Khola valley, middle mountain region. *Land Husbandry* 2(1): 59-80.
- Siakeu, J. and Oguchi, T. 2000. Soil erosion analysis and modelling: a review. *Trans. Jpn. Geomorphol.* 21(4): 413-429.
- Silburn, D.M. and Loch, R.J. 1989. Evaluation of the CREAMS model. Sensitivity analysis of the soil erosion/sedimentation component for aggregated clay soils. *Aust. J. Soil Res.* 27: 545-561.
- Singh, G. and Panda, R.K. 2017. Grid-cell based assessment of soil erosion potential for identification of critical erosion prone areas using USLE, GIS and remote sensing: a case study in the Kapgari watershed, India. *Int. Soil Water Conserv. Res.* 5(3): 202-211. <https://doi.org/10.1016/j.iswcr.2017.05.006>.
- Singh, G., Babu, R., and Chandra, S. 1981. *Soil Loss Prediction Research in India*. Soil and Water Conservation Research and Training Institute, India, 70p.

- Singh, V.P. 1994 Elementary Hydrology, Prentice Hall.
- Smith, D.D. and Wischmeier, W.H. 1957. Factors affecting sheet and rill erosion. *Trans. Am. Geophys. Union* 38: 889-896.
- Srinivas, C.V., Maji, A.K., Reddy, G.P.O., and Chary, G.R. 2002. Assessment of soil erosion using remote sensing and GIS in Nagpur district, Maharashtra for prioritisation and delineation of conservation units. *J. Indian Soc. Remote Sens.* 30(4): 198-212.
- Sun, W., Shao, Q., Liu, J., and Zhai, J. 2014. Assessing the effects of land use and topography on soil erosion on the Loess Plateau in China. *Catena* 121: 151-163.
- Suresh, R. 1993. *Soil and Water Conservation Engineering*. Standard Publishers Distributers, Delhi, 1094p.
- Svorin, J. 2003. A test of three soil erosion models incorporated into a geographical information system. *Hydrol. Process.* 17: 967-977.
- Takei, A., Kobaski, S., and Fukushima, Y. 1981. Erosion and sediment transport measurement in a weathered granite mountain area. In: *Erosion and Sediment Transport Measurement*. Proceedings of the florence symposium, IAHS, pp. 493-502.
- Tejaswini, V. 2017. Hydrologic assessment of a small watershed to combat agricultural drought. M.Tech.(Ag. Eng) thesis, Kerala Agricultural University, Thrissur, 100p.

- Tejaswini, V. and Sathian, K. K. 2018. Calibration and validation of SWAT model for Kunthipuzha basin using SUFI-2 algorithm. *Int. J. Curr. Microbiol. App. Sci.* 7(1): 2162-2172.
- Teng, H., Liang, Z., Chen, S., Liu, Y., Viscarra, R.A., Chappell, A., Yu, W., and Shi, Z. 2018. Current and future assessments of soil erosion by water on the Tibetan Plateau based on RUSLE and CMIP5 climate models. *Sci. Total Environ.* 635: 673-686. <https://doi.org/10.1016/j.scitotenv.2018.04.146>
- Tesfahunegn, G.B., Tamene, L., and Vlek, P.L.G. 2014. Soil erosion prediction using Morgan, Morgan and Finney model in a GIS environment in Northern Ethiopia catchment. *Appl. Environ. Soil Sci.* 1. <http://dx.doi.org/10.1155/2014/468751>.
- Thlakma, S.R., Iguisi, E.O., Odunze, A.C., and Jeb, D.N. 2018. Prediction of soil erosion risk in Mubi south catchment area, Adamawa state, Nigeria. *IOSR J. Environ. Sci. Toxicol. Food Technol.* 12(1): 40-67.
- Thomas, J., Joseph, S., and Thrivikramji, K.P. 2017a. Assessment of soil erosion in a tropical mountain river basin of the southern Western Ghats, India using RUSLE and GIS. *Geosci. Front.* 9(3): 893-906.
- Thomas, J., Joseph, S., and Thrivikramji, K.P. 2017b. Estimation of soil erosion in a rain shadow river basin in the southern Western Ghats, India using RUSLE and transport limited sediment delivery function. *Int. Soil Water Conserv. Res.* 6(2): 111-122. <https://doi.org/10.1016/j.iswcr.2017.12.001>.
- Tirkey, A.S., Pandey, A.C., and Nathawat, M.S. 2013. Use of satellite data, GIS and RUSLE for estimation of average annual soil loss in Daltonganj watershed of Jharkhand (India). *J. Remote Sens. Technol.* 1(1): 20-30.
- USDA[United states, department of Agriculture].1972.

- Ustun, B. 2008. Soil erosion modelling by using GIS and remote sensing: a case study, Ganos mountain. *Int. Arch. Photogramm. Remote Sens. Spatial Inf. Sci.* 37: 1681-1684.
- Vannoppen, W., Baets, S.D, Keeble, J., Dong, Y., and Poesen, J. 2017. How do root and soil characteristics affect the erosion-reducing potential of plant species ?. *Ecol. Eng.* (in press).
- Vemu, S. and Pinnamaneni, U.B. 2011. Estimation of spatial patterns of soil erosion using remote sensing and GIS: a case study of Indravati catchment. *Nat. Hazards* 59: 1299-1315.
- Vigiak, O., Okoba, B.O., Sterk, G., and Stroosnijder, L. 2005. Water erosion assessment using farmer's indicators in the west Usambara mountains, Tanzania. *Catena* 64: 307-320. <https://doi.org/10.1016/j.catena.2005.08.012>.
- Vijith, H., Seling, L.W., and Dodge-Wan, D. 2017. Estimation of soil loss and identification of erosion risk zones in a forested region in Sarawak, Malaysia, northern Borneo. *Environ. Dev. Sustain.*
- Wade, J.C. and Heady, E.O. 1978. Measurement of sediment control impacts on agriculture. *Water Resour. Res.* 14: 1-8.
- Wakindiki, I.I.C. and Ben-Hur, M. 2002. Soil Mineralogy and texture effects on crust micromorphology, infiltration and erosion. *Soil Sci. Soc. Am. J.* 66: 897-905.
- Walling, D.E. 1983. The sediment delivery problem. *J. Hydrol.* 65(1): 209-237.
- Wang, L., Dalabay, N., Lu, P., and Wu, F. 2016. Effects of tillage practices and slope on runoff and erosion of soil from the Loess Plateau, China, subjected to simulated rainfall. *Soil Tillage Res.* (in press).

- Wang, Y., Fan, J., Cao, L., Zheng, X., Ren, P., and Zhao, S. 2018. The influence of tillage practices on soil detachment in the red soil region of China. *Catena* 165: 272–278. <http://doi.org/10.1016/j.catena.2018.02.011>.
- Wang, Y., Zhang, J.H., Zhang, Z.H., and Jia, L.Z. 2016. Impact of tillage erosion on water erosion in a hilly landscape. *Sci. Total Environ.* 551: 522-532.
- Wildemeersch, J.C.J., Vermang, J., Cornelis, W.M., Diaz, J., Gabriels, D., and Ruiz, M. 2014. Tillage erosion and controlling factors in traditional farming systems in Pinardel Rio, Cuba. *Catena* 121: 344-353.
- Williams, J.R. 1975. Sediment yield prediction with universal equation using runoff energy factor. In: [Anonymous] (eds), *Sediment Yield*. Proceedings of the Workshop, USDA Sedimentation Laboratory, Oxford, Mississippi.
- Williams, J.R. and Berndt, H.D. 1972. Sediment yield computed with universal equation. *J. Hydrol. Div. ASCE* 98(12): 2087–2098.
- Wischmeier, W.H. and Smith, D.D. 1965. *Predicting Rainfall - Erosion Losses from Cropland East of the Rocky Mountains*. Agriculture Handbook No. 282, USDA, Washington, DC.
- Wischmeier, W.H. and Smith, D.D. 1978. *Predicting Rainfall Erosion Losses - A Guide to Conservation Planning*. Agriculture Handbook No. 537, US Department of Agriculture Science and Education Administration, Washington, 163p.
- Wischmeier, W.H., Johnson, C.B., and Cross, B.V. 1971. A soil erodibility nomograph for farmland and construction sites. *J. Soil Water Conserv.* 26 (5): 189-193.

- Woo, M., Fang, G., and DiCenzo, P. 1997. The role of vegetation in the retardation of rill erosion. *Catena* 29: 145-159.
- Wu, X., Wei, Y., Wang, J., Xia, J., Cai, C., and Wei, Z. 2018. Effects of soil type and rainfall intensity on sheet erosion processes and sediment characteristics along the climatic gradient in central-south China. *Sci. Total Environ.* 621: 54-66.
- Xie, Y., Liu, B., and Nearing, M.A. 2002. Practical thresholds for separating erosive and non-erosive storms. *Trans. Am. Soc. Agric. Eng.* 45(6): 1843-1847.
- Yin, S., Xie, Y., Liu, B., and Nearing, M.A. 2015. Rainfall erosivity estimation based on rainfall data collected over a range of temporal resolutions. *Hydrol. Earth Syst. Sci. Discuss.* 19: 4113-4226.
- Young, R.A., Onstad, C.A., Bosch, D.D., and Anderson, W.P. 1989. AGNPS: a non-point-source pollution model for evaluating agricultural watersheds. *J. Soil Water Conserv.* 44(2): 168-173.
- Zamani, S. and Mahmoodabadi, M. 2013. Effect of particle size distribution on wind erosion rate and soil erodibility. *Arch. Agron. Soil Sci.* 59(12): 1743-1753.
- Zare, M., Panagopoulos, T., and Loures, L. 2017. Land use policy simulating the impacts of future land use change on soil erosion in the Kasilian watershed, Iran. *Land Use Policy* 67: 558-572.
- Zerihun, M., Mohammedyasin, M.S., Sewnet, D., Adem, A.A., and Lakew, M. 2018. Assessment of soil erosion using RUSLE, GIS and remote sensing in NW Ethiopia. *Geoderma Regional* 12: 83-90.



- Zhang, X., Hub, M., Guoc, X., Yangd, H., Zhanga, Z., and Zhangf, K. 2018. Effects of topographic factors on runoff and soil loss in southwest China. *Catena* 160: 394-402.
- Zhang, Z., Sheng, L., Yang, J., Chen, X., Kong, L., and Wagan, B. 2015. Effects of land use and slope gradient on soil erosion in a red soil hilly watershed of southern China. *Sustainability* 7: 14309-14325.
- Zhao, P., Li, S., Wang, E., Chen, X., Deng, J., and Zhao, Y. 2018. Tillage erosion and its effect on spatial variations of soil organic carbon in the black soil region of China. *Soil Tillage Res.* 178: 72-81.
- Zhou, P., Luukkanen, O., Tokola, T., and Nieminen, J. 2008. Effect of vegetation cover on soil erosion in a mountainous watershed. *Catena* 75(3): 319-325.
- Zhou, W. and Wu, B. 2008. Assessment of soil erosion and sediment delivery ratio using remote sensing and GIS: a case study of upstream Chaobaihe river catchment, north China. *Int. J. Sedim. Res.* 23(2): 167-173.
- Zingg, A.W. 1940. Degree and length of land slope as it affects soil loss in runoff. *Agric. Eng.* 21: 59-64.
- Zorn, M. and Komac, B. 2011. The importance of measuring erosion processes on the example of Slovenia. *Hrvatski Geografski Glasnik* 73(2): 19-34.
- Zuazo, V.H.D. and Pleguezuelo, C.R.R. 2008. Soil erosion and runoff prevention by plant covers - a review. *Agron. Sustain. Dev.* 28: 65-86.

# **APPENDICES**

## APPENDIX I

### a) R factor calculation for the year 2013

Month	Mannarkad (2013)			Pattambi (2013)		
	Rainfall, mm	Days	Monthly R value, MJ. mm/ha/h/y	Rainfall, mm	Days	Monthly R value, MJ. mm/ha/h/y
January	0.0	0	-1.421	0.0	0	-1.421
February	51.0	2	-1.104	15.2	1	-27.95
March	0.0	0	-1.421	13.7	1	-30.31
April	117.7	5	17.801	161.3	4	25.44
May	56.8	1	1.331	94.4	4	13.32
June	767.0	20	60.171	702.2	20	58.68
July	334.8	13	41.432	397.2	15	45.81
August	262.2	9	35.907	382.6	13	44.96
September	394.8	10	45.159	331.4	8	41.71
October	390.6	12	44.917	197.9	7	30.06
November	154.2	4	23.907	121.4	3	19.01
December	0.0	0	-1.421	0	0	-1.421
	2529.1	76	265.26	2417.3	76	217.89

### Sample Calculation

To calculate monthly R value

Consider month July (Mannarkad) with monthly rainfall of 334.8 mm

According to equation

$$\begin{aligned}
 R &= 17.35 \times (1.5 \log_{10} (P_i^2 / P) - 0.08188) \\
 &= 17.35 \times (1.5 \log_{10} (334.8^2 / 2529.1) - 0.08188) \\
 &= 41.43 \text{ MJ mm ha}^{-1} \text{ h}^{-1} \text{ y}^{-1}
 \end{aligned}$$

b) R factor calculation for the year 2000

Month	Mannarkad (2000)			Pattambi (2000)		
	Rainfall, mm	Days	Monthly R value, MJ. mm/ha/ h/y	Rainfall, mm	Days	Monthly R value, MJ. mm/ha/ h/y
January	0	0	-1.421	0.0	0	-1.421
February	0	0	-1.421	0.0	0	-1.421
March	13	1	-29.612	0.0	0	-1.421
April	134	6	23.123	23.2	1	-14.25
May	37	2	-5.968	29.1	2	-9.12
June	480	17	51.966	534.0	16	56.65
July	233	5	35.628	262	5	40.55
August	462	14	51.102	468	15	53.69
September	239	8	36.203	113.4	5	21.62
October	326	11	43.221	160.6	6	29.48
November	90	2	14.126	53.2	1	4.51
December	33	1	-8.554	31.1	1	-7.62
	2047	67	208.39	1674.6	52	175.47

## APPENDIX II

### Raingauge stations with details about location and rainfall related parameters used for interpolation

Raingauge station	Latitude	Longitude	Year	Erosivity factor, R (MJ mm ha <sup>-1</sup> h <sup>-1</sup> y <sup>-1</sup> )	Annual rainfall, mm	No. of rainy days/year	Kinetic energy of rainfall, E
Pattambi	10° 48' N	76° 12' E	2000	175.47	1674.6	52	41362.62
			2013	217.89	2417.3	76	59707.71
Mannarkad	10° 59' 36" N	76° 27' 39.59" E	2000	208.39	2047	67	50560.9
			2013	265.26	2529.1	76	62468.77

#### Sample calculation for kinetic energy of rainfall (E)

$$E = R \times (29.8 - (127.5 / I))$$

Where, intensity of rainfall I = 25 mm/h, R = annual rainfall in mm

Consider data from Pattambi, year 2000

$$E = 1674.6 \times 24.7 = 41362.62 \text{ J/m}^2$$

### APPENDIX III

#### Calculation of erodibility factor K

Soil name	Vfs, %	Silt %	clay %	texture	om %	c	b	K
Vazhikadavu	3.00	17.40	33.1	Sandy clay loam	2.76	3	3	0.11
Vadavannur	15.30	18.00	22.3	Sandy clay loam	1.98	3	4	0.23
Tholuvannur	5.26	1.29	51.48	Sandy clay	2.21	4	4	0.10
Tholanur	20.10	16.80	17.4	Sandy loam	0.78	3	4	0.29
Thattengalam	2.00	33.20	30.9	clay loam	1.65	1	4	0.17
Ramapuram	0.46	30.37	32.63	clay loam	4.22	4	3	0.16
Paruthimala	11.50	18.70	23.9	sandy clay loam	5.07	3	2	0.10
Pariyanampatta	7.80	21.40	40.2	clay	0.83	3	4	0.18
Parali	10.00	23.40	32.3	clay loam	0.67	3	4	0.22
Mannur	6.10	14.16	15.3	sandy loam	2.07	3	4	0.17
Kottamala	19.50	22.50	23.75	sandy clay loam	1.14	3	4	0.29
Karuvarachundaki	10.50	28.75	37.5	clay loam	2.12	4	4	0.24
Karinganthodu	8.90	11.00	33.5	sandy clay loam	1.60	3	4	0.14
Irumpiliyam	0.53	36.41	33.98	clay loam	2.52	4	4	0.23
Churathinmel	2.11	28.12	21.72	sandy clay loam	2.43	4	2	0.17
Chelari	0.94	43.22	30.63	clay loam	0.91	3	2	0.22
Anjur	1.74	16.74	39.72	clay loam	2.72	3	4	0.12
Angadipuram	2.30	26.90	26.5	sandy clay loam	1.21	3	3	0.17
Agali	9.68	35.51	29.4	clay loam	1.03	3	4	0.29

\*vfs = very fine sand; om = organic matter; c= Permeability class; b= structural class

### Sample calculation of K factor

For Vazhikkadavu series,

$$K = \{2.1 \times M^{1.14} \times 10^{-4} \times (12-a) + 3.25 \times (b-2) + 2.5 \times (c-3)\} / 100$$

In which,  $M = (\% \text{ of silt} + \% \text{ of very fine sand}) \times (100 - \% \text{ of clay})$ , 'a' is the % of organic matter content in the soil, 'b' indicates value corresponding to structural classes and c indicates the value corresponding to the permeability class.

$$\{ M = (17.4 + 3) \times (100-33.1) = 1364.76,$$

$$a = 2.76, b = c = 3 \}$$

$$\text{therefore } K = \{2.1 \times 1364.76^{1.14} \times 10^{-4} \times (12-2.76) + 3.25 \times 1\} / 100 \\ = 0.11 \text{ t ha h}^{-1} \text{ ha}^{-1} \text{ MJ}^{-1} \text{ mm}^{-1}$$

### APPENDIX IV

#### Variation of average C factor with respect to landuse for the year 2000 and 2013

Landuse	C (2013)	C (2000)
Build-up plus barren land	0.97	0.99
Grassland	0.17	0.12
Waterbodies	1.7	1.7
Mixed crop	0.13	0.1
Forest	0.11	0.1
Rubber	0.15	0.04
Banana	0.3	0.15
Paddy	0.23	0.13
Scrub	0.26	0.12
Coconut	0.23	0.13

## APPENDIX V

Mean values of Rainfall (R), depth of overland flow (Q), rate of splash detachment (F), and % interception contributing evapo-transpiration and runoff (A) with respect to soil texture in the year 2000 and 2013

Year	2000				2013			
Texture	R, mm	Q, mm	F, kg/m <sup>2</sup>	A	R, mm	Q, mm	F, kg/m <sup>2</sup>	A
sandy clay loam	1921.05	393.87	2.49	29.58	2491.29	672.71	3.83	26.50
clay loam	1968.56	603.63	3.41	25.94	2505.55	736.22	4.06	26.82
sandy clay	1716.57	826.00	2.32	19.96	2429.9	676.91	2.19	28.08
sandy loam	1895.48	609.26	2.83	28.31	2483.61	979.76	4.52	25.74
clay	2029.82	290.72	2.56	29.78	2523.94	590.77	3.95	25.96



### APPENDIX VI

**Mean soil erosion corresponding to rainfall range and score assigned**

MODEL		RUSLE		MMF	
Rainfall range, mm	Area, km <sup>2</sup>	Mean (t/ha/y)	Score	Mean, (t/ha/y)	Score
2420-2440	152.50	13.48	0.38	16.33	0.50
2440-2460	93.49	17.95	0.51	21.92	0.67
2460-2480	84.59	22.35	0.64	23.40	0.71
2480-2500	62.30	31.43	0.90	33.14	1.01
>2500	622.12	45.11	1.29	39.70	1.21

### APPENDIX VII

**Mean soil erosion corresponding to soil texture and score assigned**

MODEL		RUSLE		MMF	
Texture	Area, km <sup>2</sup>	Mean (t/ha/y)	Score	Mean (t/ha/y)	Score
sandy clay loam	446.94	43.23	1.23	35.14	1.07
clay loam	330.58	33.56	0.96	31.77	0.97
sandy clay	3.43	6.43	0.18	14.12	0.43
sandy loam	193.55	24.60	0.70	32.76	1.00
clay	40.49	11.80	0.34	16.63	0.51

### APPENDIX VIII

**Mean soil erosion corresponding to slope and score assigned**

MODEL		RUSLE		MMF	
Slope range, %	Area, km <sup>2</sup>	Mean (t/ha/y)	Score	Mean (t/ha/y)	Score
< 5	102.94	15.20	0.43	23.60	0.72
5 - 15	413.16	25.15	0.72	28.00	0.85
15 - 30	281.52	29.30	0.83	31.00	0.95
> 30	218.12	70.94	2.02	48.49	1.48

### APPENDIX IX

**Mean soil erosion corresponding to land use and score assigned**

MODEL		RUSLE		MMF	
Name	Area, km <sup>2</sup>	Mean (t/ha/y)	Score	Mean (t/ha/y)	Score
Built-up Land	210.60	104.99	2.99	108.88	3.22
Rubber	158.87	17.30	0.49	8.17	0.25
Paddy	72.02	6.62	0.19	6.48	0.19
Banana	2.32	6.58	0.19	11.68	0.36
Coconut	25.62	4.98	0.14	7.25	0.22
Scrub	43.35	38.84	1.11	39.78	1.21
Mixed Crop	311.23	4.37	0.13	6.07	0.18
Grass Land	4.50	49.48	1.41	30.90	0.94
Forest	170.79	37.10	1.06	24.03	0.73

**SOIL EROSION RISK ASSESSMENT IN KUNTHIPPUZHA  
SUB-WATERSHED USING REMOTE SENSING AND GIS**

*by*

**SHAHEEMATH SUHARA K.K.**

**(2016-18 -009)**

**ABSTRACT OF THESIS**

Submitted in partial fulfillment of the requirements for the degree of

***MASTER OF TECHNOLOGY***

***IN***

***AGRICULTURAL ENGINEERING***

**(Soil and Water Engineering)**

**Faculty of Agricultural Engineering & Technology**

**Kerala Agricultural University**



***Department of Soil and Water Conservation Engineering***

**KELAPPAJI COLLEGE OF AGRICULTURAL ENGINEERING AND TECHNOLOGY**

**TAVANUR, MALAPPURAM-679573**

**KERALA, INDIA**

**2018**

129

## ABSTRACT

This study mainly focused to identify the erosion prone areas in Kunthippuzha sub-basin using RUSLE as well as MMF model. The effect of spatial and temporal variations of land use-land cover on soil erosion was analysed with the help of NDVI values. The estimation was performed for the year 2000 and 2013. The mean soil erosion estimated for the year 2000 was 18.30 and 20.58 t/ha/y respectively by MMF as well as by RUSLE model. Similarly in the year 2013, it was 32.78 and 35.10 t/ha/y respectively.

To find the erosion prone areas in the sub-watershed factorial scoring method was chosen, in which pixel based scoring was done based on mean soil erosion value obtained under each layers of landuse, rainfall, slope and topographic raster. From the study based on the RUSLE model, 0.15% of the area experienced very slight erosion. 40.70% of the area was with slight erosion, 28.76% area was under moderate erosion, 22.61% of the area was under severe range and 6.15% area was under very severe range. According to MMF model, the areal extent observed under slight, moderate, severe and very severe risk categories was 39.02%, 36.94%, 14.92%, 7.50% respectively.

NDVI values corresponding to land use were identified, in which negative NDVI values correspond to water pixels whereas higher NDVI values represents the thick vegetation. From the analysis of the temporal variation in land use over the NDVI, it was observed that NDVI value decreased at the points where density of the canopy decreased. The spatial variation of soil erosion varies pixel to pixel according to the landuse pattern. Highest soil erosion risk was observed under built-up plus barren land. Sediment Delivery Ratio (SDR) was calculated for the entire sub-watershed, which shows that most of the eroded sediments get deposited at intermediate location before reaching the outlet. The SDR calculation enhances the importance of adopting GIS technology in soil erosion assessment.

174472



180